Kinetic Modeling of Direct Liquefaction of Coal

by

Mehran Heydari

A thesis submitted in partial fulfillment of the requirements for the degree of

Doctor of Philosophy

in

Chemical Engineering

Department of Chemical and Materials Engineering
University of Alberta

Abstract

During the past few decades, petroleum has been the main source of liquid fuels. On one hand petroleum reserves are declining, and on the other hand coal reserve is the most abundant fossil fuel known in the world. Liquefaction aims to convert solid coal into liquid fuels. Coal can be converted to liquid and gaseous fuels and chemicals by two different processing methods, normally called direct and indirect. Direct coal liquefaction converts solid coal to liquid fuels at high temperature and pressures in the presence or absence of catalyst.

One of the advantages of direct liquefaction is that, this process can convert coal to liquid without the need for producing syngas (H_2 and CO) as in indirect process and also has higher efficiency than indirect liquefaction. In order to develop commercially practical processes for deriving liquid fuels from coal, a description of coal liquefaction kinetics is essential for design and scale-up of coal liquefaction experiments.

The liquefaction of a Canadian lignite coal has been studied experimentally and modeled mathematically. Since conventional batch autoclave is not suitable for isothermal experiments, as the time required for the autoclave to reach the reaction temperature can be substantial, the liquefaction runs were investigated with a rapid injection reactor designed specifically for isothermal kinetic study. The liquefaction experiments were carried out in a tubular bomb reactor in presence of tetralin at temperature ranged from 350 to 450˚C and reaction time range of 15 to 120 min under nitrogen atmosphere. No catalyst was used in the experiments. The results show that Canadian lignite coal is readily liquefied, with its conversion exceeds 80% at 400 °C even without catalyst. Different kinetic models have been

proposed and examined to describe distributions of products such as preasphaltene, asphaltene, oil and gas. Rate constants for each of the specified reaction network have been calculated by nonlinear regression analysis. A genetic algorithm (GA) optimization method was applied to find the optimal set of kinetic parameters.

Arrhenius activation energies were calculated for each rate constant. The high activation energies seemed to indicate that direct coal liquefaction was kinetically controlled. The results showed that at high temperature and extended time undesirable retrograde reactions may take place.

Preface

This research was funded by grant from Carbon Management Canadian Centre for Clean Coal/Carbon and Mineral Processing Technologies (C_5MPT) to Dr. Rajender Gupta.

Two journal papers were published during this study using some of materials in chapters 3 and 4. In the first paper, some materials from chapter 3 have been published as: Heydari, M., Rahman, M., & Gupta, R. (2015). Kinetic Study and Thermal Decomposition Behavior of Lignite Coal. *International Journal of Chemical Engineering*, *2015*. And in the second paper, materials from chapter 4 have been published as: Heydari, M., Rahman, M., & Gupta, R. (2016). Effect of initial coal particle size on coal liquefaction conversion. *International Journal of Oil, Gas and Coal Technology*, *12*(1), 63-80. In both papers, I was first author and responsible for the data collection, data analysis and writing the manuscript. Rahman, M. had contribution to manuscript edits and Gupta, R was corresponding author and involved in manuscript composition.

DEDICATION

To the memories of my late father, Masoud who throughout his lifetime etched in my mind the importance of education.

To my mother, Zahra

and

my brothers, Pejman and Pooya

for their support and encouragements.

Acknowledgement

I would like to acknowledge and thank my supervisor, Prof. Rajender Gupta, for his continuous guidance over the course of my studies. Without his generous encouragement, this thesis would have never been written.

 I contentedly express my gratitude to Prof. William McCaffrey and Prof. Robert E. Hayes as the members of supervisory committee for their valuable contributions, advice and support toward accomplishing this study. Their great suggestions helped me carrying out laboratory experiments, analyzing data and writing scientific papers.

Finally, I would like to thank my dear friends, Dr. Yashar Behnamian, Dr. Mehdi Mohammad Ali Pour and Dr. Moshfiqur Rahman, Dr Bardia Hassanzadeh, Mohammad Ghafelehbashi who supported me during this period which it may not have been possible to achieve this degree. I would like to thanks Quang Tran who trained me in some experiment tasks.

The financial support from Sheritt Company, Faculty of Graduate Studies and Research and Faculty of Engineering at the University of Alberta, Canadian Centre for Clean Coal/Carbon and Mineral Processing Technologies (C_5MPT) and Prof. Rajender Gupta is also appreciated.

TABLE OF CONTENTS

Contents

LIST OF TABLES

LIST OF FIGURES

Chapter 1

INTRODUCTION

Coal is the world's most abundant fossil fuel. Coal contains about 66% of Canada's hydrocarbon reserves and 92.3% of North America hydrocarbon reserves. Alberta's coal reserves represent approximately 70 per cent of Canada's total reserves. Alberta's coal reserves contain more than twice the energy of all other non-renewable energy resources in the province, including conventional oil and pentanes, natural gas, natural gas liquids and bitumen and synthetic crude.

Coal is the fuel of more than half of the world's power plants for electricity generation. About 20% of electric power generated in Canada and 50% in Alberta is coal based [1]. The amount of coal deposits is approximately ten times higher than other carbonaceous resources. Coal resources are located more broadly all over the world than oil reserves [2]. Coal appears to hold the most promise of all the possible alternatives for short-term development to meet the national requirements of energy. Coal and coal products play a major role in fulfilling the energy demands of our society. Direct liquefaction, indirect liquefaction and gasification are examples of existing processes for coal conversion into energy products [3]. Therefore coals are of significant industrial and economic importance, both as an energy source and as industrial feedstock.

Recent demands for liquid fuel (petroleum products) have increased the significance of coal liquefaction processes. Also the expectation that fuels will be needed from alternative sources is imminent, particularly in the transportation application [4]. For clean and efficient utilizing of coal, liquefaction seems to be a reliable option instead of coal combustion due to

today's stringent environmental regulations and also need for greater efficiency in power generation [5]. The production of liquid transportation fuels by direct liquefaction of coal is an active research area. Direct coal liquefaction has long been used to generate useful products such as heavy, middle distillate and light oils. The yield of these products depends on the composition of the coal used and reaction condition.

In view of the need to develop commercially applicable processes for deriving liquid fuels from coal, a description of comprehensive liquefaction kinetics is necessary for design and scale-up of coal liquefaction experiments. Kinetics studies are very important because they can provide expressions for the reaction pathway which can be used in calculating reaction times, yield and economic conditions. Several kinetic models, with varying degrees of complexity and sophistication, have been used in the literature to describe coal liquefaction behavior. However, because of heterogeneous nature of coal, experimental conditions, and different definitions and methods for measurement of coal conversion products make it sophisticated to compare the results. The kinetic of coal liquefaction is complicated due to the formation of various compounds. Thus, the approach in coal liquefaction kinetic studies is to isolate these compounds to kinetically similar compounds through some separation methods [6].

The main purpose of this project is to develop a kinetic model for direct coal liquefaction process under isothermal condition that incorporates time and temperature.

In this work, kinetic modeling of direct liquefaction of a Canadian coal has been studied at department chemical and materials engineering of university of Alberta. Since conventional batch autoclaves are not suitable for isothermal studies, as the time required for the autoclave to reach the reaction temperature can be substantial and also significant

reactions can happen, the liquefaction experiments have been carried out with a rapid injection reactor designed specifically for isothermal kinetic study. The short nonisothermal periods of heating and cooling allowed neglecting its effect on the overall process and the reaction was considered as isothermal. A literature review on description of coal and its properties, coal liquefaction concept, and types of direct coal liquid processes and their importance to industry is discussed in CHAPTER 2. The characterization methods, sample preparation and a brief overview of experimental procedures are provided CHAPTER 3. Also the results of kinetic study and thermal behavior of two coal samples are given in details in this CHAPTER. Effect of initial coal particle size on coal liquefaction conversion is studied in CHAPTER 4. This chapter is devoted to particle size selection for subsequent kinetic study experiments. CHAPTER 5 is dedicated to modeling of direct coal liquefaction of a Canadian coal. The results of CHAPTER 3 and CHAPTER 4 are employed for kinetic modeling of direct liquefaction in this CHAPTER. Several lumped kinetic models have been proposed and examined in this CHAPTER to describe distributions of main products such as preasphaltene, asphaltene, oil and gas. The mathematical models were compared to kinetic data obtained from isothermal reactor. Results of mathematical modeling and product distribution and different characterization techniques are discussed in details in CHAPTER 5. Rate constants for each of the specified reaction network have been calculated by nonlinear regression analysis. The results of (GA) optimization method are considered in CHAPTER 6. Finally, conclusions and recommendations for future works are given in CHAPTER 7,

Chapter 2

BACKGROUND

This chapter is dedicated to elucidate a general description of coal and its properties, environmental impact, coal liquefaction concept, and types of coal liquid processes and their importance to industry is discussed. Also a brief review of coal pyrolysis, direct and indirect liquefaction differences and major Factors affecting coal liquefaction is presented.

2.1   Description of coal

2.1.1 Origin of coal

Coals are complex, heterogeneous solids that vary widely in their properties and hence suitability for particular applications. Coal is an organic sedimentary rock that contains principally organic substances, inorganic mineral matter and moisture. It can be characterized by its chemical composition, chemical and physical properties. The properties and chemical composition of coal vary with the geological maturity and different types of coal can be distinguished [7].

Coal is found in deposits and formed from accumulation of plants by the chemical and geological alternation over hundreds of millions of years.

The geochemical process that transformed plant remains into coal is called coalification. Coalification refers to the progressive transformation of peat through lignite coal, subbituminous, bituminous to anthracitic coals [8].

The formation of coal involves two stages, biochemical stage and the geochemical stage. The biochemical stage starts with the accumulation of plant material settles in low, swampy

4

areas to form peat beds. At this stage, bacteria begin to decompose the plant material by eliminating oxygen and hydrogen by releasing water, methane and carbon dioxide. The biochemical stage terminates as more sediment starts to cover the peat layer. As the peat is further immersed and the sediment layer extends, bacteria stop to exist. The second stage of coalification is the geochemical stage. During this stage, the peat materials undergo more alternation due to temperature and pressure from overburden of sediment deposits. Oxygen and hydrogen are rejected as methane, carbon dioxide, and water. There is decrease in moisture and volatile matters as well as an increase in carbon percentage. This gives rise to a series of coalification that ranges from lignite to anthracite.

2.1.2 Coal Rank

The degree of maturation of coal is termed as coal rank. lignites and subbituminous are classified as low rank, while bituminous and anthracite are referred as high rank coal [9]. With increasing rank, aromaticity increases and the structure becomes more polycondensed as shown in Figure 2-2 [2]. Low rank coal like lignite coal has less aromaticity and readily liquefied under mild operation condition. With increasing rank, H/C ratio decreases. oxygen content decreases, moisture content decreases, and the heat content increases but sulfur and nitrogen change little with rank.
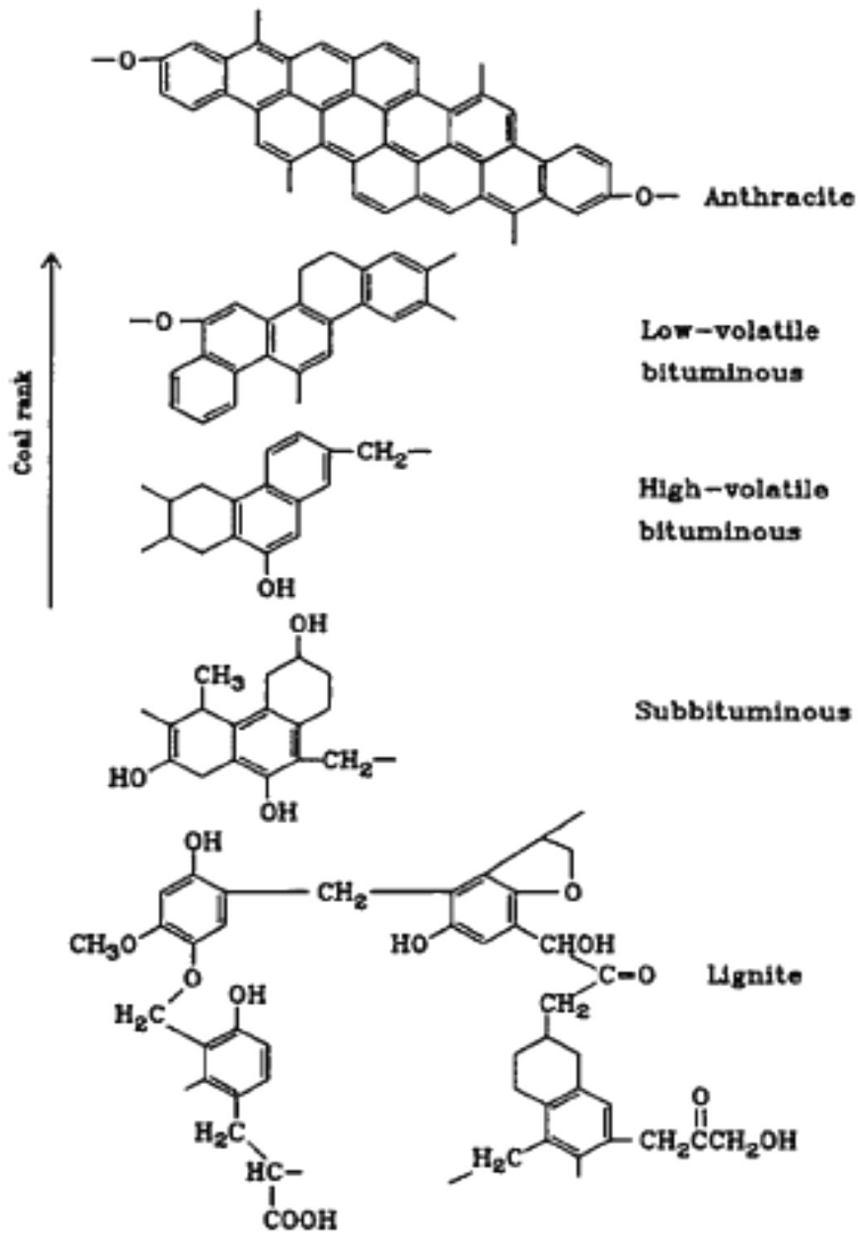
Figure 2–1: Coal rank versus aromaticity [2]

2.1.3 Coal grade

The mineral matter that is present in the coal structure indicates grade of coal and reflects coal quality. During the time of peat formation in the swampy area mineral matter present in ground water precipitate in the coal seam. Mineral matter is not always inert

during liquefaction and may affect the coal conversion and product distribution. It has been reported that some inherent mineral matters such as pyrite can act beneficially as a catalyst for coal liquefaction [10, 11].

2.1.4 Coal reserves in the world

Coal reserves are more broadly distributed all over the world as shown in Table 2.1 [9]. The United States covers the largest coal reserves about 25% of the world total.

Table 2-1 World estimated recoverable coal reserves (million tons) [9]

Region	Anthracite and Bituminous	Lignite and Subbituminous	Total
United states	126804	146852	273656
Canada	3826	3425	7251
Mexico	948	387	1335
India	90826	2205	93031
China	68564	57651	126215
Russia	54110	118964	173074
Germany	25353	47399	72753
Iran	1885	-	1885
UK	1102	551	1653
Ukraine	17939	19708	37647
Mexico	948	387	1335
Australia	46903	43585	90489
Colombia	6908	420	7328
Poland	22377	2050	24427

North America has the second largest recoverable coal reserves in the world. Most of these recoverable coal reserves are located in British Columbia, Alberta, and Saskatchewan. The

coals from Alberta and Saskatchewan are known as low sulfur coals and useful for power station fuels.

2.1.5 Coal– Environmental impact

The abundance and low cost of coal make it an attractive fuel, but environmental concerns will have the greatest influence on future coal use for power generation in the industrialized countries. Some environmentalists agree that burning coal is the polluting method and is causing environmental damage. The worst thing that happens in this process is of course the production of Particulate matter (fly ash) by burning coal. Therefore due to increasing demand for energy and stringent environmental regulations innovative technologies for utilizing of coal are required [5, 15].

Today, new technology has made it possible to use energy sources. Coal gasification/coal liquefaction will now allow us to tap the abundant energy stores without compromising the standards of environmental quality. For clean and efficient utilizing of coal, liquefaction seems to be a reliable option for the production of low sulphur and low ash fuels which can produce valuable products and reduce the environmental impacts [4, 7].

2.1.6 Advantages of lignite coals

About 45% of the world's coal reserves contains of lignite. Lignite is inexpensive and has low sulfur content [12]. Lignite coals have some advantages that make them popular as a source of energy.

-Lignite coals are young coals and found in seams with less over burden so the cost of mining is low.

- Reactivity of lignite coals is high because of high volatile matter content

-Low rank coals such as lignite have fewer impurities such as Sulphur and heavy metal

8

-Lignite coal contains several hydroxyl and carboxylic groups which have high interaction with coal liquefaction solvent such as tetralin.

-Lignite's structure is not polycondensed like high rank coals and can be liquefied readily under mild liquefaction conditions [13, 14].

2.2 Coal to liquid (CTL)

Coal can be converted to liquids by increasing the coal's hydrogen to carbon ratio and decreasing the average molecular mass. The H/C ratio of Coal is less than 1.0 which is lower than petroleum.

The hydrogen supply reservoir may be the gas phase or donor solvent. Hydrogen is also consumed in reducing the concentrations of heteroatoms in the coal (sulfur, nitrogen, oxygen).

2.2.1 History

"One of the main approaches of direct conversion of coal to liquid products via hydrogenation process is the Bergius process, created by Friedrich Bergius in 1913, leading to the Nobel Prize in chemistry. The process was further developed between 1910 and 1927, culminating in the construction between 1927 and 1943 of twelve plants that generated around 100,000 barrels per day of oil from coal in Germany during World War II. The liquefaction processes were uneconomical and involved very high temperature and pressure" [5]. The discovery of low price petroleum in Middle East in 1950s stopped essentially all the coal liquefaction developments in the world except that in South Africa due to its shortage of petroleum. With the oil crisis in 1978, the development of alternative technologies was renewed specially using coal as feedstock to produce liquid fuels. Most of the direct processes developed in the 1980s were extensions of Bergius's original concept [16].

2.2.2 Liquefaction of coal

The production of liquid fuels by liquefaction from coal involves heating pulverized coal in a solvent with or without the presence of hydrogen under pressure and with or without added catalyst. Part of the coal will decompose and dissolve in the solvent. Subsequent processing will separate the undissolved solids (mineral matter and inert macerals) from the liquids, and a portion of the liquids may be added to the solvent and recycled. The products obtained include light gases, distillate liquids and residue .The ultimate goal of liquefying coal is to increase the ratio of hydrogen to carbon and to remove the heteroatoms and ash from coal [17].

Three major types of potential coal liquefaction technologies are commonly identified: (1)-Pyrolysis (thermal decomposition of organic compounds in the absence of oxygen), (2)-Indirect coal liquefaction (initial production of synthesis gas with subsequent conversion of the primary gaseous product to liquid fuels) and (3) direct coal liquefaction (converts directly solid coal into liquid fuels without producing the synthesis gas as necessary intermediate; usually direct liquefaction takes place in the presence of hydrogen) [18].

2.3 Pyrolysis

Pyrolysis or carbonization is the method for obtaining liquids from coal which employs the approach of rejecting carbon as its method of increasing the hydrogen-to-carbon ratio of raw coal. Pyrolysis takes place as coal is treated at elevated temperature in a closed container in the absence of oxygen. During pyrolysis a series of reactions occurs. This is carried out under inert atmosphere, so that undesirable combustion reactions cannot take place. The main products of carbonization are coke or char, coal tar, gases and aqueous liquor. Their proportion is determined by a number of factors like rate of heating, type of coal, reactor

configuration [19]. Depending upon the temperature of operation, coal carbonization processes can be classified into two types:

(1) Low temperature pyrolysis: It is carried out at 500-700 ºC temperature. Char, coke and semi-coke are the main products of this process. Liquid yields are higher than high temperature pyrolysis.

(2) High temperature pyrolysis: It is known as the oldest method for obtaining liquids from coal. It is carried out at temperatures in excess of 700 ºC, to around 950 ºC and is mainly employed for the production of metallurgical coke. Besides metallurgical coke, coal tar is also produced in this process. This process results in low liquid yields and the cost of upgrading is relatively high [20].

2.4 Indirect liquefaction (ICL)

Production of liquid fuels from coal via the indirect liquefaction approach involves a number of steps: first gasification of coal with steam and oxygen to produce synthesis gas mainly composed of CO, H_2 and to a lesser extent CO_2 and CH_4 as well as impurities. Then this synthesis gas or "syngas" is cleaned from impurities to adjust the $[H_2]/[CO]$ ratio. This is followed by catalytic conversion of the synthesis gas to synthetic crude oil through methanol synthesis or Fisher-Tropsch process. Finally the synthetic crude oil can be refined to produce fuels and chemicals. Catalytic conversion of H_2 and CO into Methanol classified into two processes: Conventional gas-phase process, or the recently developed process, which is used when the syngas is rich in CO, the liquid phase methanol process [22]. The reactions are shown below:

$$2\,H_2 + CO \rightarrow CH_3OH$$

$$CO_2 + 3\,H_2 \rightarrow CH_3OH + H_2O$$

$$CO + H_2O \rightarrow CO2 + H_2$$
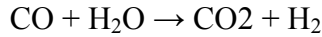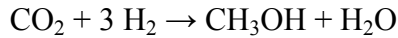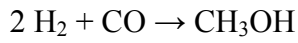
All these reactions are highly exothermic. A mixture of copper, zinc oxide and alumina are typically used as catalyst. In the Fischer-Tropsch synthesis carbon monoxide (CO) and hydrogen (H_2) in the syngas are converted into hydrocarbons of various molecular weights. In the Fischer-Tropsch synthesis carbon monoxide (CO) and hydrogen (H_2) in the syngas are converted into hydrocarbons of various molecular weights according to the below equation:

$$(2n+1)H_2 + nCO \rightarrow C_n H_{(2n+2)} + nH_2O$$
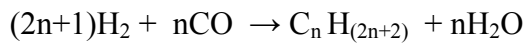
Depending on the catalyst, temperature, and type of process employed, different products ranging from methane to higher molecular paraffins, oxygenates and olefins can be obtained [23]. The following figure shows schematic diagram of ICL process [24].
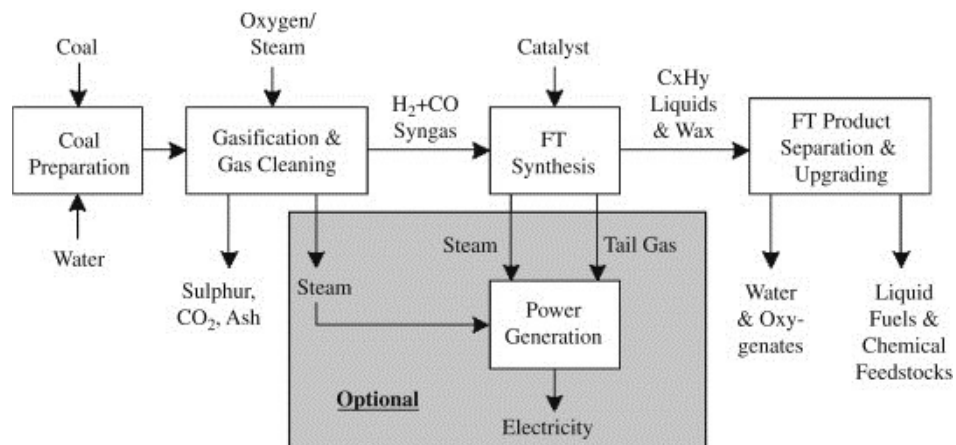
Figure 2–2: Typical indirect coal liquefaction process [24]

2.5 Direct Coal Liquefaction (DCL)

Direct coal liquefaction converts directly solid coal into liquid fuels without any intermediate; in the presence or absence of catalyst. DCL processes are more efficient and work at low temperature regime [4]. Other positive impacts of using liquefaction process involve long-term environmental advantages ranging from the reclamation of coal waste piles and the mining of secondary coal sources, to possible ways to reduce hazardous emissions in coal combustion. In addition to mitigating climate change and air pollution, liquefaction technology may also positively influence on foreign energy sources. Coal liquefaction increases energy efficiency by diversifying the power systems of a country and giving rise to more renewable sources for energy [9].

2.5.1 Major Direct Coal Liquefaction Processes

- Exxon Donor Solvent(Exxon, USA)
- H-Coal (HRI, USA)
- Solvent Refined Coal (SRC-I and SRC-II) (Gulf Oil, USA)
- NEDOL (NEDO, Japan)
- Kohleoel (Ruhrkohle, Germany) [16].

2.5.2 Exxon donor process

Research on Exxon Donor Solvent (EDS) process commenced in 1966.A 250 t/d pilot plant was created and operated in Baytown, Texas in 1980.A scheme of the basic process is given in Figure 2-4[4]. In this process pulverized coal is mixed with recycle solvent which comes from solvent hydrogenation unit and hydrogen which comes from hydrogen manufacture unit. Then the slurry introduce to reactor for coal liquefaction reaction. Vacuum distillation is used for separation of solids or heavy bottoms (containing unreacted coal and minerals) from the coal extract. The coal liquids are fractionated by distillation; the middle

fraction is hydrogenated and recycled as solvent. Coal liquid fractions are further hydro treated to products. One major advantage the EDS process is the isolate solvent treatment and there is no direct contact between mineral matter and catalyst, thus preventing catalyst deactivation [25].
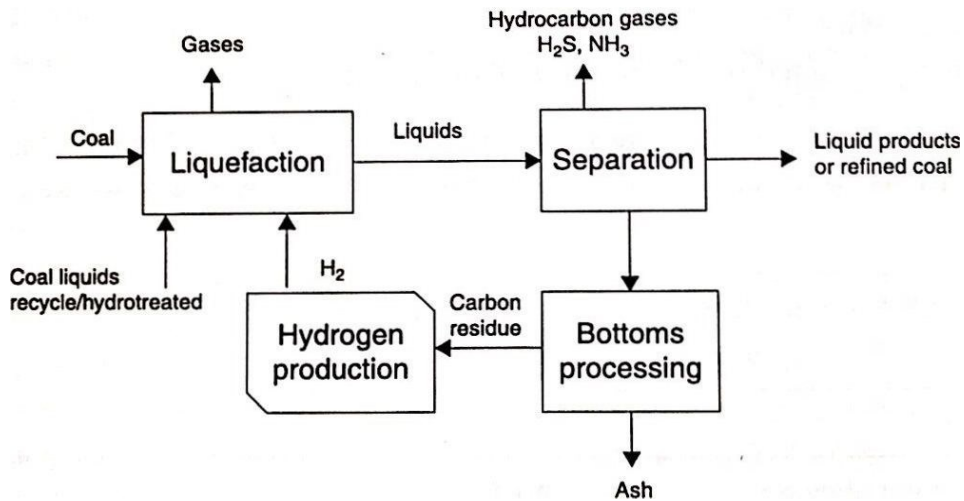
Figure 2–3: Typical direct coal liquefaction process [4]

2.5.3 H-Coal process

This process (developed by Hydrocarbon Research, Inc.) is a direct coal liquefaction process for converting solid coal into liquid products. A block diagram of the process is given in Figure 2-5. Temperatures of the order of (445°C) and pressures up to 20 MPa are used. The pulverized coal is mixed with recycle slurry and catalyst. The coal/oil slurry along with part of the recycle hydrogen is preheated to initiate the coal dissolution, and then introduced to the bottom of the ebullated bed reactor. The ebullated bed reactor is similar to a liquid entrained reactor, but larger gas bubbles help fluidize the solid particles in a fluidized bed reactor.

14
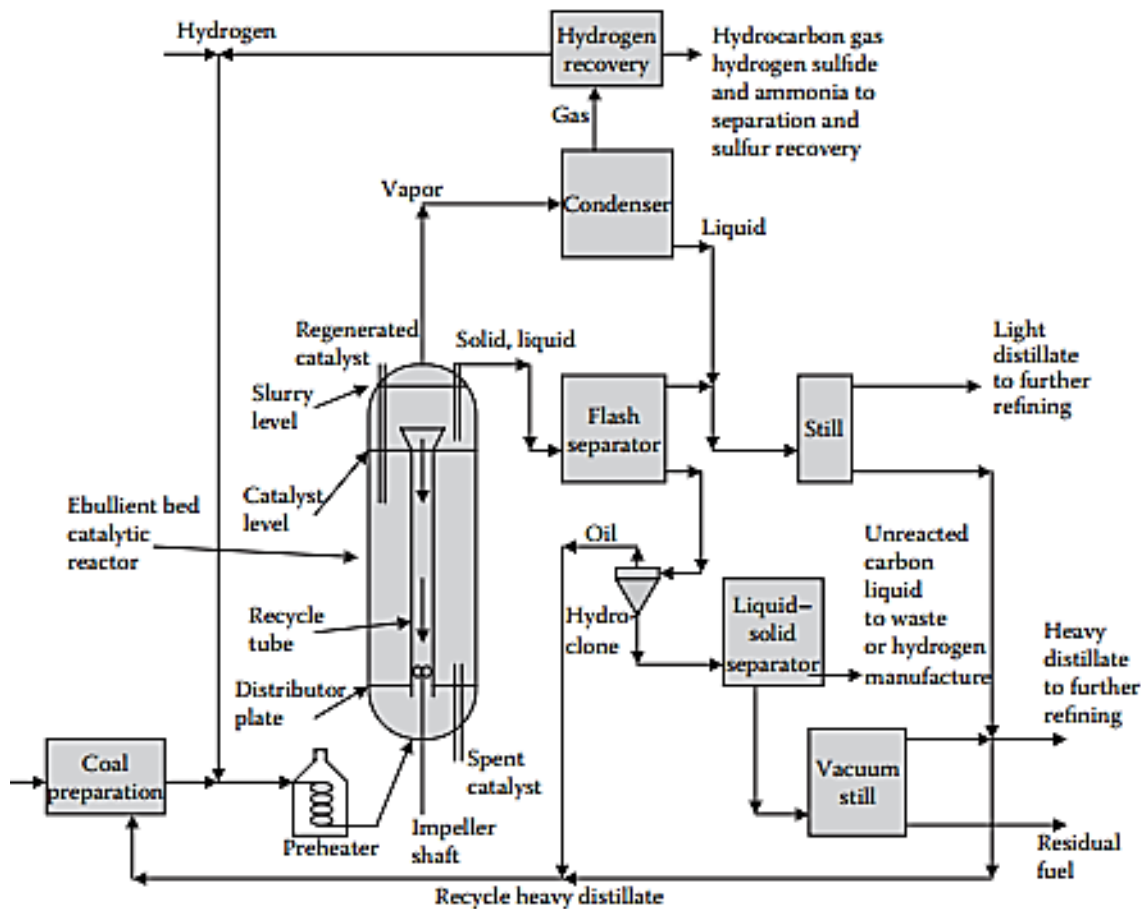
Figure 2–4: H-Coal process flow diagram [8]

The vacuum bottoms (containing the products, unconverted coal) will be gasified in gasification unit to generate hydrogen requirements of the process. Naphtha obtained from this mode can be a very good feedstock for producing high-octane gasoline [8].

2.5.4 Solvent Refined Coal

Solvent refined coal processes (SRC-I and SRC-II) were developed by Pittsburg and Midway Coal Mining Company. The process has two different modes of operation. a) SRC-I

and b) SRC II. The difference between SRC I and SRC II processes is that one produces a

solid product and the other upgrades the SRC product to coal liquid.

a)SRC I. is a thermal coal liquefaction in which coal, solvent and hydrogen are mixed in

the reactor to produce a low ash and low sulfur solid product that is useful for boiler fuel.

Figure 2-6 shows the process flow sheet for SRC-1. This process is somewhat severe than H-

coal process. The solvent is coming from the vacuum distillate. The noncatalytic condition

can reduce hydrogenation rate.
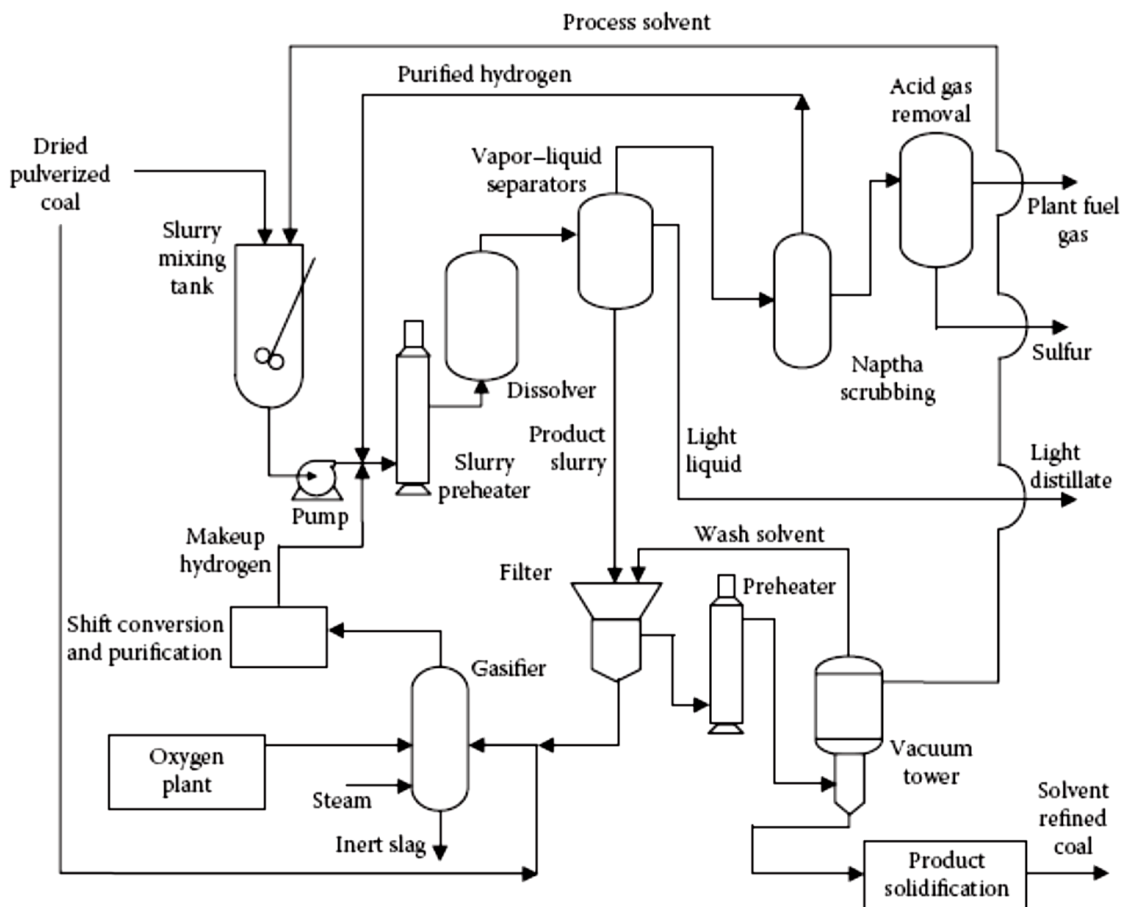
Figure 2–5: SRC I .process flow diagram [8]

b)SRC II. This process is a modification of SRC-I. It uses direct coal liquefaction in the reactor at high temperature and pressure to produce liquid products instead of solid products in SRC-I. This process is using mineral matte in the coal as catalyst. The vacuum bottoms including minerals are introduced to gasification to provide process hydrogen. The quality of liquid product is poor in comparison to H-coal process. Figure 2-7 shows the process flow sheet for SRC-II [8].
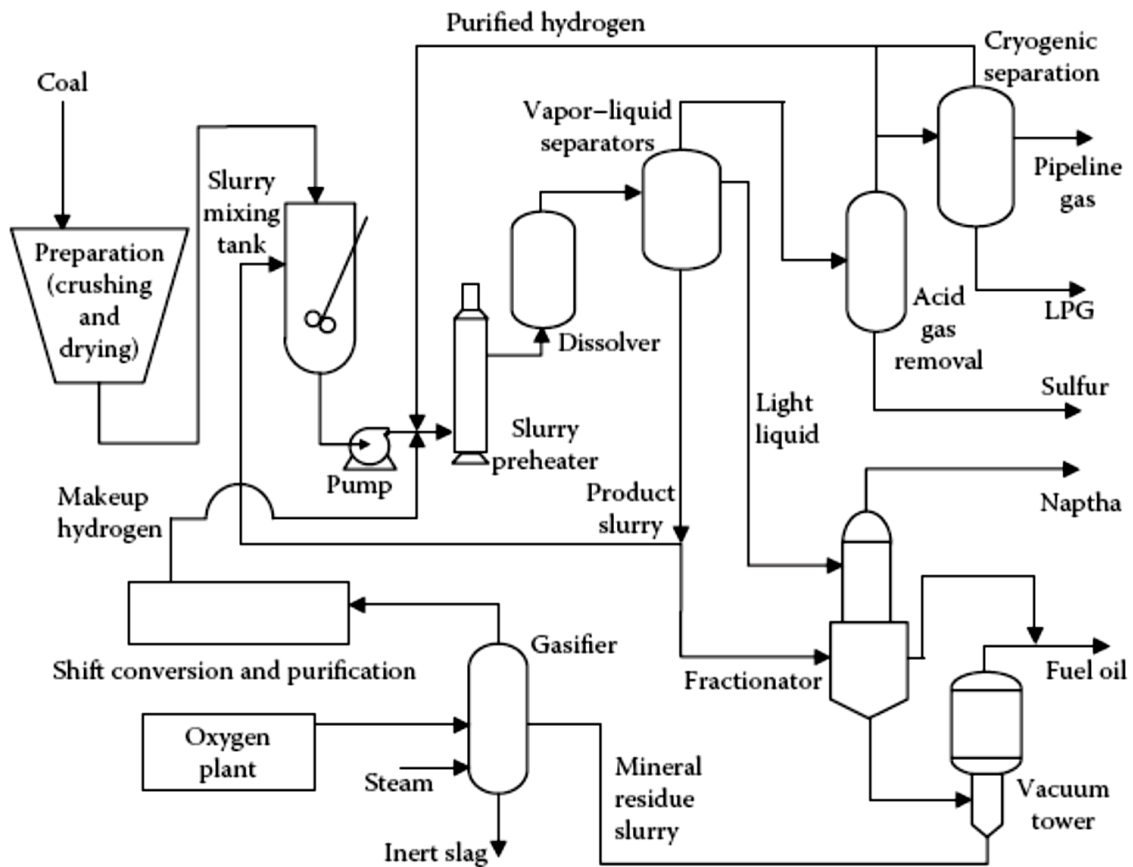
Figure 2–6: A schematic of the SRC-II process [8]

2.5.5 NEDOL process

The NEDOL process is a coal liquefaction process supported by the New Energy and Industrial Technology Development Organization (NEDO). Figure 2-8 shows a schematic flow diagram of the NEDOL process. In the NEDOL process, direct conversion of coal to oils in the presence of solvent and iron based catalyst takes place. The pilot plant comprises of four sections a Slurry preparation unit involves the grinding of coal and mixing with a recycled solvent and a iron based catalyst, a liquefaction section including a preheater, a distillation section with atmospheric and vacuum towers where products from the reactors are separated into oils and recycle solvent and a solvent hydrogenation unit to improve solvent quality. The produced oil has low quality and requires high cost of upgrading. The reaction occurs in a reactor operating at temperature in the range 430-465°C and pressures in the range 150-200bar [26].
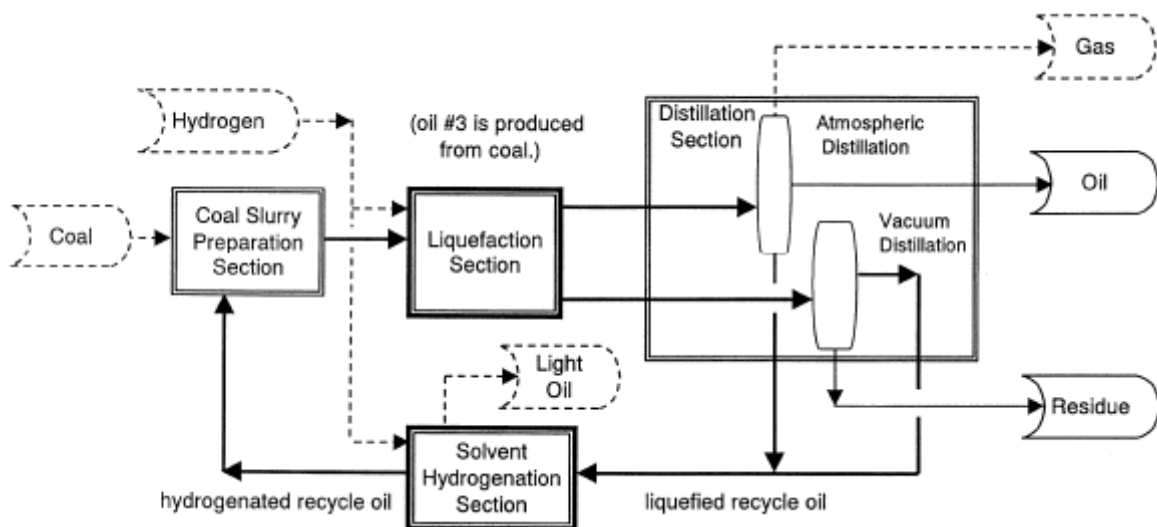
Figure 2–7: Schematic flow diagram of the NEDOL process [26]

2.5.6 Kohleoel Process

The Kohleoel Process was created by Ruhrkohle and VEBA in Germany. This plant operated from 1981 to 1987.In this process pulverized coal was mixed with recycle solvent, hydrogen and iron based catalyst. The process takes place in the reactor at the pressure of 300 bar and at the temperature of 350 -470 °C. The liquefaction products are cooled in two stages. The liquid product from the second stage is introduced to an atmospheric distillation column, yielding light oil (C5 – 200°C bp) and a medium oil (200–325°C bp) product. The vacuum column bottom involves of mineral matter, unreacted coal and catalyst and can be used as a gasifier feedstock for H_2 production [27].
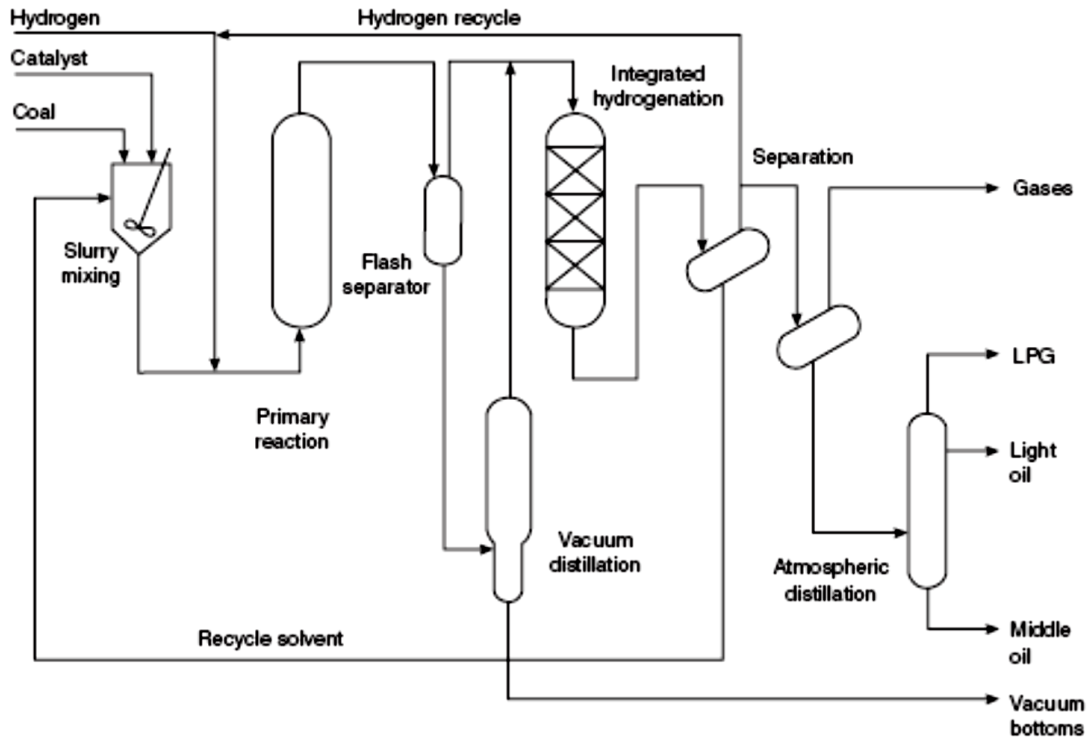
Figure 2–8: Schematic flow diagram of the Kohleoel process [27]

Table 2-2 Comparison of major DCL technologies around the world [16, 28-30]

Process	Capacity (t/d)	Temperature(°C)	Pressure(atm)	Catalyst
EDS	250	425-450	175	-
H-Coal	200	435-465	200	Co-Mo/Al2O3
SRC I	6	440	120	-
SRC II	50	460	130	-
NEDOL	150	435-465	200	Fe-based
Kohleoel	200	470	300	Fe-based
Shenhua I	6	455	190	Fe-based
Shenhua II	3000	455	190	Fe-based

2.6 Comparison of DCL and ICL

It is believed that DCL is more efficient than ICL, because it works at lower temperature regime.

- Thermal efficiency of DCL is estimated around (70-75) and for ICL approximately (40-50).

-DCL typically produces high-octane and low sulfur gasoline and also has high heating value fuel mostly due to dominance of aromatic compounds. ICL generally produces straight chain hydrocarbon which leads to have high quality Diesel.

- DCL converts directly solid coal into liquid fuels without any intermediate but ICL process requires gasification step to produce syngas in order to convert it to liquid products.

-DCL can be done in absence of catalyst while ICL requires catalyst for Fischer-Tropsch reaction. Table 2.3 compares products from DCL and ICL processes.

Table 2-3: Typical properties of DCL and ICL final products [4]

	DCL	ICL
Distillable product	65% diesel, 35%naphta	80% diesel, 20%naphta
Diesel cetane number	42-47	70-75
Diesel sulphur content	<5 ppm	<1 ppm
Diesel aromatics	4.8%	<4%
Diesel specific gravity	0.865	0.78
Naphta octane number	>100	45-75
Naphta sulphur	<0.5 ppm	-
Naphta specific gravity	0.764	0.673

2.7 Liquefaction Solvents

In the direct coal liquefaction processes, the main duty of the solvent is to stabilize the free-radicals by donating hydrogen, improve the cracking of coal macromolecules, and prevent formation of the retrograde reaction by diluting the intermediates. Furthermore, the solvent in a DCL process can facilitate the mass and heat transfer of reactions, and it carries hydrogen by shuttling hydrogen from the hydrogen gas phase to the coal matrix [31]. It is necessary to consider the temperature at which extractions are carried out. Oele and others defined four different types of solvents based on their effects on coal: non-specific solvents, specific solvents, degrading solvents, and reactive solvents. Specific and reactive solvents are of interest to direct liquefaction [32].

(1) Nonspecific solvents: These solvent can extract only a small part (~ 10%) of coal at temperatures up to 100°C. These solvents have low boiling range such as methanol, ethanol, benzene, and acetone and are not suitable for high temperature liquefaction.

(2) Specific solvents: Specific solvents such as N-methylpyrolidone (NMP) and pyridine used at lower temperatures. They can extract about 20-40% of coal at temperatures below 200°C.

(3) Degrading solvents: Degrading solvents, such as anthracene oil and phenanthridine can extract coal up to 90% at temperatures up to 400°C. Polymerization of coal may happen with these solvents which requires large amount of hydrogen to stabilize free radicals.

(4) Reactive solvents: reactive solvents such as tetralin (1, 2, 3, 4-tetrahydronaphthalene) are important when extraction is carried out at higher temperatures. Reactive solvents are generally good hydrogen donors. Tetralin will be converted to naphthalene after donation of its four hydrogen atoms. Hydrogen donor ability is important when reaction takes place at high temperatures Hydrogen donor solvents play an important role in suppressing the retrogressive reactions at this stage by capping free radicals and preventing recombination reactions.

This is the common solvent used in high temperature direct liquefaction reactions. The solvent reacts with coal by donating hydrogen to the free radicals that are formed. For liquefaction process a solvent with high hydrogen donor ability is required to obtain high extraction yields.

2.8   Chemistry of coal liquefaction

An understanding of the chemistry of coal liquefaction is essential in order to find proper kinetic model. Coal liquefaction is the cracking of macromolecule structures into smaller hydrocarbon molecules which are distillable. During the liquefaction process coal can undergo a complex sequence of physical and chemical processes as it is liquefied and hydrogenated. During the liquefaction the bridge linkages are cleaved when coal heated to

350-400 °C .At low temperatures ether bonds are ruptured and at high temperature dissolution includes methyl group cleavage [33]. Coal is a complex heterogeneous substance composed of several hydrocarbons molecules with different physical properties. Coal dissolution is governed by the extraction of these components which is temperature dependent. Chemical dissolution plays an important role in liquefaction process .During dissolution at high temperatures over 350°C chemical interactions between coal and solvent become more important. The extraction of coal with hydrogen donor solvent at elevated temperatures is of particular importance as a technological method. At high temperatures chemical dissolution is dominant. Some macromolecules in the coal matrix are enough strong to cleave physically due to its high molecular weight and can be cleaved via thermal decomposition to produce molecules with lower molecular weight [34].At this region free radicals are formed due to thermal decomposition of bond linkages which can be capped by the abstraction of hydrogen atom from the donor molecule leading to formation of products with low molecular weight that can be dissolved in the solvent. If hydrogen is not sufficient for capping the radical, recombination of free radicals occur which leads to form stable high molecular weight products that are not desirable in liquefaction processes [18-20].

2.9   Free radicals in coal liquefaction

Free radicals are now believed to play a major role in liquefaction processes. It is widely accepted that coal liquefaction involves free radicals as the key reactive intermediates. This view is supported by general observation that free radical reactions control the pyrolysis chemistry of organic substances. The aromatic units in the coal structure presumed to be dominant in coal and found to be reactive toward free radicals. General kinetic features of coal liquefaction have also been used to support this view. However, because of the chemical

complexity of coal, kinetic properties of these radicals cannot be directly obtained from experiments on coal itself [6, 36].

Curran and others were first to describe the general mechanism of coal liquefaction as a free radical. They proposed that the transfer of hydrogen to coal from a solvent follows a free radical mechanism in which coal is thermally decomposed into free radicals subsequently stabilized by abstraction of hydrogen. When coal heated, covalent bonds are cleaved and additional free radicals are formed. The extent of conversion depends on how the radicals are stabilized [38]. If hydrogen is available liquefaction yields will be high, but if there is insufficient hydrogen, radicals will repolymerize and problems such as reactor coking as well as low liquefaction yields result [39]. Wiser concluded that the thermally induced rupture of a covalent bond would leave an unpaired electron on the fragment on either side of the bond; two free radicals are formed Since free radicals are unstable and highly reactive they would seek stabilization (see Figure 2-10). These free radicals are capped in one of three ways: (1) addition of atoms (such as hydrogen) or other radical groups to the free radicals, (2) rearrangement of atoms within the free radical, and (3) polymerization of the free radicals [40]. The first method of capping the free radical is the desired method when performing coal liquefaction with a hydrogen donor solvent. This allows the large coal molecules to be thermally degraded, capped with hydrogen, and stabilized as smaller, more soluble and hydrogen-rich species. These species would typically have a molecular weight ranging from 300 to 1000.The second and third methods occur when there is not a hydrogen donor solvent available. If the free radical species contains an unstable structure such as a hydroaromatic unit, the free radical species could cap itself. Finally, if the free radical species is stable and in the presence of other free radical species, polymerization or retrograde reactions could

take place. This is the basis for the formation of coke (char), and other large and insoluble molecular weight species. Therefore, for the formation of low molecular-weight carbon-product precursors, the first method is preferred [41].
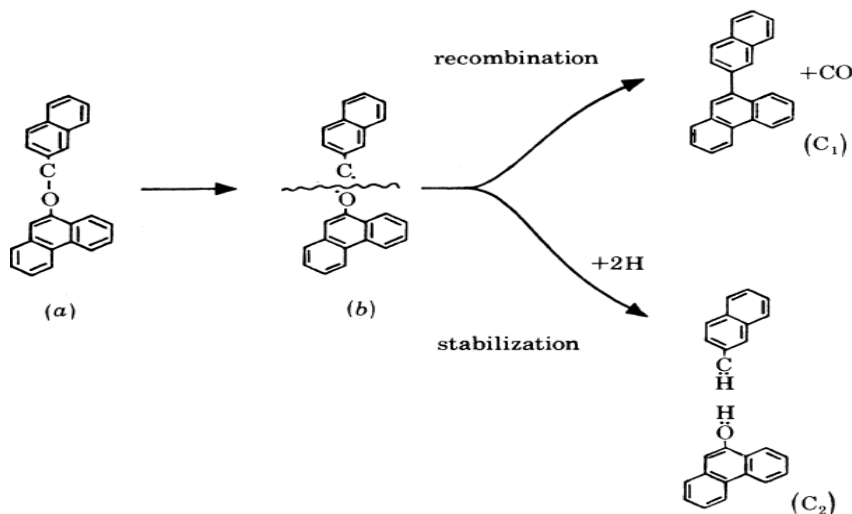
Figure 2–9: Effect of hydrogen on the fate of thermally formed free radicals [40]

Thermal direct coal liquefaction is viewed to occur primarily through a free-radical mechanism of initiation-propagation-termination. The initiation step is a thermal decomposition of the coal molecule, in which the free radicals are formed.

In this case, C-O and bonds such as ether hydroxyl group are the first to rupture due to their lower bond dissociation energies. Propagation reactions included hydrogen abstraction, β-scission, and radical addition reactions. This implies for hydrogen shuttling, retrograde type adduction of radicals back to the rigid phase, and thermal degradation of the solid coal [32, 35]. Termination reactions included radical recombination and disproportionation reactions. Radical recombination reactions are responsible for additional retrograde reactions through solvent such as tetralin and mobile phase molecule adduction to the unconverted coal matrix. At this stage, free radicals are stabilized by abstraction of a hydrogen atom from the

donor solvent. If hydrogen atoms are not enough, repolymerization of the free radical may take place and products with high molecular weight will be obtained [42].

2.10 Effect of coal properties on DCL

In order to characterize the coal, two analysis can be carried out, the proximate and the ultimate analysis.

2.10.1 Proximate analysis

The proximate analysis gives information about moisture content, volatile matter, ash and fixed carbon. This method is the simplest and most conventional technique to evaluate the coal sample.

(1) Moisture: Moisture is an important property of coal sample as most of coals are mined with high moisture content specially lignite coals. High moisture content of the coal can be detrimental for coal liquefaction as it can reduce thermal efficiency and hydrogen partial pressure thus it is recommended to dry the coal under vacuum condition prior to liquefaction [43].

(2) Volatile matter: Volatile matter in coals indicates the components of coal except moisture when coal is heated at high temperature around 950°C in the absence of oxygen. The volatile matters do not pre-exist in the coal structure and are formed by thermal decomposition of some weak bonds in the coal matrix which generates some gases such as hydrogen, carbon monoxide, methane, carbon dioxide and light hydrocarbons [44]. Generally, coals with high volatile matters content are suitable feedstock for coal liquefaction.

(3) Ash: Ash content of the coal is the noncombustible residue left after burning the coal. It is produced as a result of oxidation of mineral matter present in the coal structure. It

26

can also give information about quality of coal sample [45]. Ash content of coal reflects the coal quality. Low ash content coal is preferred for coal liquefaction as it is impurities in coal structure.

(4) Fixed carbon: The fixed carbon represents the carbon content of the coal which is left after volatile matter .There is difference between fixed carbon and carbon in ultimate analysis as some carbon is evolved to form volatile matter. Ultimate carbon is the total carbon content of the coal includes carbon present in volatile matter. Fixed carbon is useful to know how much coke can be produces in coking process.

2.10.2 Ultimate analysis

The ultimate analysis gives information about the elemental composition of the coal, carbon, hydrogen, nitrogen, sulfur and oxygen. The ultimate analysis is a helpful technique to find higher heating value of coal sample. The oxygen content is traditionally determined by subtraction of other elements from 100%. Low rank coals are rich in hydrogen that is desirable for the DCL process.

2.10.3 Petrographic analysis

The progress of coal liquefaction not only depends on coal rank but also depends on the petrographic composition of the coal. The petrographic composition refers to the components of coal that go into the process of making coal. Even the same type of coal can be different dependent on its petrographical history. Macerals can be divided in three groups: vitrinite, liptinites (exinite) and inertinite. Each type of maceral has a different behavior during coal liquefaction process. Generally, coal with high liptinites and low inertinites contain is desirable for coal liquefaction process. Maceral composition in coal plays an important role on DCL process [9, 173].

Chapter 3

Experimental Procedures and Techniques

The main purpose of this work was to develop a kinetic model for direct coal liquefaction of coal under isothermal condition and find optimal conditions for this process. Some of the results of this chapter were published as a journal paper. The parent coal used in this work was a lignite coal supplied by Sheritt Company. A brief description of this work is shown in Figure 3.1.

1. Sample Selection
(Lignite coals No.1 and
No.2)

No.1

No.2

2. Sample Characterization
2.1 Proximate and ultimate
analysis
2.2 Thermal decomposition
behavior (TGA)
2.3 XRD analysis

3. Results
3.1 No2 had better
properties in volatile
and ash content
3.2 E1<E2

Sample No.1 ✓

**4. Grinding and Drying the
sample (-45-1000µm)**
- Appropriate size rang for coal
liquefaction experiments

Eight different
particle size

150-212µm

5. Perform kinetic experiments
To obtain coal liquefaction products
(Preasphaltene, Asphaltene, Oil and Gas

Operation condition (Isothermal)
$T=350^{\circ}C-375^{\circ}C-400^{\circ}C-450^{\circ}C$
P (initial) =60 atm (N$_2$)
t= 15-120 min
Solvent=Tetralin

6. Propose different reaction networks
(Based on various reaction products)

7. Optimize kinetic constants with genetic

8. Solve differential equation to obtain product yields at different time-Temperature history

Figure 3–1: A brief overview of experimental procedures and techniques

It has been long recognized that calculating kinetic data in a massive reactor implies the problem of inaccurate reaction time due to long heat-up and cool-down times during which substantial reactions may happen. In this work, this problem was overcome by using a Micro reactor to minimize these experimental variations.

3.1   Coal and solvent preparation

It is estimated that approximately half of the coal resources of the world are low rank coal, such as lignite and sub-bituminous coal [46]. Lignite coal is abundant in Canada and plays an important role in energy production. Low rank coals like lignite coal have less aromaticity and readily liquefied under mild operation condition. Reactivity of these coals is high because of high volatile matter content and also contains fewer impurities such as Sulphur and heavy metal. It was thus chosen as the experimental sample in the present study.

Two different types of lignite coal were chosen for characterization. The bulk coal samples was crushed by means of a jaw crusher and ground in a ball mill and blended to homogenize the coal and reduce the particle size to 60 mesh (-250 μm) to characterize those samples. The representative samples were taken for proximate analysis according to the ASTM D7582 by Macro Thermogravimetric Analyzer and ultimate analysis according to ASTM D3176 in Elemental Vario MICRO Cube.

The results of the proximate and ultimate analysis (CHNS) as well as physical properties of sample used are presented in Table 3.1 and 3.2 Higher heating value of coal was also calculated with Channiwala and Parikh formula [47].

$$HHV = 0.3491C + 1.1783H + 0.1005S - 0.1034O - 0.0151N - 0.0211A \ (MJ \ kg^{-1}) \qquad (3.1)$$

Where *C*, *H*, *S*, *O*, *N*, and *A* are the mass fractions of carbon, hydrogen, sulfur, oxygen, nitrogen, and ash, respectively.

Table 3-1: Characteristic of the coal sample No.1

Proximate analysis	Mass (%)	Ultimate analysis	Mass(% daf)
Moisture	21.4	C	44.63
Volatile Matter	35.85	H	4.68
Ash	18.28	N	0.66
Fixed carbon	24.47	S	0.57
		O*	49.46
		HHV/MJkg^{-1}	15.64

*obtained by difference

Table 3-2: Characteristic of the coal sample No.2

Proximate analysis	Mass (%)	Ultimate analysis	Mass(% daf)
Moisture	25.08	C	43.97
Volatile Matter	31.47	H	3.87
Ash	20.17	N	0.48
Fixed carbon	23.28	S	0.63
		O*	51.05
		HHV/MJkg^{-1}	14.18

* obtained by difference

Solvent plays an important role in coal liquefaction process. The main duty of the solvent is donating hydrogen, improve the cracking of coal macromolecules, and prevent formation of the retrograde reaction by diluting the intermediates. The donor ability of a solvent mainly depends on structure and functional groups present in the solvent. Reactive solvents such as tetralin are generally good hydrogen donors.

Tetralin (1, 2, 3, 4-tetrahydronaphthalene) has been extensively used in coal liquefaction studies making comparison with published results more reliable. However, the using of pure solvents for industry is not economical (long time and energy needed to recovery of solvents) for industry applications but instead coal derived solvent is used in large scales. This solvent

is broadly used in the coal liquefaction studies and believed a good hydrogen donor solvent [2, 6, 17, 43, 48-50]. It was thus selected as the liquefaction solvent in the present study.

3.2   Effect of drying on coal conversion

Especially for the lignite coals which contain high amount of moisture pretreatment by drying can develop coal liquefaction conversion. High moisture and oxygen content of the low rank coals are the main drawbacks and lead to several disadvantages such as increasing the transportation cost, decreasing the thermal efficiency of the plant, increasing the GHG emission, and causes some problems during milling and coal handling including storage therefore it is considered an economic necessity to dry these coals prior to liquefaction.

The coal used in this experiment was a lignite coal containing 25% of moisture was provided by Sherritt Technologies department. The coal was dried under vacuum, air and nitrogen atmosphere at different drying times to study the effect of drying on the coal liquefaction experiments. Experiments were carried out in a 0.5 L stirred autoclave for 1 h, at 12 MPa and 415°C with a coal –derived solvent under hydrogen atmosphere. Drying of coal had significant effect on the coal liquefaction conversion. Vacuum dried and nitrogen dried samples provided higher conversion than air dried samples. The air drying gave somewhat lower conversion, which may be as a result of oxidation. Drying in air seems to increase oxidation to form more oxygen functional groups which enhances the cross-linking reactions in the initial stages of liquefaction. Both drying times and temperatures appear to be important variables which affected coal liquefaction conversion. The hydro-treated solvent HT-1007 was heavy hydrocarbon products and was also provided by Sherritt Technologies department. A 0.5L autoclave reactor (Figure3-2) was loaded with 50g of coal sample and 105g of solvent. The reactor was first purged with 10 bars of N2 gas for three times to

minimize the amount of O2 gas in the system. 40 bars of H2 gas is then purged into the system. The process took about 2 hours for reaching up to 415 °C and stay at the same temperature for 1 hour. The system then is cooled down to 100 0C within 1 hour. The system pressure was adjusted during the extraction process by venting the reactor to a specific pressure prescribed in the project, outlined by Sherritt Technologies. Once the reactor is cooled down to 100 ^{0}C, the pressurized gases are then released into the fume hood. Afterward, the reactor is cleaned using THF. All of the solution collected including THF and liquid product is then filtrated through a 0.5 μm filter paper using a vacuum pump. The solids collected are the unconverted coal. The liquid portion is then putting through rotary evaporator system to recover THF. The Moisture and Ash Analyses were conducted at two periods: beginning of the experiments and after the experiments. At the beginning of the experiments, the moisture and ash analyses are conducted on coal samples to determine Dry Ash Free (DAF) coal amount that being used in each run and to determine whether the samples are dried properly. After the experiments, the Ash Analysis is conducted on the unconverted coal to determine its ash content to determine whether the experiment is done properly without losing large amount of materials while venting. Figure 3-3 represents the time –temperature history of experiment.
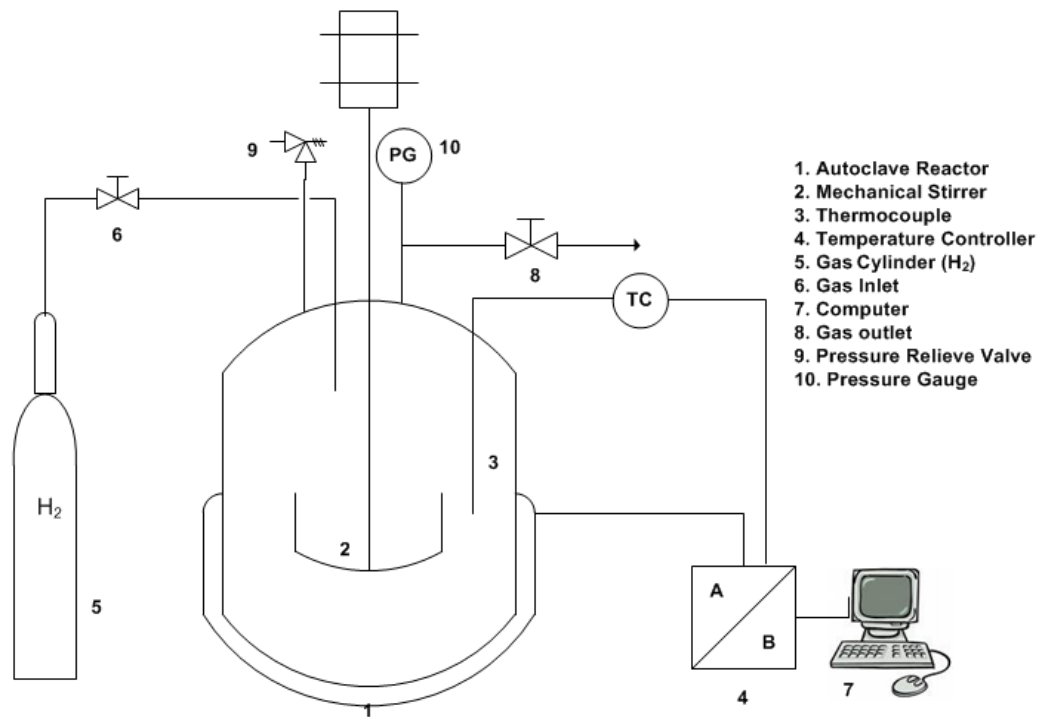
Figure 3–2: Schematic diagram of experimental setup

Key:

1. Autoclave Reactor
2. Mechanical Stirrer
3. Thermocouple
4. Temperature Controller
5. Gas Cylinder (H_2)
6. Gas Inlet
7. Computer
8. Gas outlet
9. Pressure Relieve Valve
10. Pressure Gauge
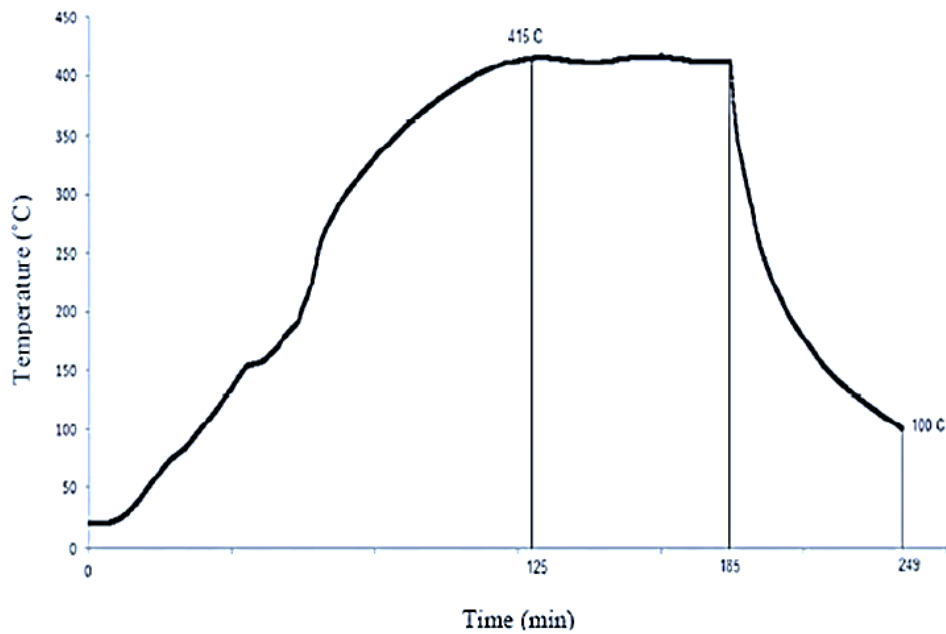
Figure 3–3: Typical time-temperature profile for coal liquefaction
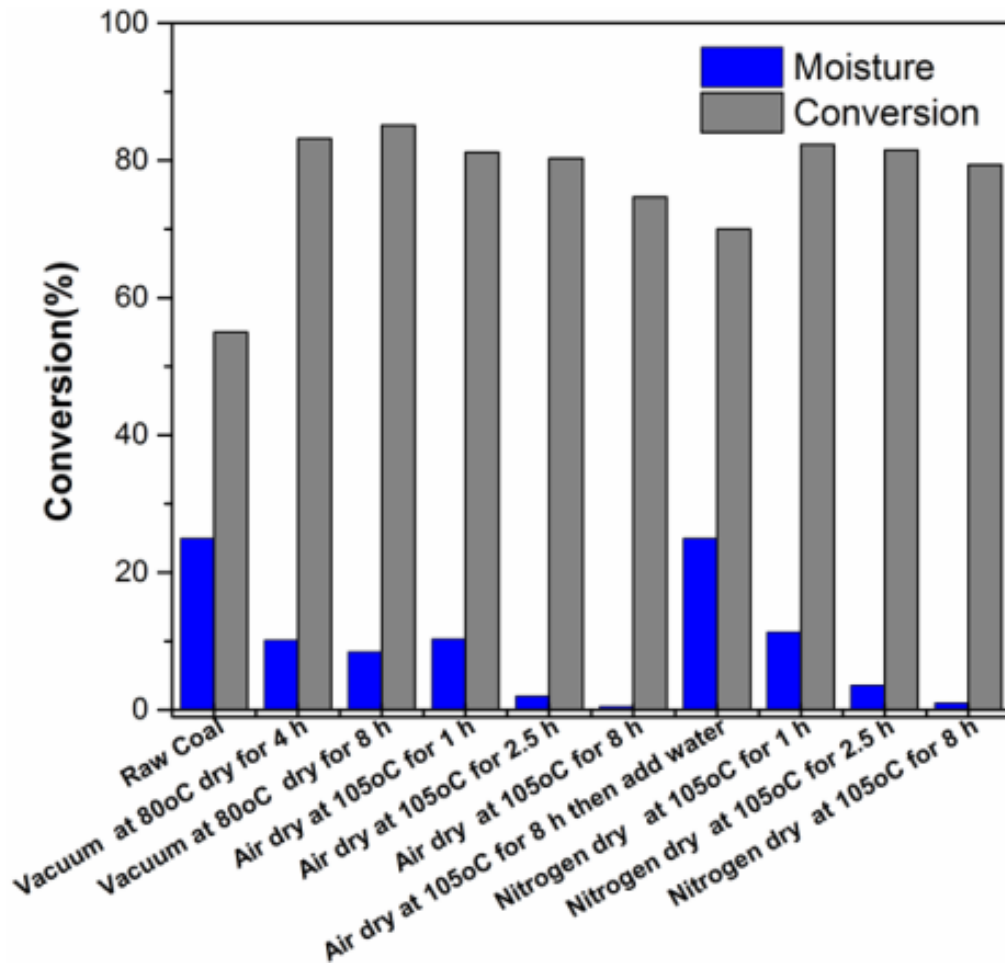
Figure 3–4: Coal liquefaction conversion versus different drying methods

Among three thermal drying methods, vacuum dry had highest conversion. However, this method is not economical for industry scale and useful for lab scale. It was observed that coal sample with lower moisture content showed higher conversion. Especially for the low rank coals, pretreatment by drying can improve the liquid yields. The storage condition of coal is essential as the coal after dried tends to adsorb moisture quickly regardless of being drying under different conditions. Removal of water from the coal prior to liquefaction reduces the cost of both separating water from the coal and wastewater treatment. Drying at air has detrimental effects on the coal conversion because significantly increase oxygen

functionality which enhances the cross-linking reactions in the coal liquefaction experiment. High moisture and oxygen content lead to several disadvantages such as increasing the transportation cost, decreasing the efficiency of the plant, increasing the GHG emission [126-128].

3.3 Kinetic study and thermal behavior of coal samples

3.3.1 Thermal behavior of samples

In large scale processes of coal conversion to valuable products through thermal treatment, determination of the kinetic parameters in the decomposition stage is one of the key problems. Many unresolved problems face a designer of coal combustors and gasifiers, including the complex physical and chemical behavior of coal and the uncertainty regarding the kinetics of the chemical reactions during thermal decomposition [51]. The design of processes for pulverized coal requires that the various stages occurring during the thermal decomposition be understood in order to provide optimum operating conditions. This greater emphasis on more efficient utilization of coal combined with its chemical complexity raises the need for a better understanding of the pyrolysis process. Pyrolysis is the method for obtaining liquid from coal by rejecting carbon and thereby increasing the hydrogen-to-carbon ratio of raw coal. Pyrolysis takes place as coal is treated at elevated temperatures in the absence of oxygen and during this pyrolysis a series of reactions occurs. This is done in the absence of oxygen, so that undesirable combustion reactions cannot take place .The main products of pyrolysis are gas, tar and char.

Pyrolysis kinetics of coal is important because it is the initial step of main coal conversion processes such as liquefaction, gasification and combustion in which coal particles undergo major physical and chemical transformations. It is customary to use a

thermogravimetric analyzer (TGA) to investigate of thermal behavior of coal sample during decomposition under inert atmosphere. For a better understanding of pyrolysis, several researchers investigated thermal decomposition of coal by thermogravimetric analysis (TGA). As coal has been used as a fuel since the beginning of industrial development, it has been among the earliest materials to be subjected to thermal analysis. To investigate the kinetics of the decomposition process, TGA is often used. In TGA, the weight change of the sample is observed as it is heated, usually at a constant heating rate under a controlled atmosphere such as nitrogen, air or other gases.

The record of weight loss with respect to the time or temperature is termed a thermogravimetric (TG) thermogram. When the rate of weight loss (the first derivative with respect to time) is recorded as a function of time or temperature, it is called a differential thermogravimetric (DTG) thermogram. The DTG has been used to study the kinetics of thermal decomposition reactions of a variety of solids, including coal. Much of this work is based on the assumption that thermal decomposition is describable by an overall first order reaction and follows the Arrhenius-type equation. The kinetics of the thermal behavior of a material can be determined by the application of a kinetic model to the rates of mass degradation. The main advantages of TGA for the study of coal pyrolysis are simplicity in implementation and utilization as well as good repeatability [52].

A large number of studies have reported on thermogravimetric and differential thermal analysis in attempts to explain kinetics of thermal decomposition of coal and to obtain qualitative information on coal pyrolysis. Literature reviews on these subjects regarding thermal analysis are present from Howard [53], Lawson [54], Anthony et al. [55], and Kirov and Stephens. Main differences in the thermobalances used for the studies of Honda (1915),

Guichard (1926), Vallet (1932), Rigollet (1934), Dubois (1935),Longechambon (1936) and Jouin (1947) were mentioned by Kirov and Stephens [56]. These thermobalances recorded mass versus temperature or time.

Van Heerdan and Huntjens studied the rates of decomposition of Dutch coals on a thermobalance that recorded mass loss data continuously over the temperature range 200-550 °C. A mathematical equation in the form of the Arrhenius equation was considered to explain the rate of coal decomposition. They concluded that the decomposition process is first order with regard to the fraction of unreacted coal. They observed that initial devolatilization is fast removal of moisture and oxides of carbon, the middle devolatilization is slow and contains of the removal of the major volatile matter from coal, and the final devolatilization is a slow process for liberating the gas from residuals.

Scaccia et al. investigated the pyrolysis of low-rank Sulcis coal by thermogravimetric techniques (TG/DTG) in the temperature range ambient to 1000°C at three different heating rates. From thermogravimetric results it was established that coal pyrolysis involved three main stages: water evaporation; devolatilization of thermally labile and more stable volatiles; and char formation [57].

The knowledge of kinetic parameters is essential for modeling the reactor and optimization of the process conditions. There are various methods for evaluating kinetic parameters from non-isothermal thermogravimetric analysis (TGA)and the most common of them can be classified into two major types: model-fitting and model-free [57-60].

In the model fitting method, different models are fit to the experimental data and the model giving the best statistical fit is selected as the model from which the activation energy (Ea) and frequency factor (A) are evaluated. Historically, model-fitting methods were

broadly used because of their ability to directly calculate the kinetic parameters from the thermogravimetric analysis results. However, these methods have several drawbacks, the most important being their inability to uniquely select the appropriate reaction model [61]. Furthermore, comparing the results of these models in the literature can be difficult especially for non-isothermal data since a wide range of kinetic parameters have been determined for the coal pyrolysis process. This led to the decline of these methods in favor of isoconversional (model-free) methods which can estimate the activation energy without evaluating the reaction model [61].

The greatest advantages of this model are its simplicity and avoidance of errors related to selecting specific reaction models. Isoconversional method is called model-free method because of its ability to determine the activation energy for different constant extents of conversion without considering any particular form of the reaction model. These methods require several kinetic curves to perform the analysis and thus are sometimes called multi-curve methods [62].These methods can calculate the activation energy at different heating rates on the same value of conversion.

The terms "model-free" and "isoconversional" are sometimes used interchangeably; however, not all model-free methods are isoconversional. For example, the Kissinger method is a model-free method but is not isoconversional because it does not calculate activation energy at different constant extents of conversion but instead assumes constant activation energy [61].

Isoconversional methods are helpful tools for the analysis of solid-state kinetics. Theoretically, they include many benefits and applications. However, practically, they have some disadvantages especially regarding reproducibility when performing a series of runs at

different heating rates which their fluctuation may enhance experimental errors. Thus, for non-isothermal experiments, each run must be conducted under the same experimental conditions (sample weight, purge gas rate, sample size) so the only variable is the heating rate. In order to obtain accurate results with high resolution curves low ranges of heating rates can be considered for the experiments.

Numerous recent studies on the TGA pyrolysis of coal [62-65] and coal–biomass blends [66-68] are available in the literature and most of them are based on model fitting techniques. There are a few reports relating to thermal decomposition behavior of coal based on model free techniques [57]. Moreover, most of the previous studies have been performed on coal-biomass blends in order to determine the kinetics of co-pyrolysis of coal and biomass mixtures. To the best of our knowledge, there is very little information regarding pyrolysis of coal itself based on model-free methods.

The aim of this section is to study the pyrolysis kinetics of Canadian lignite coal by means of thermogravimetric analysis (TGA) within the temperature range of 298-1173K at different heating rates under nitrogen atmosphere. The effect of the heating rate on decomposition will also be studied. In this study, different model free methods such as the Kissinger and the isoconversional methods of Ozawa, Kissinger-Akahira-Sunose and Friedman are employed and compared in order to analyze non-isothermal kinetic data and investigate thermal behavior of a Canadian lignite coal. The kinetic parameters of the coal decomposition process will also be determined. These results may provide helpful information for pyrolysis researchers to predict a kinetic model of coal pyrolysis and optimization of the process conditions.

3.4   Experimental method

The TGA experiments were performed using a thermogravimetric analyzer, TGA – SDT Q600 (Figure 3-5) at the coal research center of university of Alberta. About 10 mg of fine coal particle size (-150µm)was placed in a small Alumina crucible for each run and heated from 298 K to the maximum temperature of 1173 K at six different heating rates of 1, 6, 9, 12, 15 and 18 Kmin-1 respectively under nitrogen atmosphere with a flow rate of 100ml/min. During the heating, variation of the weight loss and its derivative with respect to the time and temperature was collected automatically by the instrument and determined through the TA universal analysis software. The experiments were repeated under identical conditions to check the reproducibility of the results.
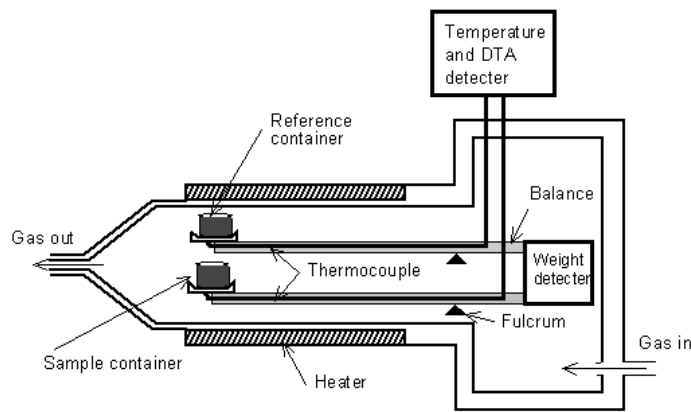
Figure 3−5: Thermogravimetric analyzer [174]

3.5   Kinetic analysis

There are a number of approaches for modelling the complex pyrolysis process. The simplest is the empirical model, which employs global kinetics, where the Arrhenius

expression is used to correlate the rates of mass loss with temperature. The pyrolysis process

of coal can be expressed by the following reaction:

$$\text{Coal} \xrightarrow{k} \text{Volatiles} + \text{Char} \tag{3.2}$$

The general expression for the decomposition of a solid sample is

$$\frac{dx}{dt} = k(T) f(x) \tag{3.3}$$

Where, x is the degree of conversion which represents the decomposed amount of the sample

at time t and is defined in terms of the change in mass of the sample

$$x = (m_i - m_t)/(m_i - m_f) \tag{3.4}$$

Where, m_i is the initial mass, m_f is the final mass, and m_t is the mass at time t of the sample

analyzed by TGA, f (x) is a function of x depending on the reaction mechanism; k(T) is the

rate constant at temperature T, which generally obeys the Arrhenius equation

$$k(T) = A\exp(^{-E_a}/_{RT}) \tag{3.5}$$

Where, A is the pre-exponential factor (min⁻¹), Equation is the activation energy (kJmol⁻¹), R

is the universal gas constant (J K⁻¹ mol⁻¹), and T is the absolute temperature (K).

Substitution of Equation (5) into Equation (3) gives the general expression to calculate the

kinetic parameters.

$$\frac{dx}{dt} = f(x)A\exp(^{-E_a}/_{RT}) \tag{3.6}$$

There are various possibilities to express the conversion function *f(x)* for the solid state

reactions. Most of the previous authors used the conversion function as follows

$$f(x) = (1 - x)^n \tag{3.7}$$

Where, n is the reaction order here is considered first order. Combining Equation (6) and (7),

the kinetic equation of decomposition is obtained as follows;

$$\frac{dx}{dt} = A\exp\left(^{-E_a}\big/_{RT}\right)(1-x)^n \tag{3.8}$$

Under non-isothermal conditions in which samples are heated at constant heating rates, the actual temperature under this condition can be expressed as

$$T = T_0 + \beta t \tag{3.9}$$

Where, T_0 is the initial temperature, β is the linear heating rate (°C/min.) and T is the temperature at time t. Non-isothermal methods are usually common in solid state Kinetics because require less experimental data in compare to isothermal methods. The following expression can be considered for non-isothermal experiments,

$$\frac{dx}{dT} = \frac{dx}{dt} \cdot \frac{dt}{dT} \tag{3.10}$$

Where, dx/dT is the non-isothermal reaction rate dx/dt is the isothermal reaction rate and dT/dt is the heating rate (β). Substituting Eq. (8) into Eq. (10) gives.

$$\frac{dx}{dT} = \frac{A}{B}\exp\left(^{-E_a}\big/_{RT}\right)(1-x)^n \tag{3.11}$$

Equation (11) represents the differential form of the non-isothermal rate law. In this study the data from non-isothermal experiments are considered to calculate kinetic parameters based on model free methods such as Kissinger and the iso-conversional methods of Ozawa, Kissinger-Akahira-Sunose and Friedman and compared in order to analyze and to investigate thermal behavior of a Canadian lignite coal.

3.6 Model-free methods

The kinetic analysis based on model free methods allows the kinetic parameters to be evaluated for different constant extents of conversion without evaluating any particular form of the reaction model. The temperature sensitivity of the reaction rate depends on the extent of conversion to products. This is partly a result of the heterogeneous nature of solid state reactions such as coal pyrolysis; It also arises somewhat because many solid state reactions follow complex mechanisms including multiple series and parallel stages with different activation energies. Model fitting methods are applied to extract a single set of Arrhenius parameters for an overall process and are not capable to show this type of complexity in the solid state reactions. Model free methods are able of addressing the aforementioned drawbacks of the model-fitting methods. The ability of model-free methods to show this type of reaction complexity is therefore a critical step toward the ability to explain mechanistic conclusions from kinetic data.

3.6.1 Kissinger method

According to Kissinger, the maximum reaction rate occurs with an increase in the reaction temperature [69]. The degree of conversion at the peak temperature of the DTG curve is a constant at different heating rates. Kissinger method is a model-free method but it is not iso-conversional method because it assumes constant activation energy with the progress of conversion. In the Kissinger's equation (eq. 12), T_m is representing the peak temperature, is expressed:

$$\ln\left(\frac{B}{T_m^2}\right) = \ln\left(\frac{AR}{E_a}\right) - \frac{E_a}{RT_m} \tag{3.12}$$

Therefore, kinetic parameters including activation energy (E_a) and pre-exponential factor (A) can be obtained from a plot of $\ln\left(\frac{B}{T_m^2}\right)$ versus $\frac{1000}{T_m}$ for a series of experiments at different heating rates.

3.6.2 Kissinger-Akahira-Sunose (KAS) method

The Kissinger–Akahira–Sunose (KAS) method was based on the following equation

$$\ln\left(\frac{B}{T^2}\right) = \ln\left(\frac{AR}{E_a g(x)}\right) - \frac{E_a}{RT} \tag{3.13}$$

Where g(x) is the integral conversion function (reaction model) which is reported in the literature [58]. For constant conversion a plot of left side of the above equation against $\frac{1000}{T}$ at different heating rates, is a straight line whose slope and intercept can evaluate the activation energy and pre-exponential factor respectively.

3.6.3 The Flynn–Wall–Ozawa (FWO) method

The Flynn–Wall–Ozawa (FWO) method is based on the following equation:

$$\ln(B) = \ln\left(\frac{AE_a}{Rg(x)}\right) - 5.331 - 1.052\,\frac{E_a}{RT} \tag{3.14}$$

Thus, for a constant conversion a plot of natural logarithm of heating rates, $\ln(B)$ versus $\frac{1000}{T}$ obtained from thermal curves recorded at different heating rates will be a straight line whose slope $\left(-1.052\frac{E_a}{RT}\right)$ will calculate the activation energy.

3.6.4 Friedman method

This method is one of the first iso-conversional methods. Using Equations (2) and (4) and taking the natural logarithm of each side, the expression proposed by Friedman can be presented as:

$$\ln\left(\frac{dx}{dt}\right) = \ln[Af(x)] - \frac{E_a}{RT} \tag{3.15}$$

The activation energy (E_a) is determined from the slope of the plot of $\ln\left(\frac{dx}{dt}\right)$ versus $\frac{1000}{T}$ at a constant conversion value.

3.7 Results and discussion

3.7.1 Thermal decomposition process

The coal samples were received wet with high moisture content over 25% and were dried in vacuum oven at 80 °C for 8 h to reduce its moisture content. The TG curves of the two Canadian lignite coals under nitrogen atmosphere are shown in Figure 3-6 and 3-7.
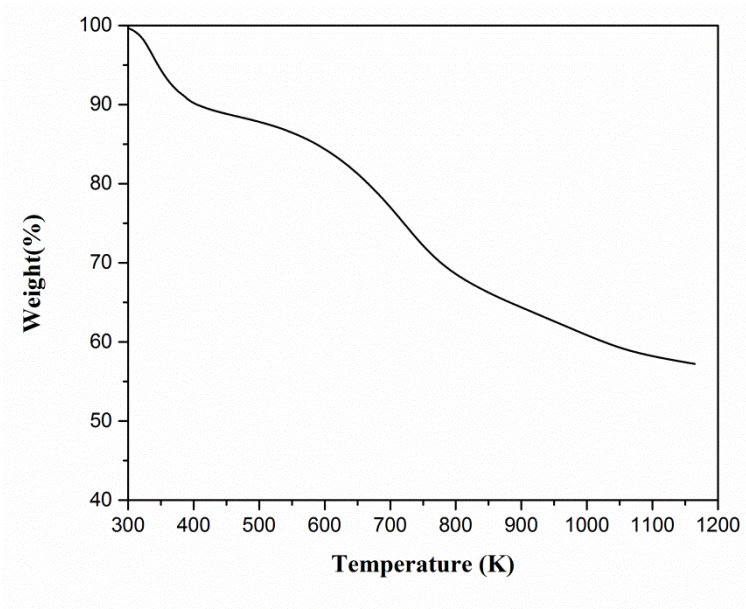
Figure 3–6: Thermal behavior of sample.1
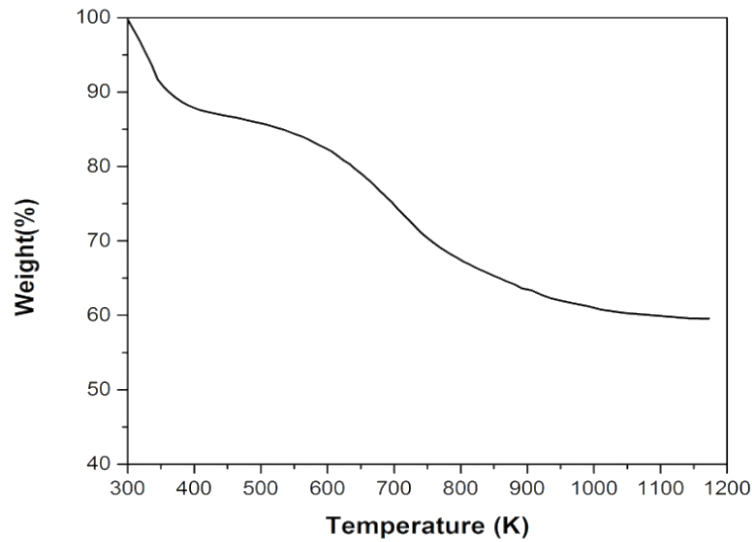
Figure 3–7: Thermal behavior of sample.2

The TG curves show the percentage mass loss of a coal sample over the range of temperature from 298 K to 1173 K. The rate of mass loss is temperature dependent: the higher the temperature, the larger the mass loss, because pyrolysis process proceeds slowly at low temperatures. As shown in these Figures, the devolatalization process launches at temperature about 450 K and proceeds fast with elevating the temperature up to 850 K and then the mass loss of the sample drops slowly to the ultimate temperature. These Figures exhibit three zones related to moisture evaporation, primary decomposition and secondary decomposition.

The first zone represents elimination of moisture which occurs below 450 K [70]. The second region is related to main decomposition stage in the temperature range 450-850 K for low heating rate and 925 K for high heating rate. At this stage most of the volatile components released which do not pre-exist in the coal structure and are formed by thermal cleavage some covalent bond such as ether bonds and methylene group in the coal matrix that form gases such as hydrogen, carbon monoxide and lighter hydrocarbons [71].

46

This region is the most significant region to examine since the major weight loss and complicated chemical reaction, such as release of tar and gaseous products and semi-coke formation take place in this temperature range [72,73]. The third zone that is the second pyrolysis stage where low decomposition rates observed can be attributed to the further gasification of the formed char due to high temperature effects. On the other hand, the coal sample contains high ash and the phase transitions of the inorganics found in the mineral matter, losses of the molecular water contents of the clay minerals and decomposition of carbonate minerals may contribute in weight loss of this step. There is only a small drop of mass observed at this stage.

In order to study a kinetic analysis via Isoconversional methods the experiments can be done at different heating rates. The results of TG and DTG curves of the pyrolysis of lignite coal (sample No.1) under nitrogen atmosphere were obtained at six different heating rates of 1, 6, 9, 12, 15, 18K min-1 are shown in Figure 3-8 and 3-9, respectively.
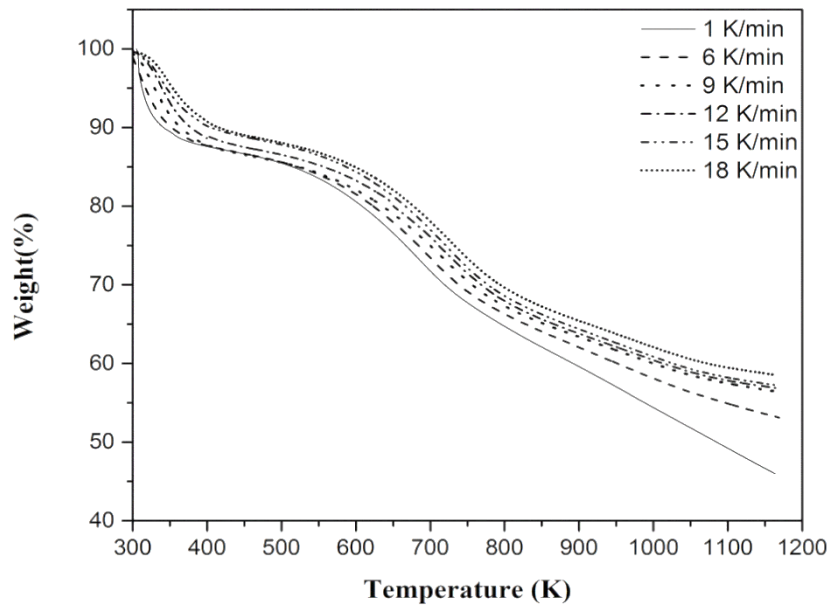
Figure 3–8: Thermal behavior of lignite coal (No.1)

at different heating rates under N2 atmosphere
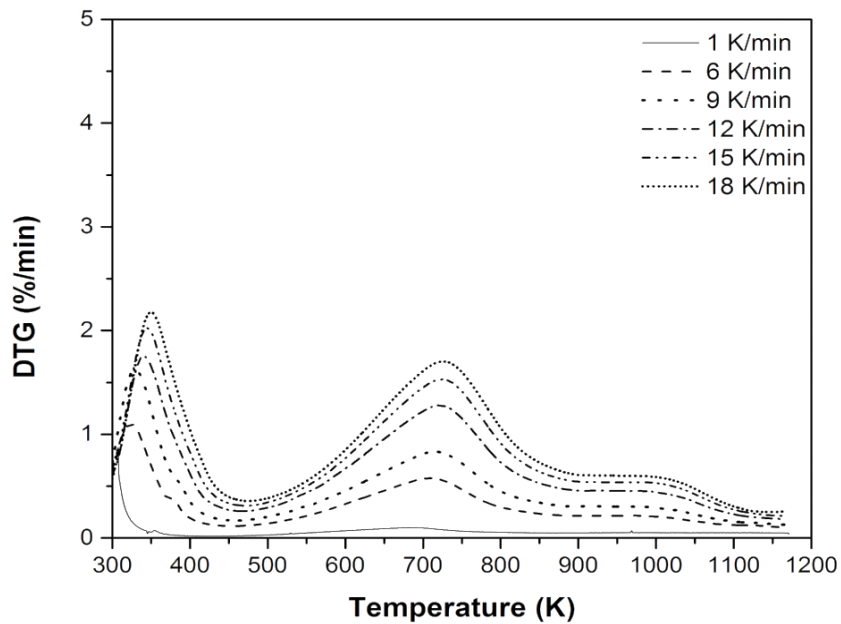
Figure 3–9 : DTG curves of Lignite coal (No.1)

at different heating rates under N_2 atmosphere.

The TGA data are normalized from 0 to 1 before analysis. The temperature at which the derivative of mass loss starts to increase is selected as the zero conversion point, and the temperature at which the mass derivative returned to the base line is chosen as end point. It is known that the heating rate affects all TGA curves and the maximum decomposition rate. When heating rate increases, the temperature of the maximum decomposition rate of the coal shifted toward higher temperature. Figure 3-10 shows conversion curves versus temperature at different heating rates. The curves showed typical sigmoid shape of kinetic curves. With increasing the heating rate, conversion values reached at higher temperatures, because at the same temperature and time a high heating rate has a short decomposition time and the temperature required for the sample to reach the same conversion will be higher. The heat transfer limitation (thermal lag) exists between furnace and sample temperature. It means that temperature in the particle can be a little lower than furnace temperature and gradient of temperature may exist in the coal sample so in order to reduce the thermal lag, the coal sample should be ground to the fine particle to increase the surface area of particle and consequently increase the heat transfer effect between the sample surface and the crucible as large as possible.
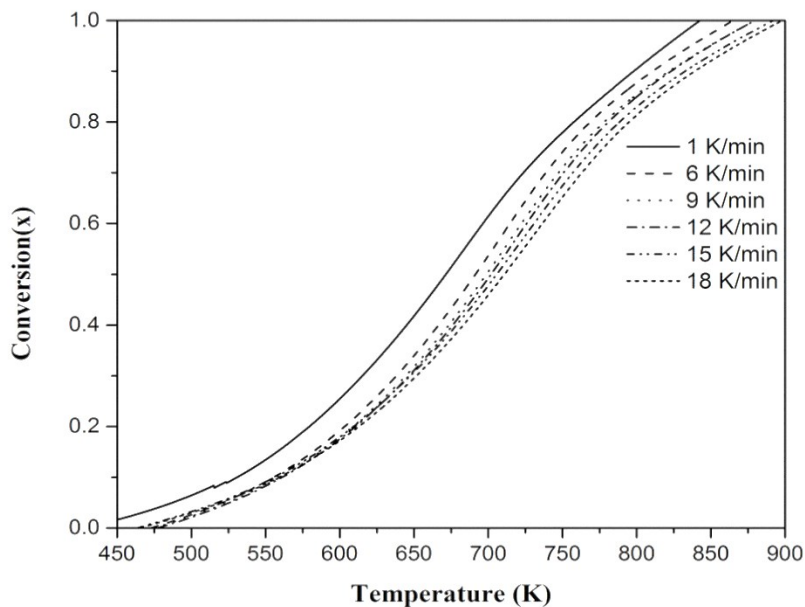
Figure 3–10: Conversion curves at different heating rates
for pyrolysis of lignite coal under N_2

3.7.2 Kinetic study results

The results of TG/DTG experimental data of coal pyrolysis obtained under non-isothermal condition under nitrogen atmosphere were used for kinetic analysis. Different model free methods such as Kissinger and the iso-conversional methods of Ozawa, Kissinger-Akahira-Sunose and Friedman are employed in order to obtain parameters like the activation energy and pre-exponential factor. In the Kissinger method the degree of conversion at the peak temperature (T_m) is a constant under different heating rates. The kinetic parameters using Kissinger method were found by linear regression line which is shown in Figure 3-11. The activation energy and pre-exponential factor were extracted from the slope and intercept are 281 kJmol^{-1} and 2.61×10^{17} min^{-1} respectively. The activation energy and pre-exponential factor were calculated as a function of conversion by using iso-

conversional methods of KAS, FWO and Friedman methods. The iso-conversional plots of these methods are shown in Figure 3-12 to Figure 3-14 respectively. Different range of conversion from 0.05-0.9 is considered for calculating the kinetic parameters based on iso-conversional method. The activation energies from the slope and pre-exponential factors from the intercept of three different iso-conversional methods were obtained and listed in Table 3.3. It can be observed from Table 3.3 that the values of activation energies are not similar at different constant extents of conversion, because most solid-state reactions are not simple one-step mechanism and follow a complex multi-step reaction. The thermogravimetric data analysis by iso-conversional technique may reveal complexity of the solid state reactions such as coal pyrolysis [74]. It means that in the pyrolysis process of coal the activation energy is a function of conversion. Figure 3-15 shows the dependence of the activation energy on extent of conversion.

The activation energy rises from about 130 kJ mol^{-1} at low conversion to approximately 350 kJ mol^{-1} at 75% conversion, and it subsequently drops to about 300 kJ mol^{-1} near the end of reaction.

The initial activation energy value was low due to cleavage of some weak bonds and elimination of volatile components from the coal matrix because at the beginning of the process all the strong bonds are not cleaved Therefore, more activation energy is required to decompose these stable molecules. With the progress of pyrolysis process the value of activation energy increased up to conversion of 75% with breaking of some strong covalent linkages. For higher conversion values above 75% the activation energy gradually decreases. The reason arises from the fact that during the decomposition process at high temperature with high conversion when most of the stable bonds are broken, less stable molecules which

51

are easier to break are present so less energy barrier is required for decomposition at this step and the value of activation energy decreases with progress of conversion.

The arithmetic means of the activation energy calculated by KAS, FWO and Friedman method are 282, 275, 283 kJ mol^{-1}, respectively, which are close to average activation energy obtained from the Kissinger method(281.03 kJ mol^{-1}). The results obtained with KAS and Friedman methods are very close and in good agreement [75]. The kinetic data obtained for pyrolysis of coal are found to agree closely with some of the literature data. However, the differences observed in the literature data can be attributed to the fact that the pyrolysis characteristics of coal highly depend on the properties of the coal which in turn differs based on origin of the coal [72-73].

The KAS and FWO methods were originally derived with constant activation energies so the errors associated with kinetic measurements from methods should be dependent on the variation of the activation energy with respect to conversion. This error does not appear in the Friedman method. Another advantage that can be attributed to Friedman method is that the activation energies obtained by the Friedman method are independent of the range of heating rates which can decrease the systematic error in evaluating the activation energy values. Thus, Friedman method can be considered to be the best among the four model free methods in order to evaluate kinetic parameters for solid-state reactions [76,77].
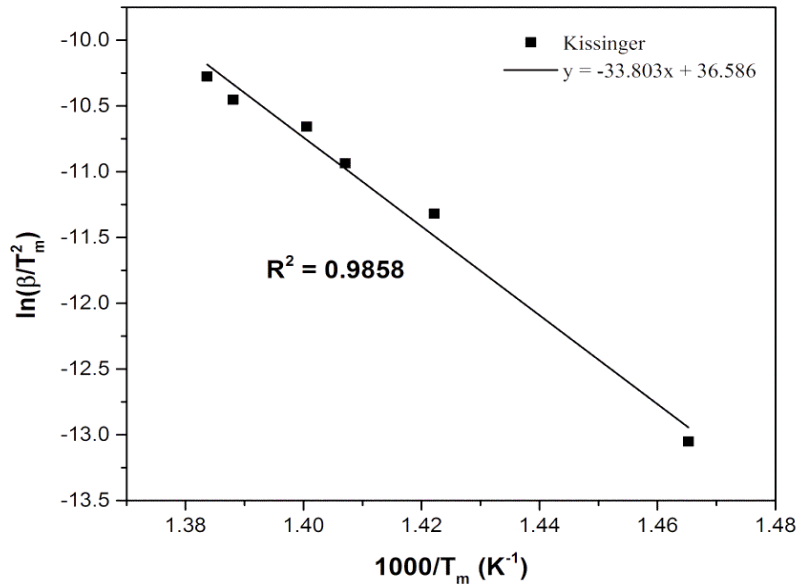
Figure 3–11: Kissinger plot of lignite coal pyrolysis at different heating rates
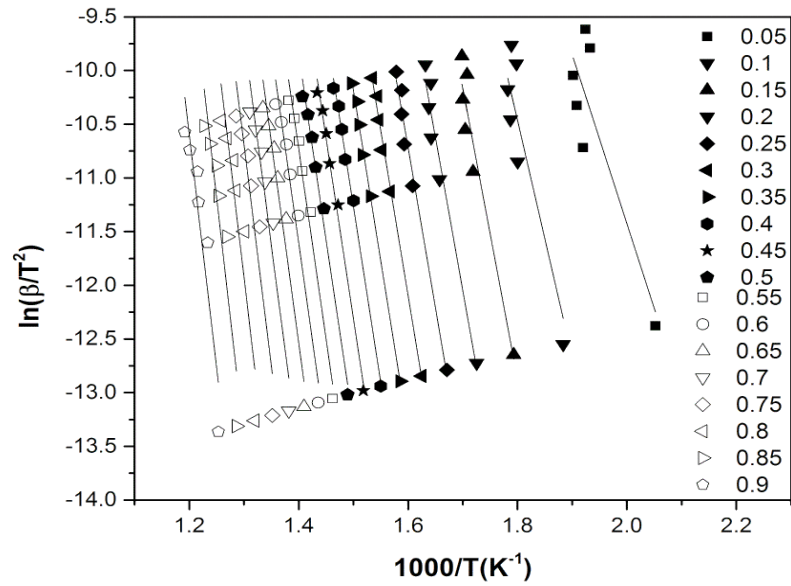
Figure 3–12: KAS plots of lignite coal pyrolysis at different values of conversion
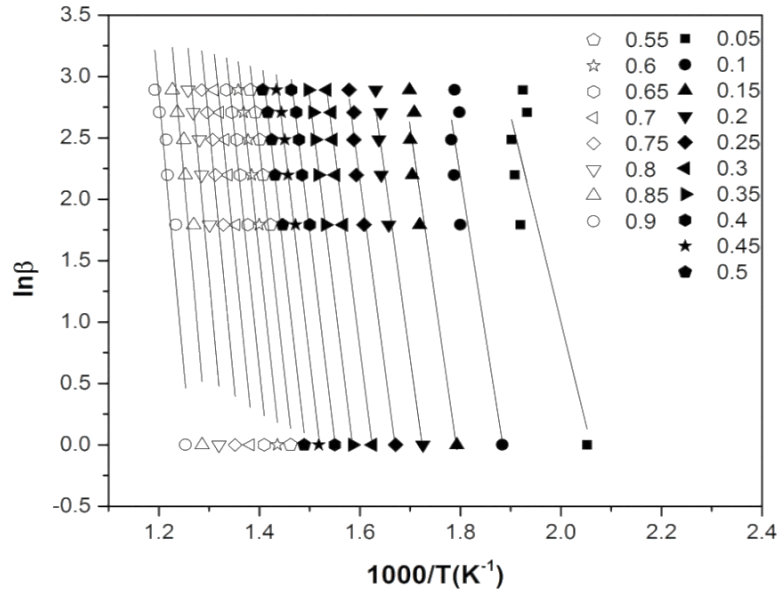
Figure 3−13: FWO plots of lignite coal pyrolysis at different values of conversion
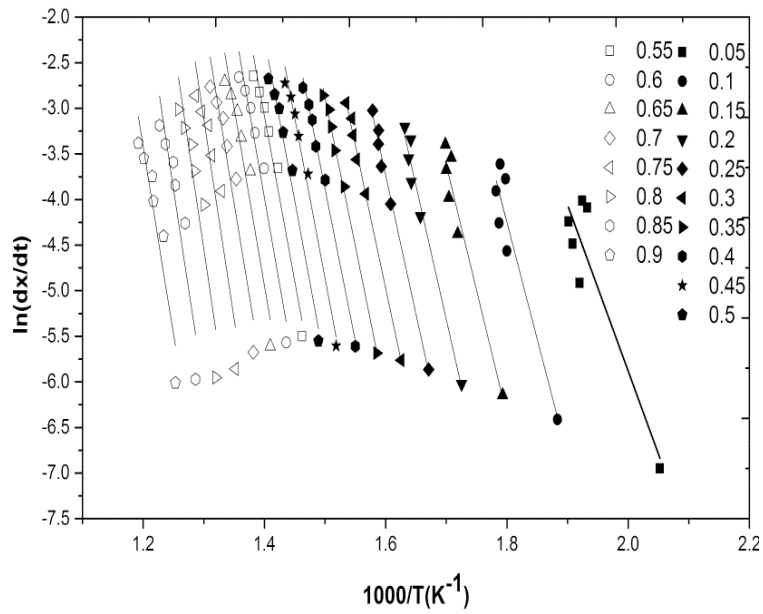
Figure 3−14: Friedman plots of lignite coal pyrolysis at different values of conversion

Table 3-3: kinetic parameters for lignite coal by different isoconversional methods

x	Friedman		KAS		FWO	
	$E_{a\,(KJmol^{-1})}$	$A(min^{-1})$	$E_{a\,(kJmol^{-1})}$	$A(min^{-1})$	$E_{a\,(kJmol^{-1})}$	$A(min^{-1})$
0.05	126.65	$2.02.10^{13}$	155.76	$4.86.10^{08}$	132.33	$1.00.10^{15}$
0.1	213.44	$1.85.10^{18}$	206.81	$2.10.10^{15}$	205.19	$1.95.10^{21}$
0.15	228.44	$6.06.10^{18}$	225.84	$1.92.10^{16}$	223.71	$1.24.10^{22}$
0.2	244.33	$3.06.10^{19}$	237.45	$4.52.10^{16}$	235.11	$2.32.10^{22}$
0.25	253.26	$4.70.10^{19}$	246.90	$8.12.10^{16}$	244.40	$3.54.10^{22}$
0.3	261.02	$6.45.10^{19}$	255.55	$1.39.10^{17}$	252.90	$5.36.10^{22}$
0.35	278.20	$1.44.10^{20}$	264.15	$2.57.10^{17}$	261.32	$8.97.10^{22}$
0.4	282.82	$2.16.10^{20}$	272.26	$4.58.10^{17}$	269.26	$1.48.10^{23}$
0.45	291.70	$1.01.10^{21}$	279.46	$7.16.10^{17}$	276.32	$2.19.10^{23}$
0.5	297.47	$1.23.10^{21}$	286.39	$1.10.10^{18}$	283.13	$3.26.10^{23}$
0.55	309.85	$1.15.10^{21}$	302.26	$1.93.10^{18}$	290.51	$5.56.10^{23}$
0.6	316.12	$6.15.10^{21}$	301.49	$3.36.10^{18}$	297.88	$9.56.10^{23}$
0.65	326.06	$9.62.10^{21}$	318.88	$7.25.10^{18}$	306.72	$2.07.10^{24}$
0.7	337.07	$3.47.10^{22}$	332.03	$2.88.10^{19}$	319.43	$1.64.10^{26}$
0.75	347.83	$1.13.10^{24}$	341.26	$1.93.10^{20}$	336.36	$5.76.10^{25}$
0.8	349.20	$1.36.10^{24}$	359.30	$1.15.10^{21}$	353.79	$3.67.10^{26}$
0.85	324.31	$1.07.10^{23}$	356.75	$1.12.10^{21}$	346.15	$4.30.10^{26}$
0.9	307.81	$8.36.10^{20}$	334.15	$9.43.10^{19}$	324.22	$5.04.10^{25}$
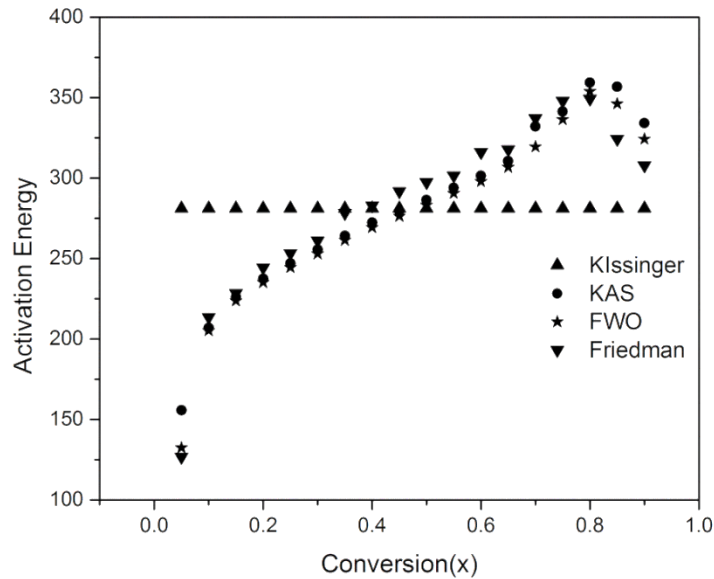
Figure 3–15: The activation energy as a function of conversion

Same calculations have been done for sample No.2 in order to compare their kinetics results.

The freedman results for sample No.2 is also shown in Figure 3-16.
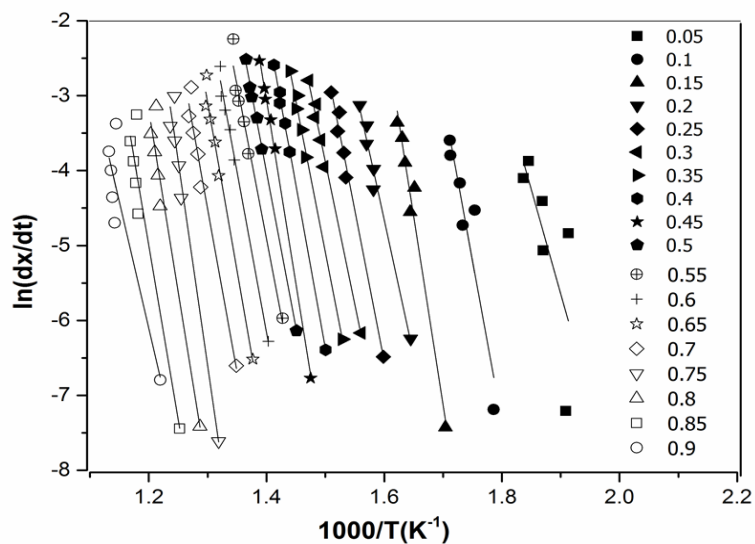
Figure 3–16 Friedman plots of coal (No.2) pyrolysis at different values of conversion.

3.8 Summary and remarks

In this study, the pyrolysis kinetics of a Canadian lignite coals were carried out by means of thermogravimetric analysis (TG) in the temperature range of 298–1173 K at six different heating rates of 1,6, 9, 12, 15 and 18 K min^{-1} under nitrogen atmosphere. It was found that the main pyrolysis process occurred in the temperature range 450-850 K. In this work kinetic study and thermal behavior of lignite coal was presented where Arrhenius parameters were determined and compared through four different methods of Kissinger, Ozawa, KAS and Friedman.

The activation energy is calculated as a function of conversion by using these methods and found to be similar. Among these methods, Friedman method was considered to be the best in order to evaluate kinetic parameters for solid-state reactions such as coal pyrolysis. Methods such as FWO and KAS are restricted to the use of a linear variation of the temperature and positive heating rate. Moreover, they are generated based on mathematical

approximation which can enhance systematic error. The advantage of the Friedman method is that it is free of mathematical approximations and is not restricted to the use of a linear variation of the heating rate. Experimental results showed that values of kinetic parameters were almost same and in good agreement. The isoconversional technique gives comparably reliable predictions of reaction rates compared to the more traditional model fitting.

The average activation energy obtained for sample No.1 (283 kJ mol^{-1}) was smaller than sample No.2 (327 kJ mol^{-1}) thus sample No.1 was considered for subsequent coal liquefaction studies. These results can provide useful information for pyrolysis researchers in order to predict kinetic model of coal pyrolysis and comparison of results for different coals also is helpful for sample selection to obtain maximum product conversion in coal liquefaction experiments. The kinetic parameters obtained in this study can be useful for pyrolysis and liquefaction researchers to predict kinetic model of coal pyrolysis and optimization of the process conditions.

CAPTER 4

Particle size selection

Despite current developments in coal liquefaction, the interactions and effects of different process variables are not completely understood. Initial coal particle size might be one of the major factors which can affect coal liquefaction conversion. The results of this chapter have been published in journal paper.

4.1 Effect of initial coal particle size on coal liquefaction conversion

Many attempts have been made to determine whether or not there are particle size effects in coal liquefaction process. Published data on particle size effects reviewed by many researchers and showed inconsistent conclusions in the literature.

Asbury studied the extraction of coal by Benzene at temperature between 220-260 °C. Four sizes of coal were selected in this work, 4 to 8 mesh, 16 to 20 mesh, 60 to 80 mesh, and one micron. Extraction at this temperature range gave approximately the same yield. For particle size ranges between 4 to 8 mesh, 16 to 20 mesh and 60 to 80 mesh, coal yielded 15.8, 17.9 and 22 % respectively but a higher yield was obtained when micron size coal was used [78].

Giri and Sharma studied the mass transfer limitations on solvent extraction of coal. They considered two range of particle size between 10-20 and 60-120 mesh. They reported that the extraction yields of coal were 13% and 33.6% respectively. They believed that finer particles increase the coal surface area and subsequently improving the extraction yield [79].

Table 4-1: Summary of particle size effects reported in the literature.

Research Group	Temperature	Coal Type	Particle size	Total Conversion (%)	Remarks
Karaca et al. (2010)	350°C-425°C	Lignite	0.25 and 1.5mm	72.57 and 72.79	The effect of particle size has been neglected
Li et al. (2008)	370°C-430°C	bituminous	Less than 149 μm	55	The effect of particle size has been neglected
Pradhan et al. (1992)	375°C - 425°C	Wyodak	Less than 841 μm Less than 149 μm	33	The effect of particle size has been neglected
Xu et al. (1996)	350°C-450°C	Argonne PCSP	106-150 and 250-500 μm	59	The effect of particle size has been neglected
Curran et al. (1967)	350°C-450°C	Pittsburgh	297-595 and 74-149 μm	72	The effect of particle size has been neglected
Szladow et al. (1981)	340°C - 400°C	Bituminous	74-250 μm	77	The effect of particle size has been neglected
Neavel et al. (1976)	400°C	HVCB	840-1000 μm	80	The effect of particle size has been neglected
Whitehurst et al. (1980)	426°C	Illinois No.6	425-600 and 45-75 μm	78.5 and 84.6	Smaller size had higher conversion
Woodfine et al. (1989)	400°C	Cresswell	2000 and 63 μm	16.8 and 35.5	Smaller size had higher conversion
Joseph et al. (1991)	400°C	Wyodak	210-2370 and 44μm	57 and 69	Smaller size had higher conversion
Ferrance (1996)	300°C - 480°C	Pittsburgh	841 297 149 74 μm	45	Smaller size had higher conversion
Vasquez et al. (1987)	380°C	Forestburg	425-841 and less than 75 μm	42	Smaller size had higher conversion
Moresi et al. (1985)	300°C - 400°C	Sulcis ,Italian	495-833 246-495 147-246 104-147 74-104	31-97	The maximum conversions are obtained with the 147-246 micron fraction
Current research	400°C	Lignite	833-1000 425-833 355-425 250-355 150-212 75-106 45-53 -45	31.6	Maximum conversions are obtained with the 150-212 micron fraction

Curran et al studied the kinetics of coal liquefaction with pure hydrogen donor solvents and reported that their runs with two size fractions, 100-200 mesh and 28-48 mesh, gave

identical results and concluded the conversion and rate of reaction are independent of particle size [80].In various studies have shown that the initial particle size has no effect on the yields of coal liquefaction process [81-83]. Table 4.1 shows summary of particle size effects reported in the literature.

Among these studies based on the effects of particle size on coal liquefaction conversion listed in Table 4.1, seven research groups have reported there was no effect of particle size, seven have reported increases in liquefaction conversion with decreasing the particle size and one has reported optimum conversion are obtained with 147-246 micron fraction. In this work, the most suitable particle size was selected as 150-212 μm which had similar behavior to Moresi's work. However, the reaction time in these studies was much longer than our work.

Joseph studied the effect of solvent preswelling pretreatments on the conversion of the 8x70 mesh (25 μm) and -325 mesh (44 μm) samples. Preswelling the samples in tetrabutyl ammonium hydroxide increased the THF solubility of both samples to about the same levels (the 8x70 mesh sample conversion increased from 57% to 77% and the -325 mesh sample conversion increased from 69% to 78%) [84].Coal pretreatment such as swelling can break weaker bonds and enhance the coal porosity, mobility of small molecules of the coal with increasing concentration of solvent in the coal matrix [85,86].

The size of coal particles can be considered a significant variable to investigate coal liquefaction conversion. If initial particle size significantly affects liquefaction yields one very important condition should be considered in which the particle must remain intact under liquefaction conditions. If the coal particle completely breaks down or dissolves almost instantaneously under high temperature in the presence of mechanical agitation and long

reaction time, then it is obvious that initial particle size has very little or no effect on liquefaction conversions. It was found that in the absence of mechanical agitation, particles can remain intact for short reaction time [87, 88].

Whitehurst et al. revealed that the coal particles were found to completely disintegrate under rapid stirring condition at conversion about 50% but in the absence of mechanical agitation, coal particles remained intact even when overall conversions reached to about 80% [87]. It seems that the coal particle remains intact for some period of time under liquefaction condition. Although the coal particle may be significantly altered morphologically and chemically during this period (i.e., swelling, breaking down to smaller fragments) the existence of a particle for even a short period of time makes it possible to investigate the effect particle size on coal liquefaction conversion. It seems that reducing the particle size decreases the distance the solvent molecule must diffuse to reach the center of a coal matrix to extract the products. For coal, the particle is the reactant and tetralin can be considered as diffusing component. If tetralin consumed faster than it can diffuse into the coal particle, then reaction in areas near the center of the particle will result in a higher level of recombination of free radicals which leads to form stable high molecular weight products that are not desirable in liquefaction processes [89-91].

In general, these studies are consistent with the hypothesis that particle size effects on liquefaction conversion may exist. Grinding of coal may result not only in particle size reduction but may also in the scission of the molecular chains with the rupture of some cross link bonds [91]. Also molecular entanglements may be inhibiting the extraction of coal because of larger association in bigger particles. Grinding the coal also can increase the surface area of coal and enhance solvent ability to more readily penetrate to the coal

structure. Most of the previous studies in the literature used long reaction time and also employed stirred autoclave reactor for their liquefaction conditions which had some drawbacks discussed above.

To the best of our knowledge, there is very little information regarding the effect of initial coal particle size on liquefaction conversion at short reaction time. The aim of the present work is to study the effect of initial coal particle size on liquefaction conversion at short reaction time up to 5 minutes. To reduce the mechanical disintegration effect on particles in this study, the experimental studies of particle size have been performed in a short contact time reactor where there is no internal stirring device, and mixing is accomplished by shaking the reactor vertically in a fluidized sand bath. Scanning electron microscope (SEM) was employed to follow the changes of coal physical structure. These results may provide helpful information for coal liquefaction at short reaction time in order to optimize the coal conversion into energy products.

4.2 Sample preparation

The bulk coal sample was crushed by means of a jaw crusher and ground in a ball mill and blended to homogenize the coal and reduced the particle size below 45to 1000 μm. The as received coal sample was wet with high moisture content and was dried in vacuum oven at 80 °C for 8 h until a moisture content of 9.5 % was achieved. The representative samples were taken for proximate analysis according to the ASTM D7582 by Macro Thermogravimetric Analyzer. The crushed samples were sieved with standard sieve series to obtain eight different fractions. Proximate analysis of each size fraction is given in Table 4.2. As seen in Table 4.2 finer sizes contain more ash content than larger sizes since the ash-forming minerals are naturally fine in size and have high specific gravity in comparison to

the organic part of the coal and can be broken easily and pass through mesh sieves during the sieving process. Also the fuel ratio which defines as volatile/fixed carbon is also presented in the table with low standard deviation.

Table 4-2: Proximate analysis of coal sample at different sizes

Particle size (µm)	Moisture (%)	V (%)	Ash (%)	F.C (%)	STD	Fuel ratio
833-1000	10.73	43.3	19.6	26.4	0.36	0.62
425-833	9.66	41.7	19.1	29.6	0.42	0.58
355-425	9.97	42.7	18.8	28.5	0.28	0.60
250-355	9.72	40.2	19.4	30.7	0.32	0.57
150-212	9.34	44.3	20.9	25.5	0.34	0.64
75-106	9.18	43.1	24.6	23.1	0.31	0.65
45-53	8.82	36.2	29.0	26.1	0.38	0.58
-45	8.35	38.5	33.7	19.4	0.25	0.66

Particle size distribution of the coal particles was determined using Malvern-MasterSizer 3000 analyzer which operates based on the theory of laser light scattering for comparison purposes. However, in sieve analysis pin shaped particles can vertically pass through the mesh sieves whereas in Mastersizer they can be detected with their longest dimension. The results of particle size distribution of samples are shown in Figure 4-1. A closer look at Figure 4-1 shows ranges over 45 µm contain some fine particles. This is because during the sieving process some of the fine particles attached to the larger particle sizes and thus can be detected with Mastersizer. The difference between the two measuring methods can be the reason for the discrepancy. The Mastersizer techniques however are purely for comparison purposes.
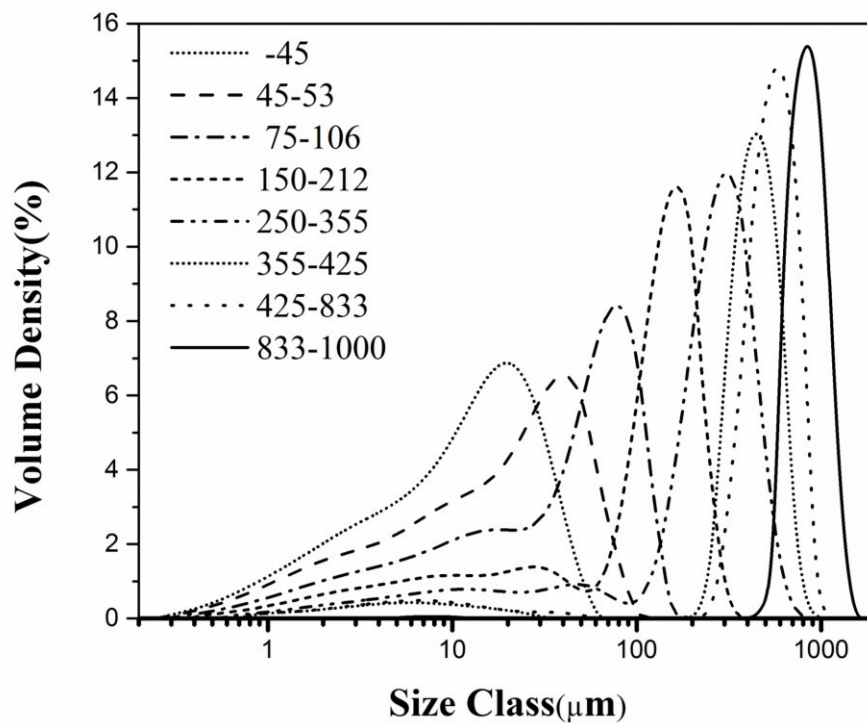
Figure 4–1: Particle size distribution of lignite coal

4.3 Experimental method

In this study eight different size fractions were considered for investigating the effect of initial coal particle size on coal liquefaction conversion. In this study a short contact time batch reactor (SCTBR) of 15 mL of capacity was used to carry out the liquefaction experiments without catalyst. In the typical experiment, the reactor was assembled and leak tested under nitrogen pressure. Figure 4-2 schematically illustrates the experimental setup. Typically, about 3 g of tetralin as a solvent was introduced into the reactor and pressurized to 35atm with nitrogen to keep the solvent in the liquid phase at reaction temperature. Then coal-solvent slurry consisting of 1 g of coal in 4 g of tetralin was introduced to the sample container and pressurized to 70 atm keeping the release valve closed. To provide high heat-

up rates, reactors were immersed in a heated fluidized sand bath and mixing was accomplished by shaking the reactor vertically. The sand bath was preheated 10^oC above the reaction temperature and micro reactor was submerged in the sand bath. The solvent was initially preheated in the reactor to a temperature of 10^oC above the reaction temperature. Once the temperature reached to the reaction temperature, the sample released valve was opened and the slurry was injected to the reactor for coal liquefaction reaction. At this instant, zero time was defined. The final solvent to coal ratio in the reactor was 7:1 in all experiments. After injection of the cold slurry, the reactor temperature was dropped by approximately 30^oC however, it immediately recovered and stabilized to the reaction temperature in about 20 s as can be seen in a typical temperature-time profile shown in Figure 4-3. In this study, reaction time was considered 5 min for all experiments to measure the coal liquefaction conversion. After the desired reaction time, the reactor was rapidly cooled down by liquid nitrogen to 80^oC, afterwards the reactor was depressurized, washed with tetrahydrofuran (THF) and the mixture was then taken out of the micro-reactor and placed on the filter media to separate solid from liquid using a vacuum pump.

Figure 4–2: Schematic diagram of Experimental setup

Following expression can be considered for calculating coal liquefaction conversion based on the dry and ash-free basis,

$$X(daf\ wt\%) = \frac{Wc - W_R}{Wc} \qquad (4.1)$$

Where, Wc and W_R are the weight fractions of the raw coal and residue respectively.

The experiments were repeated under identical conditions to check the reproducibility of the results. The liquefaction residues were dried overnight in the vacuum oven at $80^{\circ}C$ and submitted for visual observations with scanning electron microscope (SEM). Subsequently, the THF in the mixture was removed from coal liquid using rotary evaporator prior to gas chromatograph (GC) analysis.
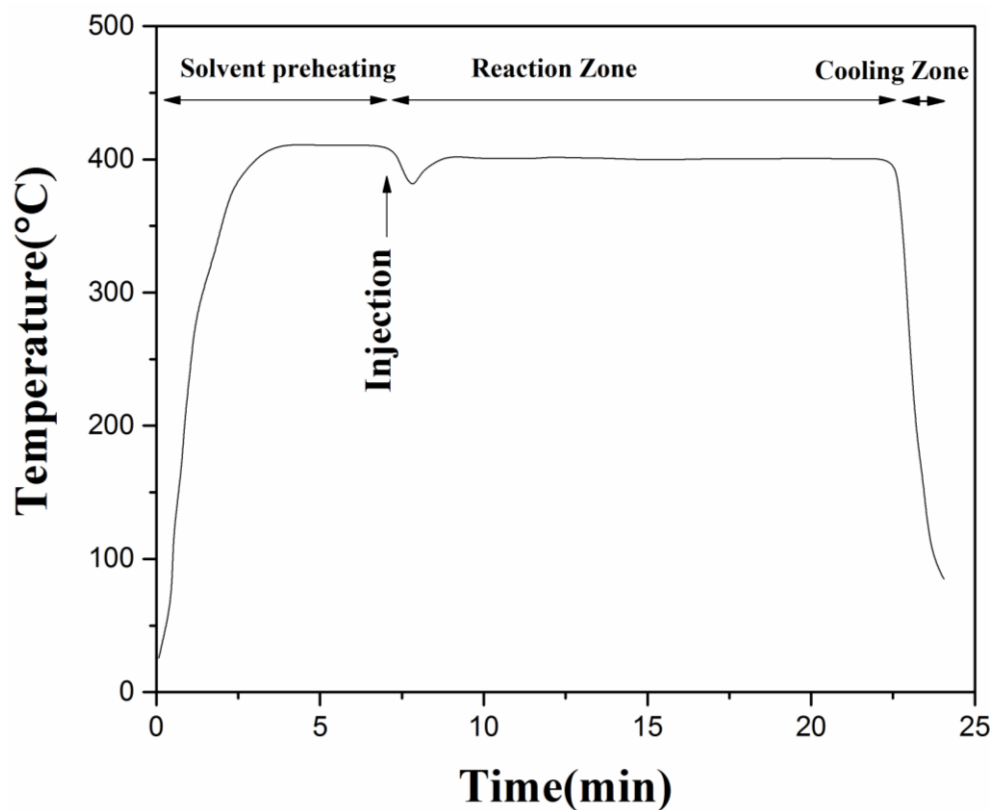
Figure 4–3: Typical time-temperature profile for micro reactor set up.

4.4 Results and Discussion

In order to investigate the effect of initial particle size on the coal liquefaction, solvent to coal ratio is considered constant at 7/1, reaction time at 5 min, and reaction temperature at 400˚C, where the particle size is varied as -45 to 1000 μm in the liquefaction process. The experiments were carried out under non-catalytic and isothermal conditions. The total coal liquefaction conversion of coal at different size fractions were calculated from equation 2 and shown in Figure 4-4. As can be seen in Figure 4-4, the reduction of particle size from 833-1000 to 150-212 μm changed the total conversion at short reaction times. However, the effect will be gradually diminished at longer reaction times. When the particle size decreased from 833-1000 to 150-212, the total conversion changed from 16.54% to 31.6%. With reducing the particle size the distance the solvent molecule must penetrate to reach the center of a coal matrix to drag out the products will decrease. Grinding of coal had synergetic effect on coal liquefaction conversion. However, as the energy costs increase with the reduction in particle size, the most suitable particle size found to be 150-212 μm. Reducing the particle size from 150-212 μm to -45 μm, e.g. below 45 μm, total conversion gradually decreased. The reason arises from the fact that during the coal liquefaction at high temperature fine particle can attached each other and produce larger particle where agglomeration of particles occur at this stage. As can be observed in Figure 4-1, association of fine particles (e.g. below 20 μm) in small particle size ranges are dominant in comparison to large particle size ranges. Thus these fine particles can increase the agglomeration process which may restrict solvent access to the inner coal network that is undesirable in coal liquefaction processes. In order to compare the variations in char morphology at different particle size ranges, scanning electron microscopy was employed using a JEOL 6301F device. Several images were taken and

representative images were selected for further investigation. In this study, among eight particle size fractions, three particle size ranges, -45, 150-212 and 833-1000 μm were chosen and presented for visual observation and comparison. These results are shown in Figure 4-5 to 4-7. Figure 4-5 shows the SEM images of largest particle size, e.g. 833-1000 μm and its residue. This residue was not expected to show major alteration as a result of solvent swelling and decomposition as discussed above. Indeed, by comparing the raw coal particles with their corresponding residue particles at the same level of magnification. Figure 4-6 shows SEM images of selected particle size range. A closer look at Figure 4-6 shows evidence of swelling and thermal decomposition of these particles. It can be seen that the residue particles were smaller even at short reaction time and no evidence of agglomeration was observed at this particle size range.
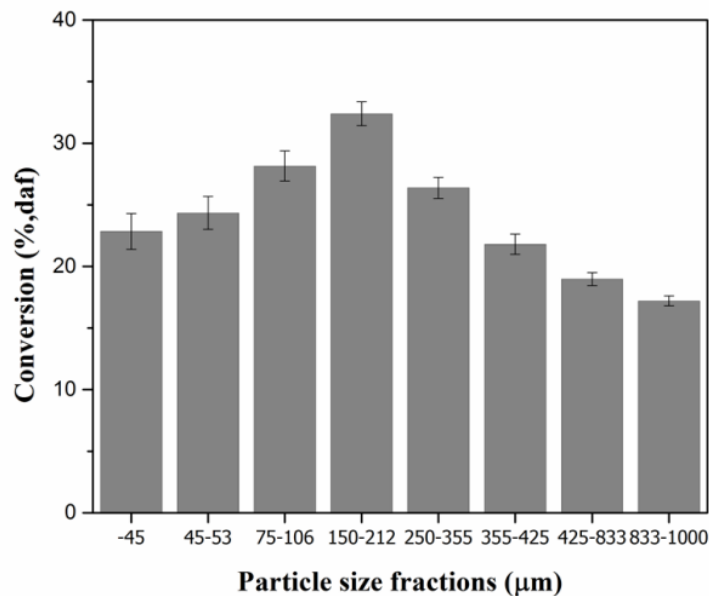
Figure 4–4: Effect of particle size on coal liquefaction conversion
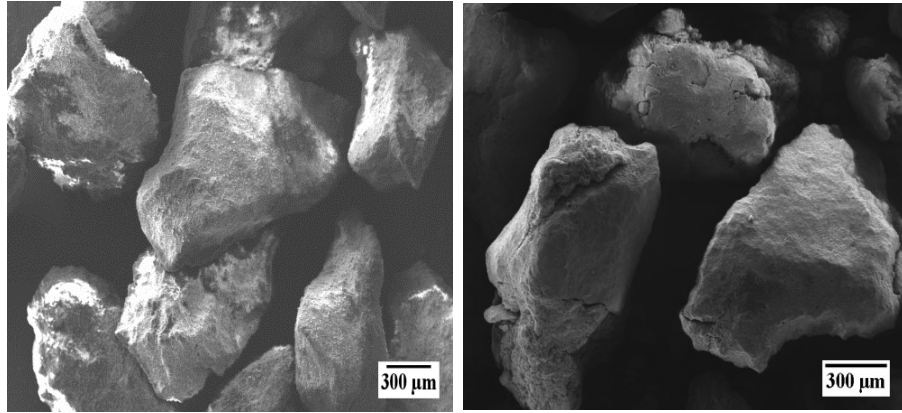
Figure 4–5: SEM images of 833-1000 µm size fraction at
100X magnification; (a) raw coal and (b) residue

.
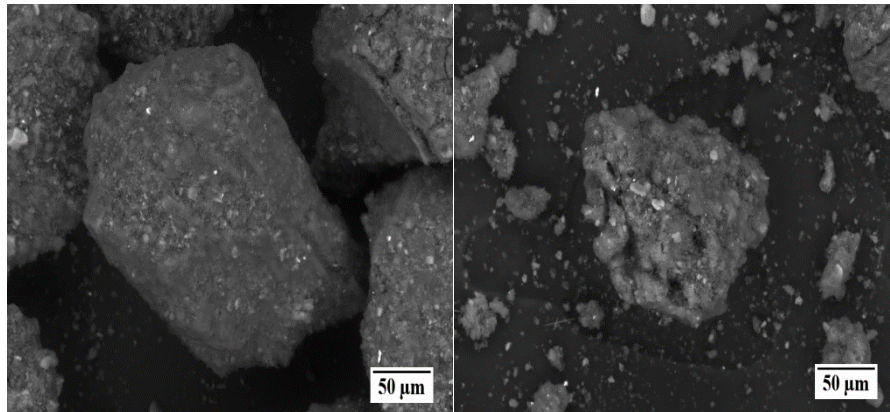
Figure 4–6: SEM images of 150-212 µm size fractions at
800X magnification; (a) raw coal and (b) residue
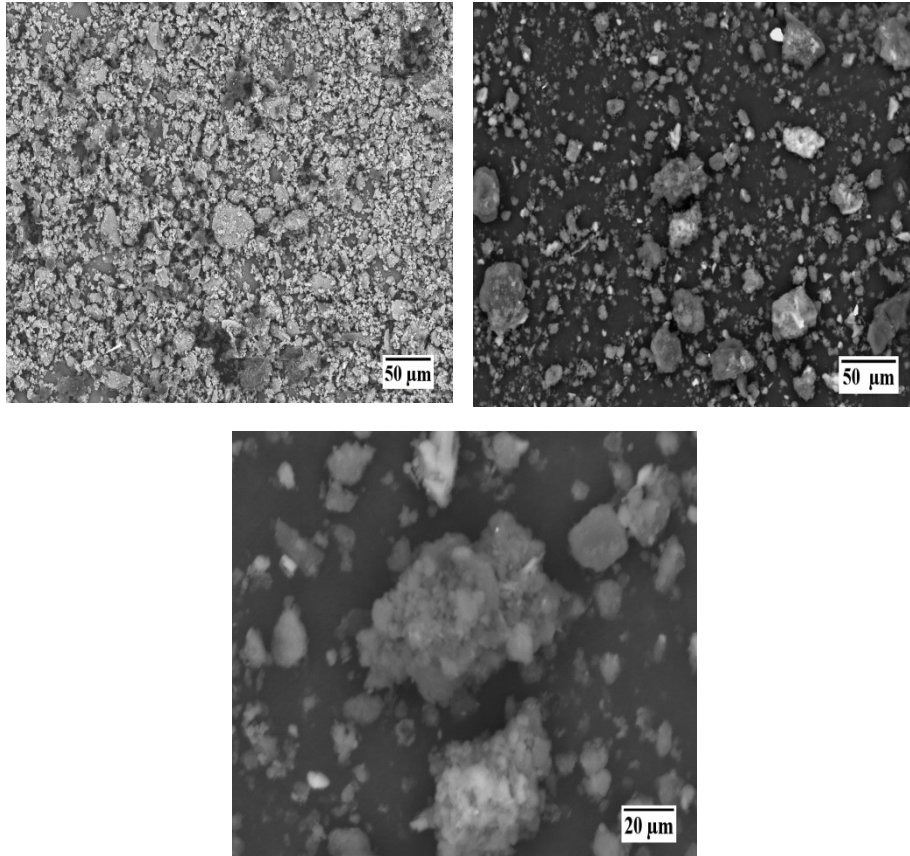
Figure 4–7: SEM images of -45 µm size fraction at 600X magnification;
(a) raw coal and (b)residue and (c) higher magnification at 2000 X

Figure 4-7 presents SEM images of smallest size fraction at three different magnifications. Both char photographs (Figure 4-7(b) and 4-7(c)) show visual evidence of agglomeration. It can be seen that some particles are highly smaller than its corresponding raw coal. Coal particles were partially cleaved and dissolved during the liquefaction experiment and some others were agglomerated and generated larger size fraction than its original raw size during short reaction time. These effects might be more pronounced at longer reaction times.
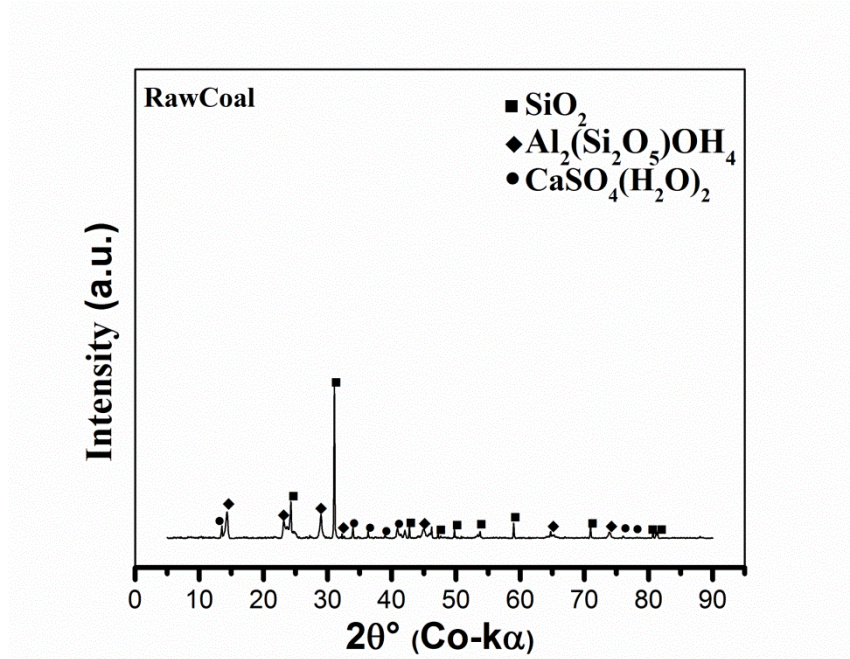
Figure 4–8: XRD spectra for the pulverized coal sample.
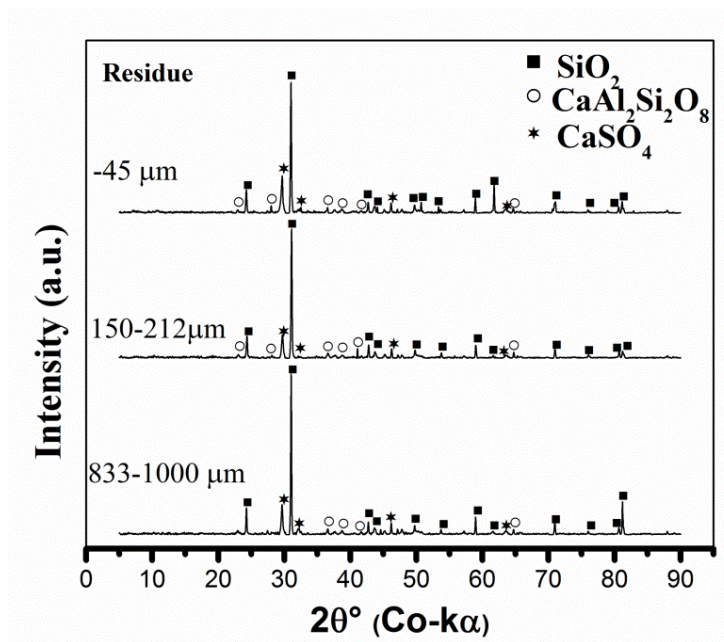
Figure 4–9: XRD patterns of residue at three different sizes

Powder XRD patterns were obtained using a Rigaku Powder X-Ray diffractometer which is equipped with a cobalt tube, graphite monochromator and scintillation detector.

XRD analysis has been performed on samples of the raw coal and of residues at different size fractions. Three particle size ranges same as before were selected for X-ray diffraction analysis. Quartz and calcium sulphate were the main composition of the sample. The Gas chromatography (GC-MS) analysis was performed for analyzing the coal liquid. The extract was obtained after short reaction with tetralin as solvent at 400°C and diluted in CS_2 to inject into gas (GC-MS).The results of gas chromatography of coal liquid at three main particle sizes are presented in Figure4-10. A closer look at Figure 4-10, products from the dehydrogenation of tetralin such as naphthalene and dihydronaphthalene can be identified. The first peak of the GC spectra is decalin and the highest peak represents tetralin as hydrogen donor solvent. Main compounds of coal liquefaction are listed in Table 4.3. These products reveal that even at very short reaction times under inert atmosphere hydrogen shuttling takes place. At this region free radicals are formed due to thermal decomposition of bond linkages which can be capped by the abstraction of hydrogen atom from the donor molecule leading to formation of products with low molecular weight that can be dissolved in the solvent. Hence, it can be seen that even at short reaction time, product upgrading occurs which may provide the possibility for coal liquefaction at short reaction time to reduce energy consumption. It has been shown that the number of peaks as well as the intensity of peaks in the coal liquid obtained from appropriate particle size was partially changed and therefore the product distribution was formed in higher level compared to other particle size ranges. This result is in agreement with those previous results which discussed before. Combination of the results suggests that initial coal particle size can play an important role in coal liquefaction conversion.
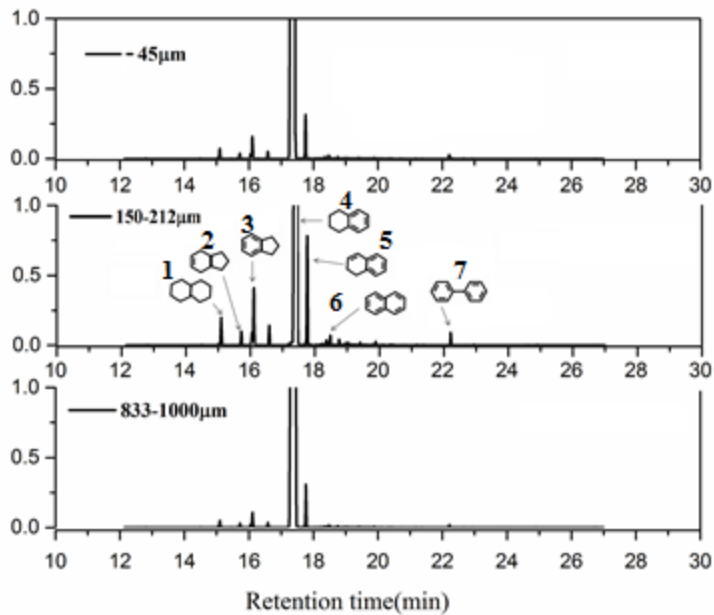
Figure 4–10: GC of coal liquid at 400°C and 5 minutes

Table 4-3: Residence time for different components in coal liquid [162,163,177,178]

Residence time(min)	Species
15.2	decalin
15.8	2,3,4,5,6,7-Hexahydro-1H-indene
16	Indene
16.5	1-methylindene
17.5	tetralin
17.8	dihydronaphthalene
18.5	naphthalene
22.5	biphenyl
19.6	1-Methylnaphthalene
23.5	fluorene
29.5	fluoranthene
30	pyrene

4.5 Summary and Remarks

In this study, coal liquefaction of a Canadian lignite coal was carried out in a tubular bomb reactor at short residence time. Eight different size fractions between -45 to 1000 μm were considered for coal liquefaction experiments to show whether or not there are particle size effects in coal liquefaction conversion. Advanced analytical techniques such as SEM, GC-MS and XRD were employed in this work and discussed in order to determine the importance of initial coal particle size on coal liquefaction conversion. The results showed that liquefaction of coal in the presence of hydrogen-donor solvent (tetralin) significantly affected total liquefaction conversion at short reaction time. With Grinding of coal solvent has more ability to penetrate to the coal structure. However, as the energy costs increase with the reduction in particle size, the most suitable particle size was selected as 150-212 μm. Reducing the particle size from 150-212 μm to -45 μm, e.g. below 45 μm, total conversion gradually decreased. The reason arises from the fact that during the coal liquefaction at high temperature fine particle can attached each other and produce larger particle where agglomeration of particles occur at this stage. Thus fine particles may promote the agglomeration process which may restrict solvent access to the coal matrix that is undesirable in coal liquefaction processes. These results may provide helpful information for coal liquefaction researchers to find suitable coal particle size for coal conversion into energy products.

CHAPTER 5

Kinetic modeling of direct coal liquefaction

This chapter is dedicated to modeling of direct liquefaction of coal. A brief review kinetic modeling of coal liquefaction, results of mathematical modeling and product distribution and different characterization techniques are discussed. Some of the results of this chapter have been submitted as a journal paper.

5.1   Introduction

As mentioned before one of the main advantages of direct liquefaction is that, this process can convert coal to liquid without the need for producing syngas (H2 and CO) as in indirect process and also has higher thermal efficiency than indirect liquefaction. One aim of coal liquefaction kinetic models is to predict the results of coal liquefaction experiments in order to determine optimal processing conditions. A second goal is to identify those processing variables which have the most influences in the system. This can decrease the number of experiments which needed to investigate new systems by centering on the most significant variables [94].

Kinetics studies are very important because they can provide expressions for the reaction pathway which can be used in calculating reaction times, yield and economic conditions. Several kinetic models, with varying degrees of complexity and sophistication, have been used in the literature to describe coal liquefaction behavior. However, because of heterogeneous nature of coal, experimental conditions, and different definitions and methods for measurement of coal conversion products make it sophisticated to compare the results.

The kinetic of coal liquefaction is complicated due to the formation of various compounds. Thus, the approach in coal liquefaction kinetic studies is to isolate these compounds to kinetically similar compounds through some separation methods. Most traditional and current process models have implemented complex feedstock, reaction network and products are represented based on global lumped models. In this way similar components are grouped into a few cuts or lumps. The number of lumps of the proposed models for the reactions has been consecutively increasing to obtain a more detailed prediction of product distribution. Because coal has heterogeneous nature and contains several species, a model for the reaction of a complex material such as coal might be lumped methodology, and the selection of a suitable network is very important [95-98]. The lumping criteria are mainly based on analytical capabilities, the level of understanding of the chemical mechanism, and degree of interest in various reaction products. If too complex, it becomes difficult to isolate a particular reaction pathway and measure its rate; if too simple the rates of a group of pathways are being measured effectively as the rate of one step, so that information about intermediate or concurrent steps is omitted.

5.2 Overview of kinetic modeling of coal liquefaction

Global lumped models were first proposed by Weller et al to model the conversion of coal to asphaltenes and then to oil. These solubility models have been made more complicated over the years to incorporate both preasphaltenes and an asphaltenes fraction. They studied the liquefaction of a bituminous coal in a batch autoclave in temperature range of 400-440 °C. This kinetic model allowed for the description of coal, the reactant, and its transitions into oil and asphaltenes. Rate parameters were regressed and an excellent fit of the model to the experimental data was found.Kinetic parameters were calculated and an

excellent fit of the model to the experimental data was found. The limitation of this model is that single reaction network is considered for liquefaction condition and other reaction intermediates such as preasphaltenes were not determined [99].

Falkum and Glenn studied the hydrogenation of Spitsbergen coal in the presence of hydrogen gas and absence of solvent. They found that the coal hydrogenation involves two distinct stages and one of them decomposed faster than the other. In this work other fraction like preasphaltenes and gas were not considered in reaction network [100].

Pelipetz et al. studied the catalyzed and uncatalyzed liquefaction of lignite coal and assumed that only a single thermal decomposition occurs. They also concluded that in the presence of a catalyst, a unit of coal produces more benzene-soluble material than uncatalyzed conditions. The drawbacks of this model are that single reaction network cannot describe liquefaction behavior and also in this model the asphaltenes and oil products are considered as one lump since the path of formation of oils is different from asphaltenes [101].

Hill et al examined the mechanism and kinetics of coal liquefaction in tetralin. Solubility of the liquefied products in benzene was used as a measure of conversion. They proposed that coal liquefaction can be explained by a series of independent first-order reactions and the unreacted residue from a reaction being the reactant for the subsequent reaction forming liquid and gaseous products. In the first step, all the coal bulk which is readily available in the mixture of coal and solvent goes to R_1 which is solid, L_1 which is liquid, and G_1 which is gas. They concluded that this reaction network is based on Dryden's model. This reaction based on Dryden's model may describe the extraction at low temperatures, but at

temperatures above 350°C when increasing the temperature, increases the reaction rates and the assumption of indestructible micelles is not tenable [102].

Curran et al examined liquefaction of bituminous coal in the autoclave. The reaction network composed of a reactive fraction and an unreacted material which simultaneously react for the formation of oils and asphaltenes [103].

Struck et al employed batch autoclaves for hydrocracking a coal and proposed a kinetic model consisting of two independent parallel reactions. In this model the asphaltenes and oil products were lumped together [104].

Another model by Liebenberg et al discussed the transition of bituminous coal to asphaltene to oil under hydrogenation conditions (batch reactor, tetralin, 2500 psig of H2 in more detail, and on a molar rather than a mass basis. They postulated a parallel network where coal can directly convert into an oil (n-hexane soluble) product. A kinetic model using molar data for a coal would be ambiguous since coal has a complex matrix consists of a broad distribution of molecules with different molecular weights and cannot be defined as elementary kinetic unit [105].

Yoshida et al suggested that coal produced two different oil fractions during liquefaction. The experiments conducted in a shaking autoclave under isothermal conditions followed by Soxhlet extractions to isolate the oils and asphaltenes, enabled estimation of the three rate constants in the network. They assumed that the first oil fraction (S1) occurred directly from the coal and a second oil fraction (S2) was produced from the asphaltene .The first hexane-soluble oil fraction was produced from short contact time liquefaction experiments (4-29 min at 400°C), and the second hexane-soluble oil fraction was produced from reactions with the coal-derived asphaltene (10-120 min at 400°C). It might speculate

that the evolution of the mobile phase produced the S 1 oil fraction while the thermal degradation of the coal produced the majority of the S2 oil fraction [106].

Cronauer et al performed thermal liquefaction of a Belle Ayrsubbituminous coal in a CSTR reactor. They considered parallel reactions for gases and asphaltenes formation. Gas formation was the only one which was observed that the model predict in a better way compared to previous models. The addition of the preasphaltene fraction to the kinetic network allowed more kinetic detail, but it did not allow for greater understanding of oil formation. The activation energy were very low maybe because of the kinetic model cannot describe the reactions happen in an accurate ways [107].

Shah et al proposed different reaction network for direct coal liquefaction. They classified the product according to the boiling point range where O_1, O_2, O_3 and BP are heavy fuel oil, furnace oil, naphtha and byproduct respectively. This model is classified on the basis of physical properties and ignored the chemical properties of the molecules [108]. Chiba and Sanada proposed a generalized model for coal hydrogenation reactions based on batch autoclave experiments. They suggested that coal consists of two reacting parts (C_1 and C_2) which C_1 was less active component and formed asphaltene and C_2 was active portion of coal and directly formed oils product .In this work preasphaltene and gas are not considered in the reaction network [109].

Shalabi et al. postulated a further complicated network by assuming Preasphaltenes can directly convert into asphaltenes and oils. Their work centered around liquefaction of a high volatile bituminous coal in a 300 cm3 batch reactor with tetralin as the solvent and under 350 psig of hydrogen gas. They incorporated the concept of a reactive fraction of coal which is necessary to adequately model the data since the final concentration of unreacted coal will

not be zero. They assumed all reactions to be first order and irreversible. They considered three reaction models based on various presumed theoretical mechanism of coal liquefaction. Model 1 represent a pure series reaction network, model 2 differs from model 1 in producing of oil and gas directly from preasphaltenes and also asphaltenes. In model 3 preasphaltenes are formed directly from the coal and also are the precursors for the formation of asphaltenes and oil and gas. First Model could not provide an adequate representation for the liquefaction process. The results for the second model was a little better than first Model since adding one step to the pure series reaction allows two compounds to be adequeately modeled here coal and asphaltene. Finally, Model 3 was more accurate than the other two models since adding parameters to the model allows more variation in the data set to be accounted for by the regression scheme. These models had some limitations. First, temperature regimes where regressive reactions began to become important were avoided secondly, in these models the gaseous and oil products are considered as one lumped since the path of formation of oils is different from gaseous products [110].

Mohan and Silla proposed two models in which reversible reactions of asphaltenes, preasphaltenes and oils are present. First model could describe liquefaction behavior at high temperature and the second one was only valid at low temperature. In these models production of Gas has not been considered [111].

Gertenbach et al proposed a reversible reaction model for coal liquefaction experiment. The fit to this model was poor and the model predicted high amount of oil yield in plug flow reactors.

Gas fraction is not included in this reaction network and the reversible reaction path from preasphaltene to coal is not right since preasaphaltene can produce coke and cannot be distinguished from coal [112].

Abichandani et al studied a kinetic of short contact time liquefaction of Coal in the CSTR reactor. They assumed coal fragments into smaller species instantaneously which is fuction of temperature. They showed in the reaction network the possibility of direct formation of asphaltene and oil from an active portion of coal [113].

Abusleme et al. proposed a kinetic model for the catalytic liquefaction of two Chilean subbituminous coals (Pecket and Catamutan). In this reaction network, formation of asphaltene from oil fraction is described as a result of recombination of free radical at long reaction time which accelerates retrogressive reaction that is undesirable in coal liquefaction process [114].

Radomyski et al.studied mathematical analysis of three kinetic models of coal liquefaction in the absence of catalyst and found that a series-parallel model was the most appropriate among the models based on either only-series or only-parallel reaction. [115].

Ozawa et al. studied catalytic direct coal liquefaction in the absence of donor solvent. The results showed that the catalyst had great effect on the conversion of preasphaltenes to asphaltenes but little effect to accelerate gasification and oil formation reactions [116]

Gollakota et al. developed a parallel thermal and catalytic kinetics for coal liquefaction. This model contained four thermal rate constants, two catalytic, and a stoichiometric parameter. The reaction of coal to preasphaltenes and gas were mainly thermal in nature and the last reaction was thermal as well as catalytic in nature. They also recommended for effective

conversion of large preasphaltene molecules, catalysts with large pores must be utilized [117].

Nagaishi et al developed a kinetic model for evaluation of coal reactivity for liquefaction experiment. The model assumes that coal consists of three different components I_0 (inert), C_1(less reactive), and C_2 (reactive), all of which can be quantified experimentally. In this kinetic model the gaseous and oil products are considered as one lumped while the path of formation of oils is different from gaseous products [118]. Another kinetic model based on a set of irreversible pseudo-first-order reactions proposed by Giralt et al. The experiment performed under isothermal condition with two different solvent, tetralin and anthracene oil. Oil and gas components were lumped together in this reaction network and reactive part of coal was considered to this network [119].

Angelova et al studied kinetics of Bulgarian brown coal in the tubing micro reactor under isothermal conditions. This model assumed that gas is formed directly from the brown coal. The initial stage was found to be strictly temperature sensitive. Products of the initial thermal reactions were mainly preasphaltenes and asphaltenes. Lighter materials are usually formed through hydrocracking of these heavy products [120].

Salvado et al carried out catalytic hydroliquefaction of lignite coal under various reactive atmospheres. The use of commercial hydrodesulphurization catalyst did not increase the conversion of coal into liquid but it could improve the production of hydrogen sulphide and methane. Oil and gas fractions were grouped as a lump in this reaction network [121].

Pradhan et al studied a kinetic model based on both series and parallel conversion of coal into oils. It is similar to one employed by Radomyski who found that a series-parallel model was more accurate than the models based on only series or only-parallel pathways. The products

of coal liquefaction were unreacted coal, asphaltenes, oils, and gases. Unreacted coal included char and was defined as methylene chloride insolubles. All reactions in this Model were irreversible with a first order reaction rate constant. The formation of asphaltenes from coal was found to be based on thermal effects not catalytic effect [122].

Ferrance developed a general model for coal liquefaction which differs from previous models. Two things included in the kinetics of this model which were not considered in previous works, concenrrarion of reactants and hydrogen pressure. The only drawback of this model was considering oil and gas fractions as a lump into the reaction network [123]. A kinetic analysis of coal liquefaction in flow reactors was reported by Ikeda et al. Coal was concluded to consist of two different solid components with different reactivities and different reaction paths. They assumed first-order reversible successive reactions in three continuous stirred tank reactors. According to this scheme, retrogressive reactions were not negligible during the coal liquefaction process. Oil and gas fractions grouped as a lump into the reaction network while formation of oil is as a result of hydrocracking of heavy materials and gas fraction is formed because of thermal decomposing of light hydrocarbon in the coal matrix [124].

Kidoguchi et al developed a kinetic model for the initial stage of reaction in the direct coal liquefaction of subbituminous coal. The model assumed that coal consists of three components where CA, CB and C1 are larger rate of decomposition, smaller rate of decomposition and negligible rate of decomposition respectively. In this reaction network preasphaltene and asphaltene are grouped as a lump and no reaction path was considered for decomposition of heavy materials like preasphaltene and asphaltene [125].

Li et al investigated kinetics of coal liquefaction in a 500 ml autoclave during heating-up and isothermal stages. Temperature range of non-isothermal stage in this work was from 370°C to 430 °C and the isothermal stage temperature was 430 °C. This Model differs from the other previous studies about lumped category. In this study coal was divided into three parts, easy reactive part, hard reactive part and unreactive part. This type of reactivity classes of coal generates more accurate Model. They considered some assumptions for their kinetic scheme which may not be advantage for studying of coal liquefaction process. For example in their kinetic study asphaltene and preasphaltene and also oil and gas yield were considered as one for simplifying calculation process. This may increase experimental variation when various components with different solubility are assumed as one lump [126]. A summary of recognized coal liquefaction kinetic models can be found in Table 5.1.

Table 5-1: Summary of direct Coal liquefaction kinetic models

NO	Research group	Kinetic Sheme	Coal Type	Solvent	T (°C) and P (MPa)
1	Weller et al. 1951	C → A → O	Pittsburgh	None	T:400-440 P:41
2	Falkum et al. 1952	C1, C2 → A + O	Spitsbergen	None	T:400 P:NA
3	Pelipetz et al. 1955	C → A + O	Wyoming	None	T:400 P:3.4-27.6
4	Hill et al. 1966	C → A + O	Utah	Tetralin	T:440 P:34.5
5	Curran et al. 1967	C1, C2 → A + O	Pittsburgh	Tetralin	T:324-441 P:NA
6	Struck et al. 1969	C1, C2 → A + O	Pittsburgh	None	T:371-427 P:10.34-24.13
7	Liebenberg et al. 1973	C → A / O	Bituminous	Tetralin	T:380-440 P:16-20
8	Yoshida et al. 1976	C → A → O, O	Japanese	Anthracene oil	T:400 P:19.6-21.6

#	Reference	Scheme	Coal	Solvent	Conditions
9	Cronouer et al. 1978	C→G; C→A, C→O; P→A→O	Belle Ayr	Hydrogenated phenanthrene	T:400-470 P:13.79
10	Shah et al. 1978	BP ← C → O₂ → O₃; C→G, C→W, C→O₁	SubBituminous	Hydrogenated Anthracene oil	T:413 P:24.13
11	Chiba et al. 1978	C1→A→O; C2→O	Yubari bituminous	Tetralin	T:375-440 P:NA
12	Shalabi et al. 1979	C→P, C→A, C→O; P→A; A→O; P→O	Kentucky No. 9 bituminous	Tetralin	T:350-400 P:13.79
13	Mohan and silla 1981	C→P; P→A, P→O; A⇌O	Illinois No. 6	Tetralin	T:330-450 P:7.1
14	Gertenbach et al. 1982	C⇌P; C→O, C→A; P⇌A; O←A	Kentucky No. 9 bituminous	Recycle oil	T:360-440 P:13.89
15	Abichandani et al. 1982	G; A←C→P; C→O, A→O, P→O	Pittsburgh	Recycle solvent	T:350-450 P:13.8
16	Radomyski et al. 1984	G; C→A→O; C→O	NA	Tetralin	T:400-460 P:29.4
17	Ozawa et al. 1984	G←C→O₁, C→P, C→A; A→O₂	Yubari bituminous	None	T:400 P:7.9
18	Gollakota et al. 1985	C +αO→P→A→O; C→G, P→A→O	Elkhorn No. 3	Anthracene oil	T:425 P:8.6
19	Nagaishi et al. 1988	C⇌P→A→O+G	Akabira	Tetralin	T:450 P:10.1
20	Giralt et al. 1988	C→P; C→A, C→O+G; P→O+G, P→A; A→O+G	Catalan	Tetralin	T:350-400 P:NA
21	Angelova et al. 1989	P; C→A→O; C→P→O; C→O	Bulgarian coal	Tetralin	T:350-400 P:NA
22	Salvadó et al. 1990	C→P; C→A, C→O+G; P→A; A→O+G	Bergued lignite	Anthracene oil	T:400-450 P:5
23	Pradhan et al. 1992	G←C→A→O; C→O	Wyodak	methylene chloride	T:375-425 P:6.9
24	Ferrance et al. 1996	C→P; C→A, C→O+G; P→A, P→O+G; A→O+G	lignite	Tetralin	T:350-400 P:15.2
25	Ikeda et al. 2000	C⇌P⇌A⇌O+G	Tanito-Harum	Recycle solvent	T:450-465 P:16.8

| 26 | Kidoguchi et al. 2001 | | Tanitoharum | Recycle solvent | T:200-450 P:10.1 |
| 27 | Li et al. 2008 | | Shenhua | cycle oil | T:370-430 P:8 |

In summary, there are drawbacks to these models in reference to extensions to liquefaction. First, some of these models (1-8), employed simple reaction network which information about intermediate or concurrent steps is omitted. Second, some of these models, the gas fraction has not been considered (1-8,11-14,18,21) and in some other cases, gaseous and oil products are not considered as a separate lumped while the path of formation of oils is different from gaseous products (20,22,24,25,27). Reversible reaction is also not considered in most of kinetic networks except those presented in the table (13, 14, 19,25). Finally, most of these models have been performed under non-isothermal condition. This condition may lead to experimental variations due to the time required to reach the desired temperature where significant reactions occurred in advance. To the best of our knowledge, there is little information regarding kinetic modeling of direct coal liquefaction under isothermal condition.

The aim of the present work is to develop a kinetic model for direct coal liquefaction process under isothermal condition. Since conventional batch autoclave is not appropriate for isothermal runs, as conventional autoclaves require long heat-up and cool-down times to reach the desired temperature, during which significant reaction may happen. Thus the liquefaction experiments were conducted with a tubing bomb reactor designed to suppress secondary reactions and have more reliable kinetic data. Consequently, the reproducibility of conversions obtained is far superior to those taken in conventional massive reactors.

5.3   Experimental method

Many investigators considered massive reactors of various capacities for their experiments. It has been long recognized that calculating kinetic data in a large reactor indicates the problem of inaccurate reaction time due to long heat-up and cool-down times during which significant reactions can happen [37, 80, 92, 93]. The approaches used to minimize these nonisothermal heat-up times have been considered to use Micro reactors. This problem was overcome by heating solvent to desire temperature and injecting slurry consist of coal and solvent into the reactor.   The liquefaction runs were investigated with a rapid injection reactor designed specifically for isothermal kinetic study. Figure 5-1 schematically illustrates the experimental setup. The micro reactor was 15 ml stainless steel (10 cm height and 1.4 mm diameter) manufactured at university of Alberta. Connection included a 3/4″ sample injection line, 1/4 ″gas injection line to introduce gas to the system and stainless steel wire type thermocouple for reading the reactor temperature. The raw coal sample was received from Sherritt Company. The coal sample was crushed, sieved to particle size fraction (150-212 μm) as obtained in chapter 4 and dried under vacuum condition until a moisture content of about 9.5 % was achieved. The representative sample was stored under vacuum condition prior to liquefaction. In a typical run, 3 g of solvent (tetralin) was placed in into the reactor. The set up was purged three times with nitrogen to remove the air present inside the reactor and leak tested with nitrogen and vented. Then reactor pressurized to 35atm with nitrogen to keep the solvent in the liquid phase at reaction temperature. The slurry consisting of 1 g of coal in 4 g of tetralin was introduced to the sample container and pressurized to 70 atm keeping the release valve closed. To provide high heat-up rates, reactors were immersed in a heated fluidized sand bath and mixing was accomplished by

shaking the reactor vertically. The sand bath was preheated 10°C above the reaction temperature and micro reactor was submerged in the sand bath. The solvent was initially preheated in the reactor to a temperature of 10°C above the reaction temperature. Once the temperature reached to the reaction temperature, the sample released valve was opened and the slurry was injected to the reactor for coal liquefaction reaction. At this instant, zero time was defined. The short nonisothermal periods of heating and cooling allowed neglecting its effect on the overall process and the reaction was considered as isothermal. The final solvent to coal ratio in the reactor was 7:1 in all experiments. After injection of the cold slurry, the reactor temperature was dropped by approximately $30^{o}C$. Recovery to the desired temperature required about 20 sec. After the desired reaction time, the reactor was rapidly cooled down by liquid nitrogen to about $80^{o}C$ within 30 sec, afterwards the reactor was depressurized under the hood and amount of gas released was calculated from reactor weight before and after experiment.
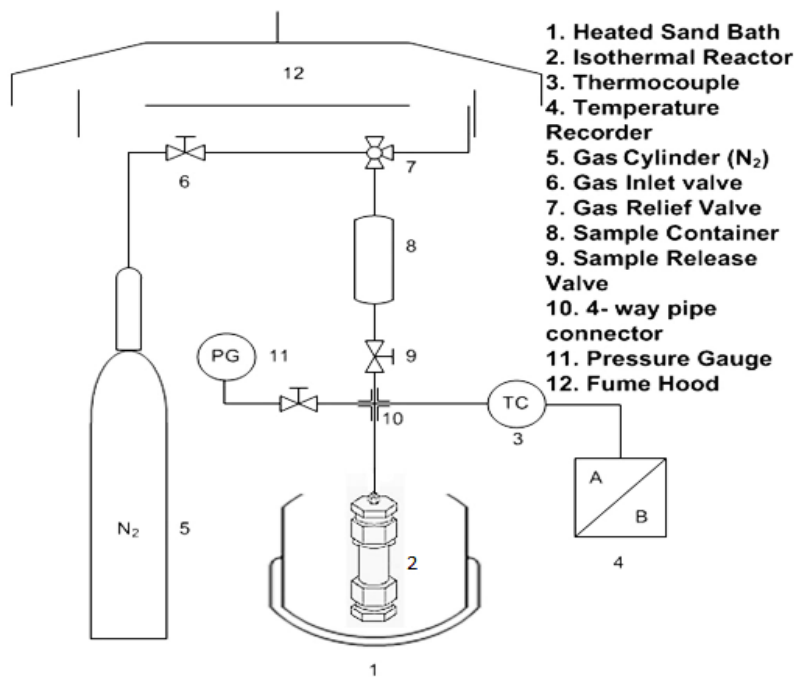
Figure 5–1: Diagram of Experimental setup

89

The reactor then washed with tetrahydrofuran (THF) and the contents were then taken out of the reactor. The residue was separated from liquid by filtration the slurry with a vacuum pump. Unconverted coal samples or liquefaction residues were dried overnight in the vacuum oven at $80^{o}C$ and submitted for visual observations with scanning electron microscope (SEM) and TGA analysis for further characterization. Subsequently, the THF in the mixture was removed from coal liquid using rotary evaporator prior to gas chromatograph (GC) analysis. The experiments were carried out at four isothermal temperatures from 350 to 450°C. Temperatures below 350°C are ineffective for coal liquefaction resulting in low conversions and temperatures higher than 450°C lead to excessive coke formation [97,129-131]. Reaction times of 15, 30, 60 and 120 minutes were selected for all the experiments. No catalyst was used in the experiments. The results showed that at high temperature and extended time undesirable retrograde reactions may take place.
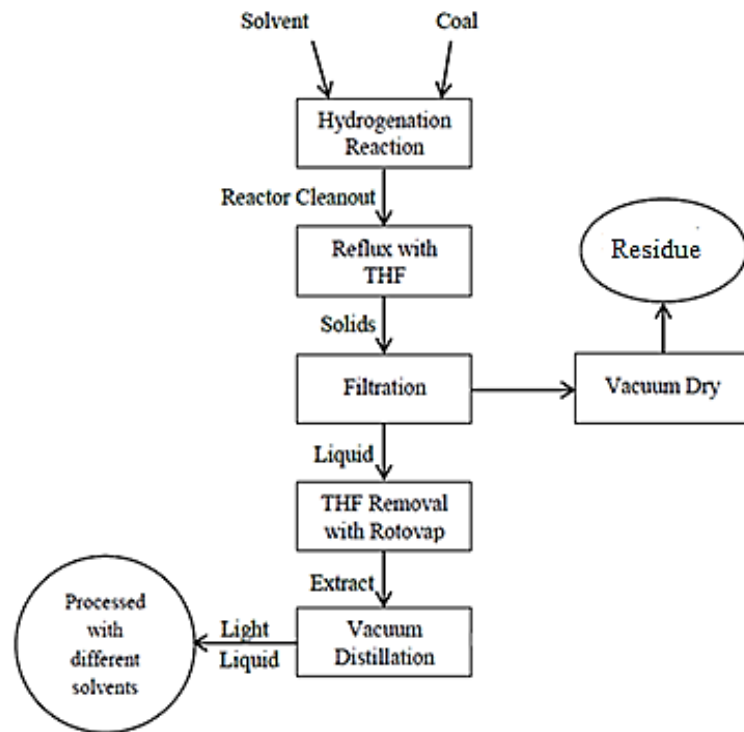
Figure 5–2: Direct Liquefaction Block Flow Diagram

Solvent extraction is a method for separation of materials of different chemical types and solubilities by selective solvent action. It utilizes the fact that some materials are more soluble than others in certain solvents, resulting in preferential extraction. In coal liquefaction studies, coal conversion is often described in terms of solubility of products in various solvents. The experimental procedure that is followed by most of the authors, during the liquefaction process, is shown in Figure 5-2.

A Buchi Roto-vapor R210 was used to separate (THF) from the extracts. The water bath was set to 60 °C and the vacuum to 260 mbar. The separation process took approximately 2 hours. After THF removal with rotary evaporator (Figure 5-3) coal liquids are processed with different solvents to obtain weight fraction of each lump such as asphaltenes, preasphaltenes and oils. Preasphaltenes material can be precipitated with benzene or toluene.

The extract was first processed with 100ml toluene to obtain (toluene insoluble) material present in the coal liquid. The residue (toluene insoluble) was left at room temperature overnight to eliminate remaining toluene to measure the weight percent. The toluene soluble was distilled in a rotary evaporator from the mixture at 60°C and 76 mm Hg to remove toluene. Then the liquid sample without toluene was treated with n-Heptene causing precipitation of asphaltenes.
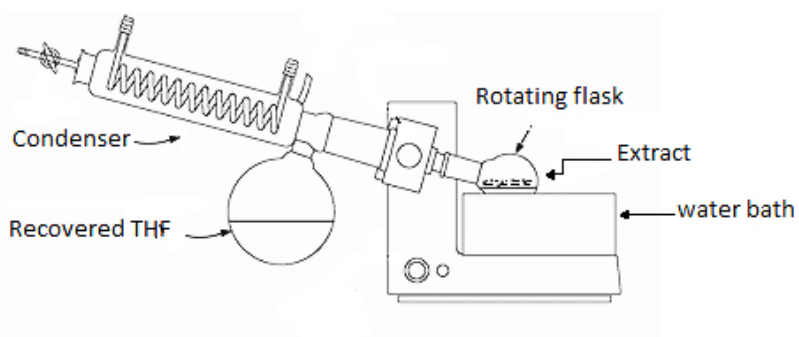
Figure 5–3: Rotary Evaporator for the Recovery Solvent [175]

Figure 5-4 shows sequence of direct coal liquefaction experiments which are proposed by most of the authors. The kinetics models can be proposed based on the data obtained from the mass balance and different time-temperature history. Different kinetic models have been proposed and examined to describe distributions of products such as preasphaltene, asphaltene, oil and gas. Rate constants for each of the specified reaction network have been calculated by nonlinear regression analysis.
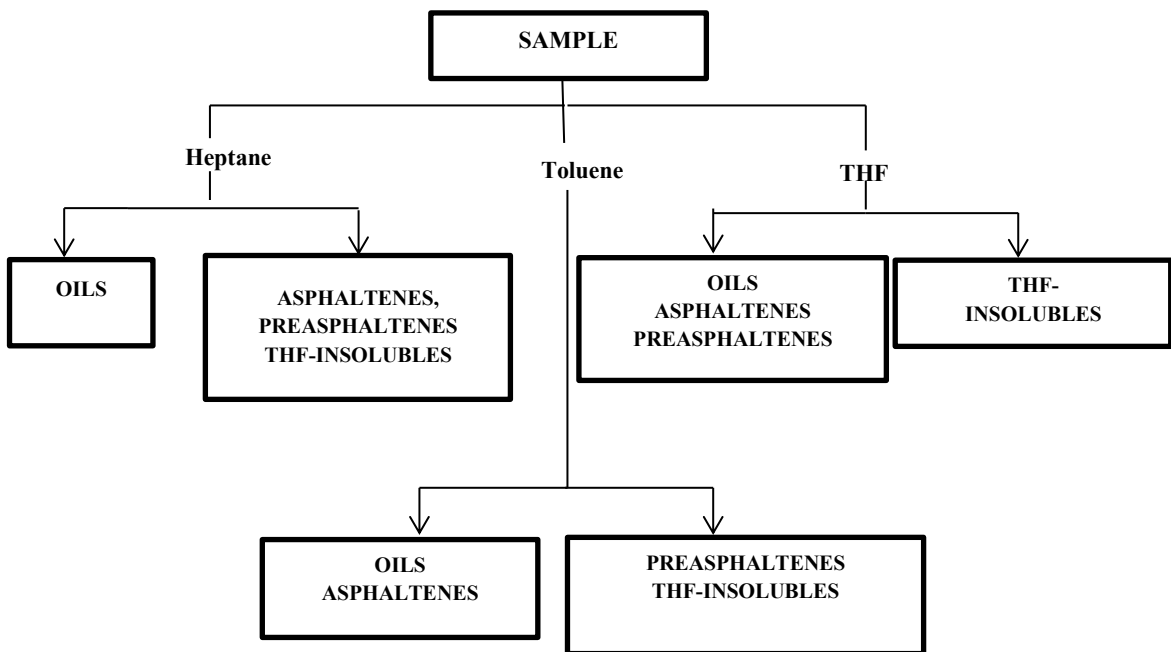
Figure 5–4: Direct Coal Liquefaction Sequence [107]

Preasphaltenes:

This fraction is consisted of complex polyaromatic compounds containing a certain amount of nitrogen and polar functional groups such as OH, generally having molecular weights between 400 and 2000. Preasphaltene is one of the heavy products of direct coal liquefaction which can be generated as a result of thermal cleavage of coal network. This

product includes the highest heteroatoms and the lowest hydrogen to carbon ratio among all other coal products. Preasphaltenes fractions are called polar compounds since they comprise polar functional group such as hydroxyl group in their structures. The formation this product can reduce the efficiency of coal liquefaction process [138].

Asphaltenes:

The term refers to a chemically complex fraction described mainly by its solubility in an aromatic solvent such as benzene or toluene but insoluble in solvents such as pentane or heptane.

This component is obtained as a result of hydrocracking of larger molecular size such as preasphaltenes. This fraction has higher hydrogen to carbon ratio and less average molecular weight around 500 in comparison to preasphaltenes [139,140].

Oils:

Oils are defined as those components which are soluble in solvents such as heptane or pentane with higher hydrogen to carbon ratio among other coal liquid products. Oils generally produced as a result of hydrogenation of higher molecular weight components and contain less heteroatom which make them more readily suitable as a clean fuel for industry applications [82].

5.3.1 Proximate and ultimate analysis

The as received coal sample contained high moisture content and was dried in vacuum oven at 80 °C for 8 h until a moisture content of 9.5 % was achieved. The representative samples were taken for proximate analysis according to the ASTM D7582 by Macro Thermogravimetric Analyzer and ultimate analysis according to ASTM D3176 in Elemental Vario MICRO Cube.

Three crucibles was filled with approximately one gram coal and placed into Macro Thermogravimetric Analyzer. All calculations for obtaining proximate analysis have been done by this equipment.

Density of lignite coal also measured by adding 10 g dry coal to 40.0 ml deionized water. The density of coal sample was calculated by subtracting of volume of coal plus water from volume of water. The density of 1.35 g/cm3 was obtained for lignite sample. These results are presented in Table 5.2

Table 5-2: Characteristic of the lignite coal sample

Proximate analysis	Mass (%)	Ultimate analysis	Mass(% daf)
Moisture	9.46	C	44.63
Volatile Matter	43.12	H	4.68
Ash	21.15	N	0.66
Fixed carbon	26.27	S	0.57
Density/gcm^{-3}	1.35	O*	49.46

daf =Dry and ash free basis; *Obtained by difference.

5.4 Factors affecting coal liquefaction

Despite current developments in coal liquefaction, the interactions and effects of different process variables are not completely understood. In order to optimize coal liquefaction process, some major process factors should be balanced. The optimal product yield can be achieved by managing the temperature-time, pressure, solvent to coal ratio. Some of these variables are studied here.

5.4.1 Temperature-time

Generally, the direct coal liquefaction process includes decomposition of the macromolecular structure of coal into free radicals at high temperature and stabilization and hydrogenation of those free radicals to prevent retrogressive reactions in order to have low molecular weight products.

At low temperatures usually below 350 ºC conversion is low and very little chemical reaction takes place and small molecules are dragged out of the coal matrix due to interactions between the hydrogen donor solvent and the coal molecules. The cross-linking is provided by relatively weak bonds such as methylene, sulfide, disulfide, or ether linkages, and it is the thermal rupture of these labile bonds at temperatures around 350 ºC that is responsible for the initial stage of coal dissolution. With increasing the temperature, thermal decomposition of these bonds results in the formation of large free-radical species. Effect of temperature is remarkable at the early stage of liquefaction. The free radicals react by abstracting a hydrogen atom from a solvent molecule or from hydrogen atmosphere or by repolymerizing. If the free radical is successfully capped by hydrogen, products in lower molecular weight and richer in hydrogen than the original coal will be formed ,but if the free radical species is stable and in the presence of other free radical species, polymerization or retrograde reactions could take place. This is the basis for the formation of coke, char, and other large and insoluble molecular weight species [131]. These processes take place at very high temperature and time when the rate of decomposition is lower than recombination of free radical.

Huang et al. performed kinetics of coal liquefaction at low reaction times and high temperature. They believed that the liquefaction process does not normally occur at a low

temperature and hydrogenation of coal does not produce valuable products, while at a high temperature around 420 °C undesirable retrograde reactions could be dominant. Understanding this onset of retrograde reactions is of great importance for improvement of the direct coal liquefaction process. The Temperature not only affects the conversion, but also the degree and quantity of retrograde reactions, and the quality of liquid products [132]. Flatman et al. showed that an increased reaction temperature from 380 to 400 °C improved product yields by promoting the secondary decomposition reactions, while when the temperature increased to 450 °C retrograde reactions took place [131]. Rodriguez et al demonstrated that with increasing the temperature, the formation of free radicals increased and the optimal temperature for this process, based on quality of the products and reaction conversion took place at 425 °C [133]. Studying the reaction temperatures in these studies helps us to find appropriate temperature range and subsequently optimal temperature which maximum extraction yield takes place.

Thermal decomposition depends on temperature only. The free radical formation is also due to thermal effects (Temperature dependence) during dissolution process. Temperature influences on reaction rates, ultimate conversion, hydrogen availability from the coal and solvent, finding the optimal temperature is very significant to have high quality liquid products. Most of studies have been done under non-isothermal condition and kinetic model is not considered on complete time temperature history as the time required for the massive autoclave to reach the reaction temperature can be substantial.

Effect of time is also remarkable at early stage of liquefaction when most of component can be extracted at this stage. It has been reported that coal conversions are not considerable improved at longer residence times over 2 hours, although some changes may occur in the

product distribution. Moreover, the gas production is excessive at long reaction times in the reactor [134]. Temperature-time is thus the most important factor that alters quality of product and reaction rate.

5.4.2 Pressure

In direct coal liquefaction process, high pressure is desirable as it keeps the solvent in liquid phase in order to prevent solvent evaporation and avoids the retrograde reactions.

The hydrogen can come from different sources: the solvent, gaseous H_2 or from the coal itself. The most efficient source of hydrogen for quenching the free radicals is the hydroaromatics in the solvent. However, when their concentration is low, molecular hydrogen can take part in quenching the free radicals [141]

Tang et al investigated the effect of initial hydrogen pressure on liquefaction process with tetralin as a solvent and concluded that the conversion of coal and yield of oil increased when the initial pressure of hydrogen changed from 6MPa to 8MPa, the change is 3.48% and 5.3%. The trend was little when changing from 9MPa to 10MPa. The results showed the effect of pressure on conversion was prominent at lower pressures rather than higher pressures [142].

In contrast several researchers believe that pressure has no considerable effect on coal liquefaction and conversion.

In study by Abichandani et al about short contact time coal liquefaction, they reported that the hydrogen pressure had no significant effect on the conversion and production distributions [113].

Okuma also showed that no pressure effects were found between 14.7 and 18.6 MPa [143]. Cai et al studied rapid injection of lignite coal by using a tubular reactor and found

total conversion marginally increased from 25.4% to 26.1% when pressure was increased from 10 to 15 MPa [144].

Miura et al examined the effect of the pressure on the product yields and concluded that no appreciable difference was found in the extraction yield at 10 and 20 MPa of pressure [145].

In some literatures the experiments have been done at low residence time and the authors investigated the effect of pressure at short reaction time. This arises from the fact that in the initial stage of reaction where free radicals formed from thermal reactions seek stabilization by abstracting hydrogen from solvent rather than hydrogen gas atmosphere. In the presence of a good donor solvent, coal liquefaction can proceed even at lower pressure and under nitrogen atmosphere [145]. It was found that when using a good donor solvent for liquefaction high conversion can be achieved under inert atmosphere [146].

In this study nitrogen is considered as gas atmosphere since excess good hydrogen donor solvent was available for all experiments and there was no need to use hydrogen gas atmosphere for coal conversion.

5.4.3   Solvent to Coal ratio

The solvent to coal ratio might be expected to have an influence on the coal liquefaction process. Investigators in the past have used ratios in the range of 1 to 18.

Hill et al performed a series of solubility experiments to find the optimum ratio of solvent to coal. They investigated the effect of solvent to coal ratio on coal liquefaction in tetralin at constant temperature and time. They found ratios greater than 8:1 the coal dissolved did not

increase. They used ratio of 10 for their kinetic studies to make sure that excess solvent was always available [102].

Rudnick et al showed that the coal conversions are not significantly improved for solvent to coal ratios greater than 7 [135]. Longanbach et al also concluded that changes in coal conversions at 425-440°C are relatively small for solvent to coal ratios between 2 and 5[136]. Abichandani et al studied Kinetics of Short Contact Time Coal Liquefaction at temperature and pressure ranges of 573-723 K and 10.3-13.8 MPa. They reported the solvent-to-coal ratio has no significant effect on the individual yields of pentane and toluene solubles, but for the THF solubles with an increase in the solvent-to-coal ratio the yields of products are significantly increased [113]. Shalabi et al considered a solvent to coal ratio of 10: 1 to remove solvent starvation effects and to assure that a sufficient supply of hydrogen donor species was available in the reaction condition to obviate the need for hydrogen for the experiments [110].

In the study by Vimal Kumar et al who investigated the solvent extraction of two different types of coal with solvent to coal ratio between 6:1 to18:1 and it was found that with increasing the solvent to coal ratio from 6:1,9:1,12:1,15:1 and 18:1 the extraction yields increased from 45.9% and 46.6% to 55% for both type of coals and then with further increasing it dropped to 48% and 49%.They found that the maximum extraction yield was obtained for 12:1 solvent to coal ratio [137]. Retrograde reactions which are dominant at high temperatures and long reaction times depend on hydrogen availability and can occur at temperatures as low as 400°C if very low solvent to coal ratios are used [133]. The solvent to coal ratio required for liquefaction should be optimum.

In this work to find the optimum solvent-to-coal ratio four experiments were carried out at constant temperature (400°C) and time. It was found that with increasing the solvent to coal ratio from 3:1, 5:1, 7:1 and 9:1 the extraction yields increased from 26.7%, 29.8 %, 31.6% and 31.8 % respectively. Lower limit for this experiment was kept 3:1 so that fluidity of the coal liquid can be maintained during the liquefaction experiment. Upper limit was kept 9:1 and above that was not tested because recovery of solvent would consume more energy and no significant effect was observed even at higher limit. Thus, the appropriate solvent-to-coal ratio of 7 was kept for all experiments to ensure that excess solvent was always present.

5.5 Result and discussion

5.5.1 Coal liquefaction conversion

Coal liquefaction conversion was calculated based on dry and ash-free by Equation (4-1) as discussed in chapter 4. The experiments were repeated under identical conditions to check the reproducibility of the results. In this experiment isothermal temperature was changed from 350°C to 450°C and the reaction time was changed from 15 to 120 min. The changes in total conversions are shown in Figure 5-5. The results show that the temperature had a strong positive effect on total conversion. This effect was most pronounced at the early stage of liquefaction as can be observed that slope of curves were sharper at initial stage where most of volatile matters are trying to evolve at this stage. Therefore, initial stage of coal liquefaction is highly temperature sensitive. On the other hand, the effect of time was also important at initial stage and this effect was lost for extended times at higher temperatures. This indicates that most of the liquid products were already extracted at the early stage of liquefaction.
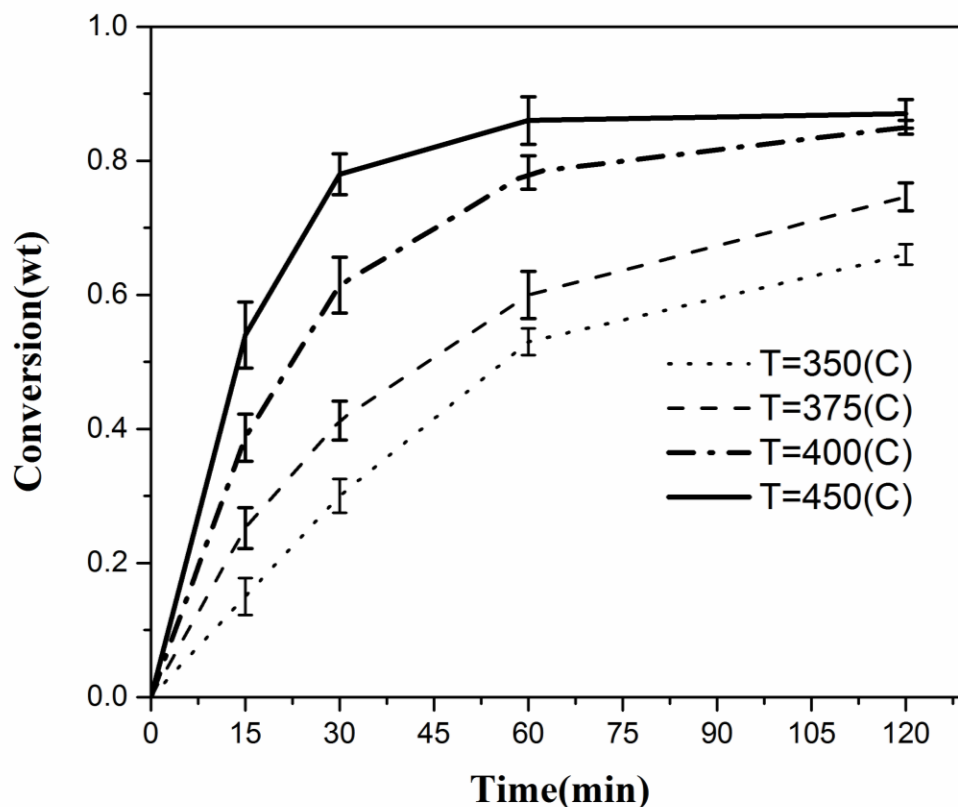
Figure 5–5: DCL conversion at different time-temperature

5.5.2 Mathematical Modeling

In order to obtain a better understanding of coal liquefaction process, a number of kinetic models have been undertaken. Several reaction networks have been proposed by various scientists in catalytic and non-catalytic condition as discussed in this chapter. Although almost all researchers have suggested first order irreversible reaction for their kinetic network, reversible reaction is also considered in the current study. Analysis of the reaction network needs estimation of parameters such as reaction rate constants, determination of the accuracy of parameter estimates and evaluation of the suitability of fit theoretical mechanism to the experimental data. The solidification of systematic methods for specification of parameters in non-linear models, and for selecting between alternative models is essential

and has been discussed a lot in the literature. Non- linear estimation of several parameters from data for these types of reaction systems is sometimes challenging. The data obtained in this work were correlated using six different kinetic models include series and parallel and were assumed based on various presumed theoretical mechanisms of direct coal liquefaction to preasphaltene, asphaltene, Oil and gas. One of the main goals of this study is to find which of these models can best describe coal liquefaction behavior. Based on the preferred model, a set of differential equations can be written to indicate the rate of formation of the products. Different six lumped kinetic models are considered to predict the product distribution. The assumptions made in the development of these kinetic models are briefly summarized below:

1. The reaction is considered as isothermal.

2. The reactions are first order with respect to the reacting species and the rate constants. This assumption is supported from previous research reported in the literature [99-126].

3. Reversible reaction is also considered in the reaction network. The results showed that at high temperature and extended time undesirable retrograde reactions may take place. Thus incorporation of reversible reactions in needed to predict residual concentration at high temperature.

4. Products of coal liquefaction include asphaltenes, preasphaltenes, oil and gas.

5. Mass transfer effect is negligible in this work. Coal disintegrates into smaller species almost instantaneously and particle does not remain intact under liquefaction condition. Moreover, the high activation energies suggested by previous scientists indicate that direct coal liquefaction was kinetically controlled rather than mass transfer controlled.

6. Hydrogen donor solvent is assumed to be present in excess in all runs and there was no need to use hydrogen gas atmosphere for experiments.

Based on these assumptions the rate of formation or depletion of various species can be explained as follows:

$$\frac{dX_i}{dt} = \sum k_i X_i \tag{5.1}$$

Where X_i represents weight fraction value of species i and k_i represents the specific rate constants.

Model 1

This model represents coal decomposition as a series and parallel reaction scheme involving the following steps:
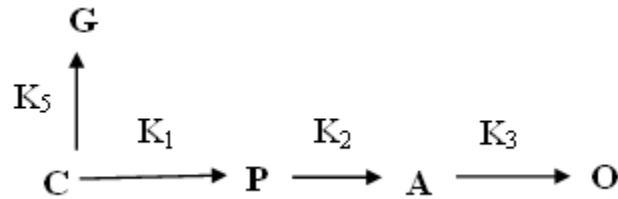
Where: C, reactive fraction of parent coal; P, preasphaltenes; A, asphaltenes; D, oils and G, gases.

The following differential equations display the rate of depletion and formation of reactants and products.

$$\frac{dC}{dt} = -(k_1 + k_5)C \tag{5.2}$$

$$\frac{\mathrm{d}P}{\mathrm{d}t} = k_1C - k_2P \qquad (5.3)$$

$$\frac{\mathrm{d}A}{\mathrm{d}t} = k_2P - k_3A \qquad (5.4)$$

$$\frac{\mathrm{d}O}{\mathrm{d}t} = k_3A \qquad (5.5)$$

$$\frac{\mathrm{d}G}{\mathrm{d}t} = k_5C \qquad (5.6)$$

The initial conditions represented by weight fractions are:

t = 0; C = a, P = A = O = G = 0.
t = t; C' = 1 - a + C

Where C' = unreacted coal, C = reactive fraction of coal at time t.

1 - a = unreactive fraction of coal and is found experimentally at longest reaction time.

a = reactive fraction of coal at time t = 0.

Incorporation of the concept of term (1 - a) is necessary since not all C will react at infinite time

These equations are first order differential equations and can be solved by the above initial conditions. First order differential equation is defined as:

$$\frac{\mathrm{d}y}{\mathrm{d}t} + yP(t) = q(t) \qquad (5.7)$$

$$\mu(t) = e^{\int p(t)dt} \qquad (5.8)$$

$$y(t) = \frac{\int \mu(t)q(t)dt + C}{\mu(t)}$$

(5.9)

Where $\mu(t)$ is integrating factor and $y(t)$ is weight fraction of components at specific time.

The analytical solutions of the differential equations are given by:

$$[C'] = 1 - a + ae^{-k_A t} \qquad , \qquad k_A = k_1 + k_5$$

(5.10)

$$[P] = \frac{ak_1}{k_2 - k_1}(e^{-k_A t} - e^{-k_2 t})$$

(5.11)

$$[A] = \frac{ak_1 k_2}{k_2 - k_A}\left[\frac{(e^{-k_A t} - e^{-k_3 t})}{k_3 - k_A} - \frac{(e^{-k_2 t} - e^{-k_3 t})}{k_3 - k_2}\right]$$

(5.12)

$$[O] = \frac{ak_1 k_2 k_3}{k_2 - k_A}\left[\frac{1}{k_3 - k_A}\left(\frac{e^{-k_3 t}}{k_3} - \frac{e^{-k_A t}}{k_A}\right) - \frac{1}{k_3 - k_2}\left(\frac{e^{-k_3 t}}{k_3} - \frac{e^{-k_2 t}}{k_2}\right)\right] + \frac{k_1}{k_A}$$

(5.13)

$$[G] = \frac{ak_5}{k_A}(1 - e^{-k_A t})$$

(5.14)

Model 2

This model is similar to model 1 but somewhat modified. In this model oils can be generated directly from preasphaltenes. The reaction network of this model is given here:
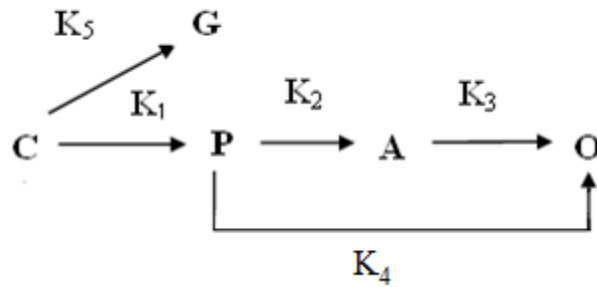
The following differential equations display the rate of depletion and formation of reactants and products.

$$\frac{dC}{dt} = -(k_1 + k_5)C \tag{5.15}$$

$$\frac{dP}{dt} = k_1 C - (k_2 + k_4)P \tag{5.16}$$

$$\frac{dA}{dt} = k_2 P - k_3 A \tag{5.17}$$

$$\frac{dO}{dt} = k_3 A + k_4 P \tag{5.18}$$

$$\frac{dG}{dt} = k_5 C \tag{5.19}$$

The solutions of the differential equations are given by:

$$[C'] = 1 - a + ae^{-k_A t} \qquad , \qquad \begin{aligned} k_A &= k_1 + k_5 \\ k_B &= k_2 + k_4 \end{aligned} \tag{5.20}$$

$$[P] = \frac{ak_1}{k_B - k_A}(e^{-k_A t} - e^{-k_B t}) \tag{5.21}$$

$$[A] = \frac{ak_1 k_2}{k_B - k_A} \left[\frac{(e^{-k_A t} - e^{-k_3 t})}{k_3 - k_A} - \frac{(e^{-k_B t} - e^{-k_3 t})}{k_3 - k_B} \right] \tag{5.22}$$

$$[O] = \frac{ak_1 k_4}{k_B - k_A} \left[(\frac{e^{-k_B t}}{k_B} - \frac{e^{-k_A t}}{k_A}) \right] +$$

$$\frac{ak_1 k_2 k_3}{k_B - k_A} \left[\frac{1}{k_3 - k_A}(\frac{e^{-k_3 t}}{k_3} - \frac{e^{-k_A t}}{k_A}) - \frac{1}{k_3 - k_B}(\frac{e^{-k_3 t}}{k_3} - \frac{e^{-k_B t}}{k_B}) \right] + \frac{k_1}{k_A} \tag{5.23}$$

$$[G] = \frac{ak_5}{k_A}(1 - e^{-k_A t}) \tag{5.24}$$

Model 3

This model is very similar to model 1 with a minor change in the reaction network. In this model oils can be generated directly from coal. It is similar to one employed by Radomyski

who found that a series-parallel model was more accurate than the models based on only series or only-parallel pathways.
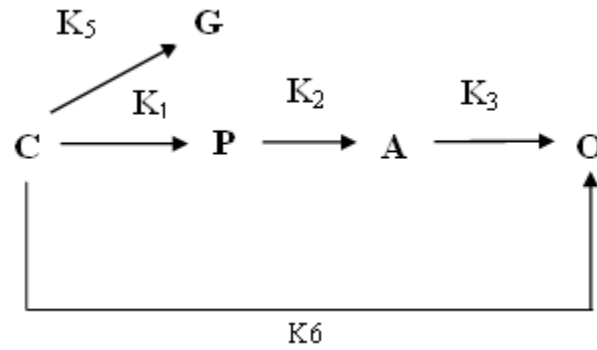
The following differential equations represent the rate of disappearance and formation of species.

$$\frac{\mathrm{d}C}{\mathrm{d}t}=-(k_1+k_5+k_6)C \tag{5.25}$$

$$\frac{\mathrm{d}P}{\mathrm{d}t}=k_1C-k_2P \tag{5.26}$$

$$\frac{\mathrm{d}A}{\mathrm{d}t}=k_2P-k_3A \tag{5.27}$$

$$\frac{\mathrm{d}O}{\mathrm{d}t}=k_3A+k_6C \tag{5.28}$$

$$\frac{\mathrm{d}G}{\mathrm{d}t}=k_5C \tag{5.29}$$

The solutions of the above differential equations based on the mentioned methods are given by:

$$[C'] = 1 - a + ae^{-k_A t} \quad, \quad k_A = k_1 + k_5 + k_6 \tag{5.30}$$

$$[P] = \frac{ak_1}{k_2 - k_1}(e^{-k_A t} - e^{-k_2 t}) \tag{5.31}$$

$$[A] = \frac{ak_1 k_2}{k_2 - k_A}\left[\frac{(e^{-k_A t} - e^{-k_3 t})}{k_3 - k_A} - \frac{(e^{-k_2 t} - e^{-k_3 t})}{k_3 - k_2}\right] \tag{5.32}$$

$$[O] = 1.0 - (C' + P + A + G) \tag{5.33}$$

$$[G] = \frac{ak_5}{k_A}(1 - e^{-k_A t}) \tag{5.34}$$

Model 4

This model is combination of model 2 and 3 and all reactions are considered irreversible. In this model oils can be produced directly from coal, preasphaltenes and asphaltenes. The reaction network is given by:
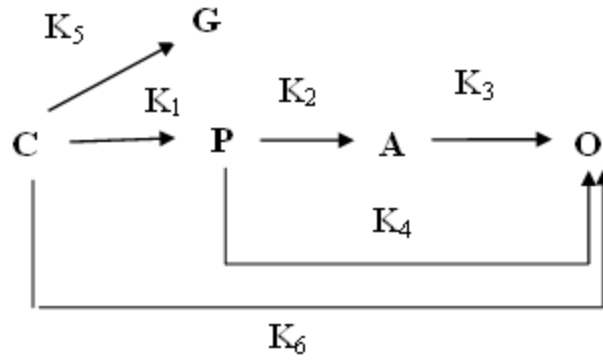
The following differential equations represent the rate of disappearance and formation of species.

$$\frac{dC}{dt} = -(k_1 + k_5 + k_6)C \qquad (5.35)$$

$$\frac{dP}{dt} = k_1 C - (k_2 + k_4)P \qquad (5.36)$$

$$\frac{dA}{dt} = k_2 P - k_3 A \qquad (5.37)$$

$$\frac{dO}{dt} = k_3 A + k_4 P + k_6 C \qquad (5.38)$$

$$\frac{dG}{dt} = k_5 C \qquad (5.39)$$

The solutions of the above differential equations based on the mentioned methods are given by:

$$[C'] = 1 - a + ae^{-k_A t} \quad , k_A = k_1 + k_5 + k_6 \quad \& \quad k_B = k_2 + k_4 \tag{5.40}$$

$$[P] = \frac{ak_1}{k_B - k_A}(e^{-k_A t} - e^{-k_B t}) \tag{5.41}$$

$$[A] = \frac{ak_1 k_2}{k_B - k_A}\left[\frac{(e^{-k_A t} - e^{-k_3 t})}{k_3 - k_A} - \frac{(e^{-k_B t} - e^{-k_3 t})}{k_3 - k_B}\right] \tag{5.42}$$

$$[O] = 1.0 - (C' + P + A + G) \tag{5.43}$$

$$[G] = \frac{ak_5}{k_A}(1 - e^{-k_A t}) \tag{5.44}$$

Model 5

This model is combination of previous models and includes all possible irreversible reactions. In this model coal can be converted directly to all liquid products. The number of kinetic constants in this model makes it more difficult to analysis in comparison with other previous models. The reaction scheme of this model is given here:
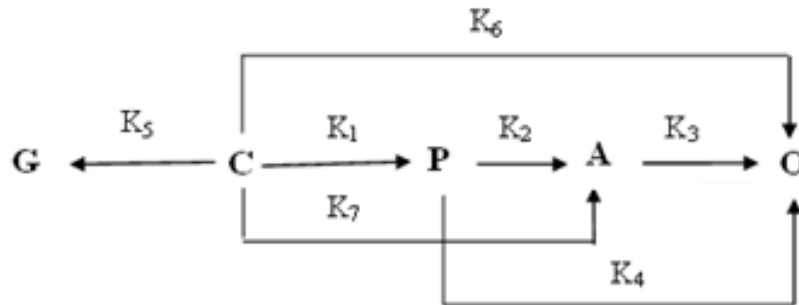
The following differential equations represent the rate of disappearance and formation of species.

$$\frac{\mathrm{d}C}{\mathrm{d}t} = -(k_1 + k_5 + k_6 + k_7)C \tag{5.45}$$

$$\frac{\mathrm{d}P}{\mathrm{d}t} = k_1 C - (k_2 + k_4)P \tag{5.46}$$

$$\frac{\mathrm{d}A}{\mathrm{d}t} = k_2 P - k_3 A + k_7 C \tag{5.47}$$

$$\frac{\mathrm{d}O}{\mathrm{d}t} = k_3 A + k_4 P + k_6 C \tag{5.48}$$

$$\frac{\mathrm{d}G}{\mathrm{d}t} = k_5 C \tag{5.49}$$

The analytical solutions of the above differential equations based on the mentioned methods are given by:

$$[C'] = 1 - a + ae^{-k_A t} \tag{5.50}$$

$$[P] = \frac{ak_1}{k_B - k_A}(e^{-k_A t} - e^{-k_B t}) \tag{5.51}$$

$$[A] = \theta(e^{-k_A t} - e^{-k_3 t}) - \beta(e^{-k_B t} - e^{-k_3 t}) \tag{5.52}$$

$$[O] = 1.0 - (C' + P + A + G) \tag{5.53}$$

$$[G] = \frac{ak_5}{k_A}(1 - e^{-k_A t}) \tag{5.54}$$

Where $k_A = k_1 + k_5 + k_6 + k_7$, $k_B = k_2 + k_4$

$$\theta = \frac{ak_7(k_B - k_A) + ak_1 k_2}{(k_B - k_A)(k_3 - k_A)} \quad \text{and} \quad \beta = \frac{ak_1 k_2}{(k_B - k_A)(k_3 - k_B)}$$

Model 6

This model is the preferred model in this study which assumes reversible reaction from oils to asphaltenes at higher temperatures. This model contains all possible reactions from coal to products. The reaction scheme of this model is given here:
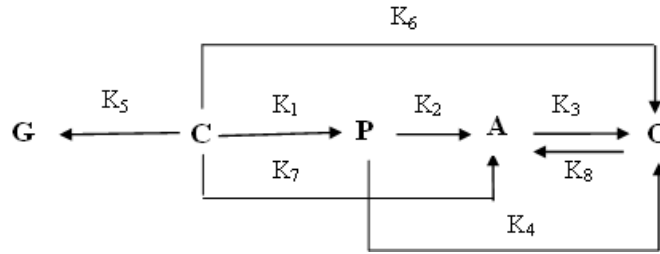
The following differential equations represent the rate of disappearance and formation of species.

$$\frac{dC}{dt} = -(k_1 + k_5 + k_6 + k_7)C \tag{5.55}$$

$$\frac{dP}{dt} = k_1 C - (k_2 + k_4)P \tag{5.56}$$

$$\frac{dA}{dt} = k_2 P - k_3 A + k_7 C + k_8 O \tag{5.57}$$

$$\frac{dO}{dt} = k_3 A + k_4 P + k_6 C - k_8 O \tag{5.58}$$

$$\frac{dG}{dt} = k_5 C \tag{5.59}$$

The analytical solutions of the above differential equations based on the mentioned methods are given by:

$$[C'] = 1 - a + ae^{-k_A t} \tag{5.60}$$

$$[P] = \frac{ak_1}{k_B - k_A}(e^{-k_A t} - e^{-k_B t}) \tag{5.61}$$

$$[A] = C_1(e^{-(k_3 + k_8)t} - 1) + C_2(e^{-k_A t} - 1) + C_3(e^{-k_B t} - 1) \tag{5.62}$$

$$[O] = 1.0 - (C' + P + A + G) \tag{5.63}$$

$$[G] = \frac{ak_5}{k_A}(1 - e^{-k_A t}) \tag{5.64}$$

$$C_1 = \frac{-(C_2 k_A + k_8 C_3 + k_7 a)}{k_3 + k_8}$$

$$C_2 = a\left[\frac{-k_1 k_2 k_A + k_1 k_2 k_8 + k_1 k_4 k_8}{(k_B - k_A)(k_A{}^2 - (k_3 + k_8)k_A)} - \frac{k_7 k_A - k_7 k_8 - k_6 k_8}{k_A{}^2 - (k_3 + k_8)k_A}\right]$$

$$C_3 = a\left[\frac{k_1 k_2 k_B - k_1 k_2 k_8 - k_1 k_4 k_8}{(k_B - k_A)(k_B{}^2 - (k_3 + k_8)k_B)}\right]$$

Where $k_A = k_1 + k_5 + k_6 + k_7$, $k_B = k_2 + k_4$

In general, the fit of these models to the experimental data becomes progressively better with an increase in the number of allowable transitions between the different lumped-classes. It might be argued that there is an optimum complexity of a reaction model can usefully be applied to coal conversion: If too complex, it becomes difficult to isolate a particular reaction pathway and measure its rate; if too simple the rates of a group of pathways are being measured effectively as the rate of one step, so that information about intermediate or

concurrent steps is omitted. Coal liquefaction reactions follow complex mechanisms including multiple series and parallel stages with different activation energies. Single reaction networks are not capable to show this type of complexity. In order to have a more accurate kinetic model, a multiple reaction network should be considered which can state explicitly the behavior of liquefaction process.

5.5.3 Product distribution

The comparison between model6 prediction and experimental product distributions at four different temperatures of 350°C, 375°C, 400 °C and 450°C are presented in Figure 5-6 to 5-9. The initial stage of process was found to be highly temperature sensitive. Products of initial reactions were largely preasphaltenes and asphaltenes with high dependency to reaction temperature. As could be seen from data, preasphaltenes were dominant during the first 30 min of the reaction time. Preasphaltenes have the highest average molecular weight in comparison with other coal products and was expected to be produced with high concentration at the beginning of the reaction as thermal cracking reactions are dominant at this stage. Asphaltenes, oils and gases are also formed at the beginning of the reaction with lower yields than preasphaltenes. The positive slope of concentration versus time for asphaltenes at the beginning of the reaction indicates that asphaltenes is also the primary product which is formed directly from coal and parallel to the preasphaltenes. This behavior was seen at all temperatures and can be properly described by the mechanism of coal liquefaction. Asphaltenes yield improved dramatically to a value of 24% and leveled off around 26% during the reaction at 400 °C, however this component at lowest temperature kept increasing almost linear. This behavior can be also explained mathematically with

115

respect to exponential factor of this component in the specific differential equation. As can be seen at lowest temperatures, the behavior of preasphaltenes, asphaltenes and oils are similar and follow almost linear trend. With the progress of time, the yield of oils and gases continued to increase at higher temperatures whereas yield of preasphaltenes gradually declined. Preasphaltenes yield at 375 and 400 °C increased to the maximum amount of 27% and 18 % then decreased. With the progress of thermal cleavage and hydrogenation of heavy products, lighter liquid products such as oils were formed. The highest oil concentration in the liquid product was obtained at 400 °C after 120 min of the reaction. This temperature can be considered optimum for producing oil as the most important component of liquefaction. Lower temperature regimes did not give considerable yield as the maximum oil yield about 20 % was observed after 2 hr. Figure 5-9 shows the product distributions at highest temperature. A good agreement has been found between experimental and predicted values by the model at this temperature. As discussed in the previous chapters, reversible reaction is considered in this model which occurred between asphaltenes and oils products at longer reaction time. Incorporation of retrograde reaction which is undesirable in coal liquefaction process allowed us to predict the residual high molecular weight concentrations at the end of reaction. Retrograde reactions can convert desirable small product molecules into undesirable larger macromolecules and can influence on liquefaction behavior observed at longer reaction times. As can be seen in the figure, the amount of oils leveled off and slightly decreased at this temperature in comparison with lower temperatures especially at 400 °C. Understanding onset temperature of retrograde reactions is substantial for development of DCL process. This behavior was also observed in GC-Ms analysis which will be discussed later in this chapter. These predictions are not predicted by previous works.
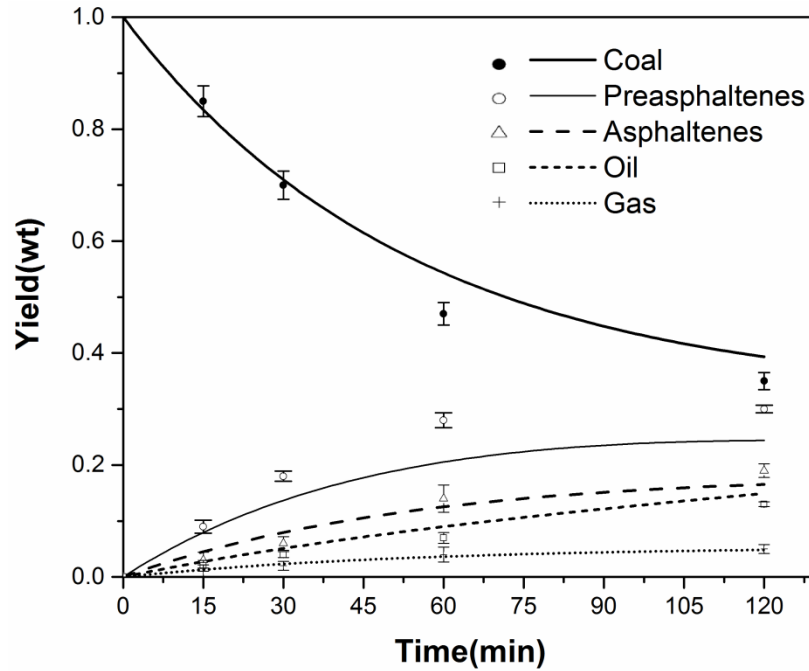
Figure 5–6: Comparison of experimental data (dots) and predicted values (lines) of product yield at 350 °C.
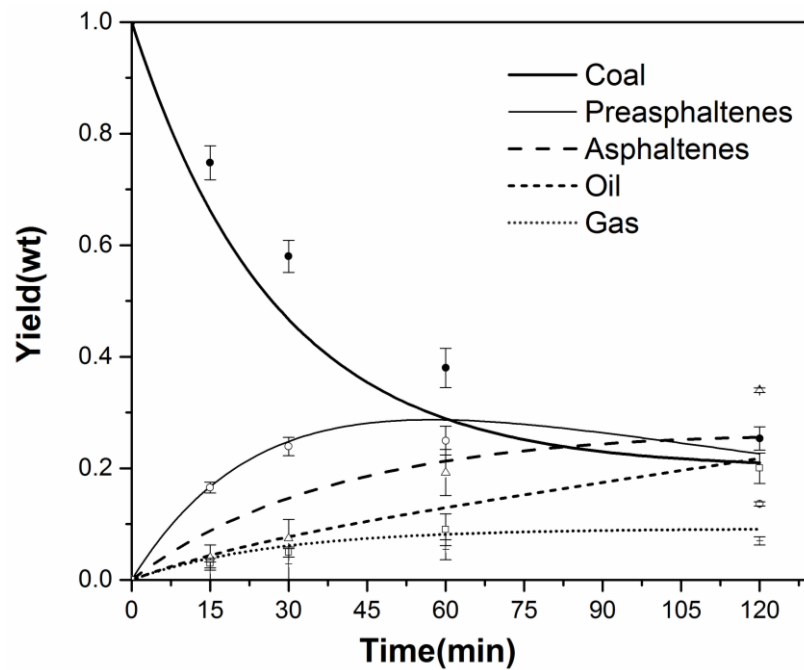
Figure 5–7: Comparison of experimental and predicted values of product yield at 375 °C.
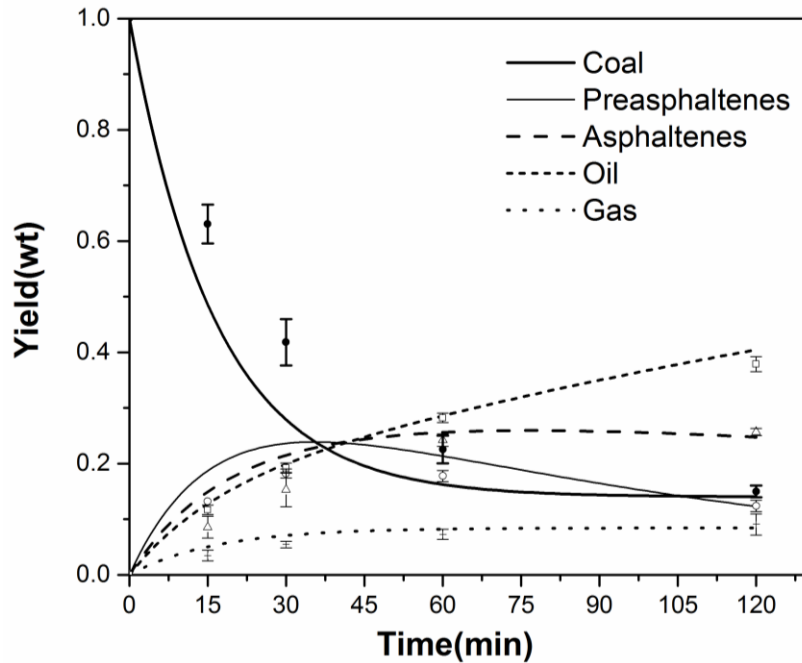
Figure 5–8: Comparison of experimental and predicted values of product yield at 400 °C.
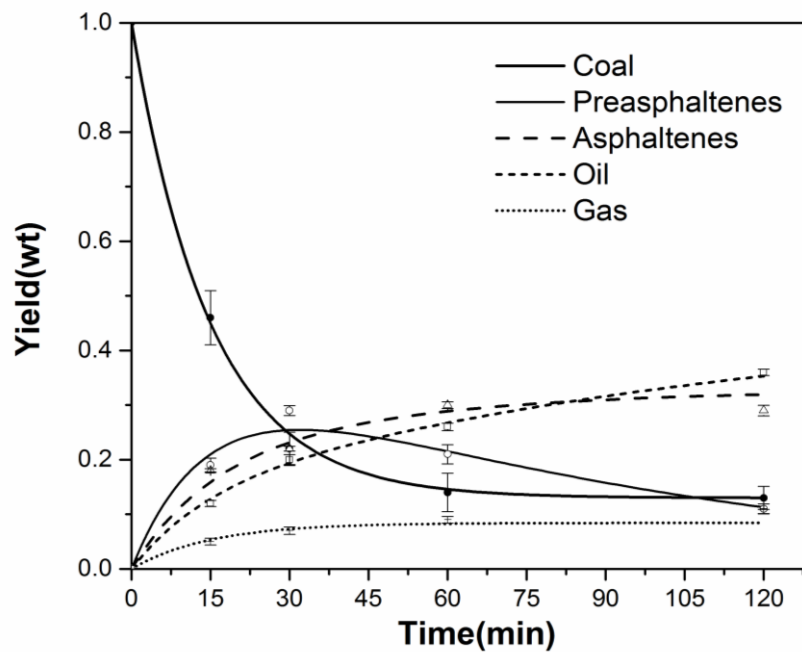
Figure 5–9: Comparison of experimental and predicted values of product yield at 450 °C.

The other five models were used also to fit the experimental data using the same procedure described earlier. These models are compared to their experimental data at 400°C. Model 1 exhibited the poorest fit to the data. This is because this model consists of sequential formation of products which the parallel reaction is not considered for other species except for one step. This result indicates that coal liquefaction cannot be explained in such simple models especially at high temperature. Model 2 was created by adding another possible reaction between preasphaltenes and oils. The error of this model was lower in comparison with previous model. Model 3 has different step which was not included in model 1 and 2. In this model oils can be formed directly from coal. It is obvious that series-parallel model is more accurate than the models based on only series or only-parallel pathways. This is because of the complex nature of coal liquefaction. Model 4 gave reasonably good fit especially at 400°C. This model is combination of model 2 and 3 and all reactions are considered irreversible. Model 5 is combination of previous models and includes all possible irreversible reactions. This model gave the best fit to experimental data in comparison with other previous model except for 450°C where reversible reactions become dominant at this temperature. Model 6 gave the best fits at all temperatures as discussed earlier and was considered the best model to describe the direct coal liquefaction behavior.

The accuracy of the six models under study was tested by calculating sum of square residuals between experimental data and predicted values. The model discrimination has been also evaluated by Bayesian information criterion (BIC) developed by Schwarz [167]. These deviations are shown in Table 5-3. It can be observed that the selected model gave minimum deviation among the six models which indicates the superior fit to the data.

$$BIC = n \ln\left(\frac{RSS}{n}\right) + k \ln(n) \qquad (5\text{-}65)$$

Table 5-3: Model discrimination

Model NO	RSS	BIC
Model 1	0.0938	-283.93
Model 2	0.0684	-295.22
Model 3	0.0347	-327.79
Model 4	0.0141	-367.15
Model 5	0.0095	-382.23
Model 6	0.0064	-397.31
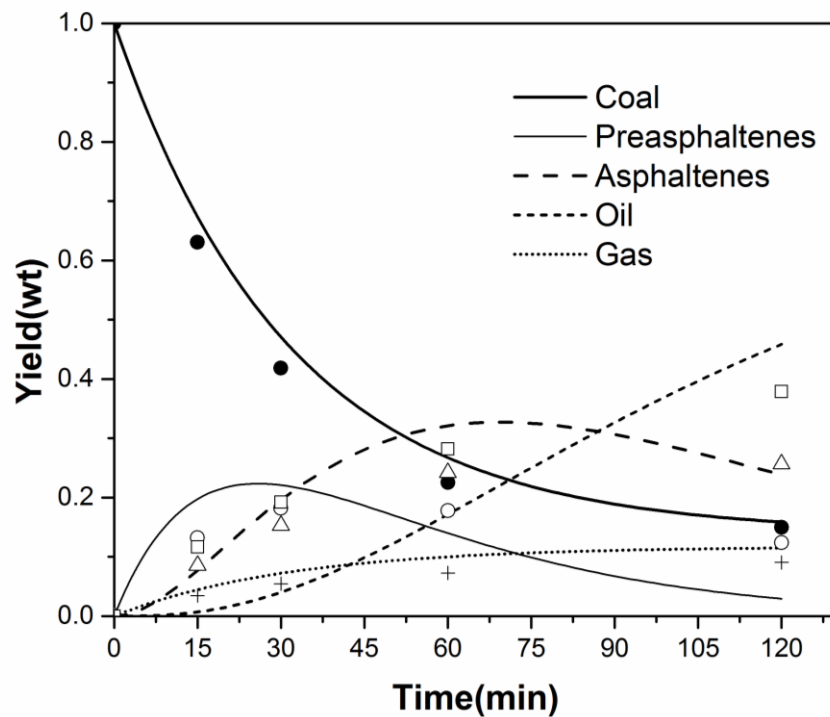
Figure 5–10: Comparison of experimental and predicted values of model 1 at 400°C
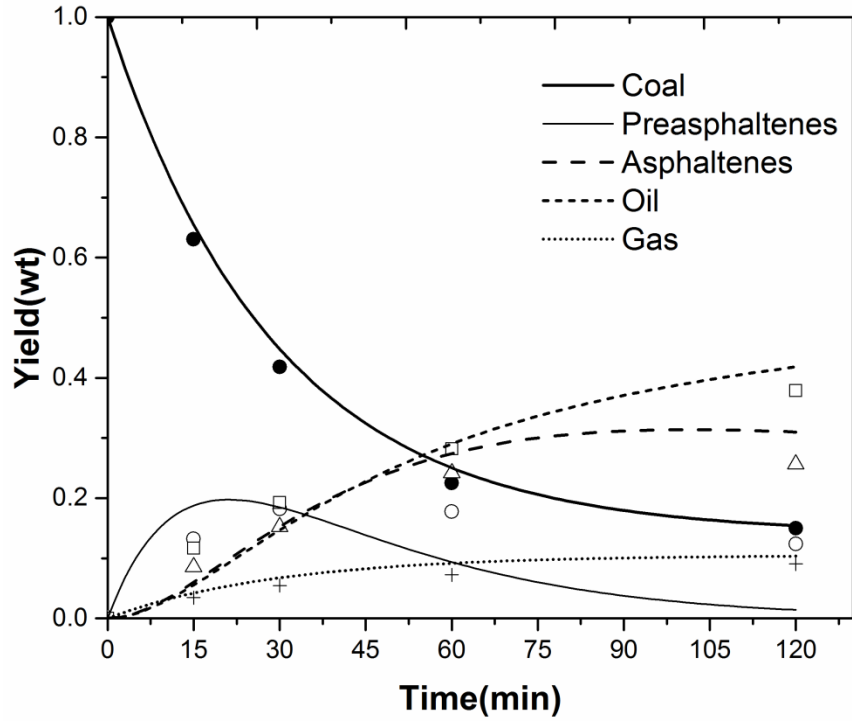
Figure 5–11: Comparison of experimental and predicted values of model 2 at 400°C
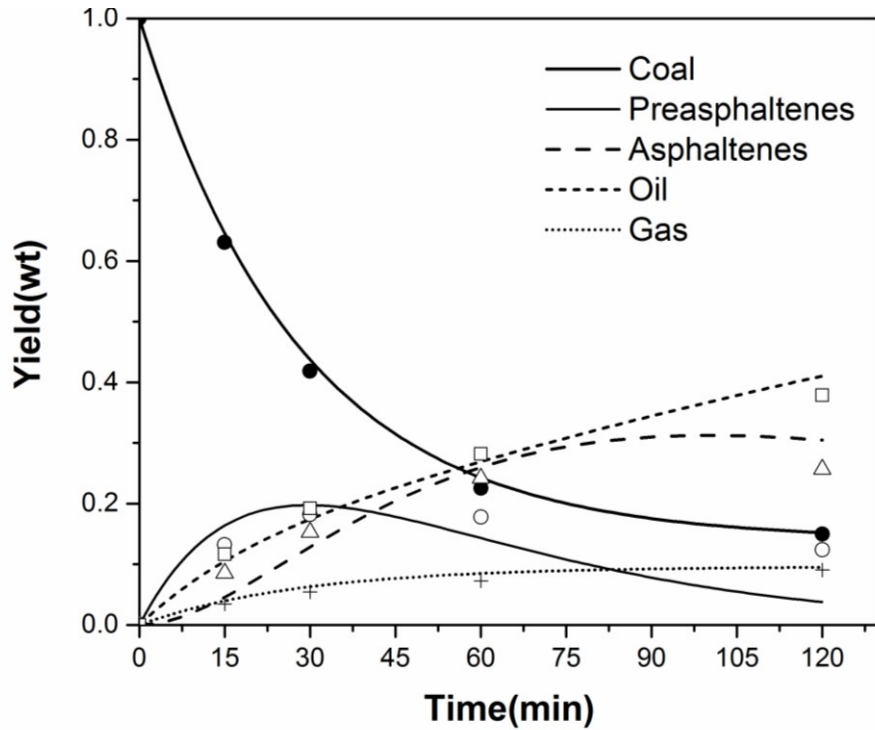
Figure 5–12: Comparison of experimental and predicted values of model 3 at 400°C
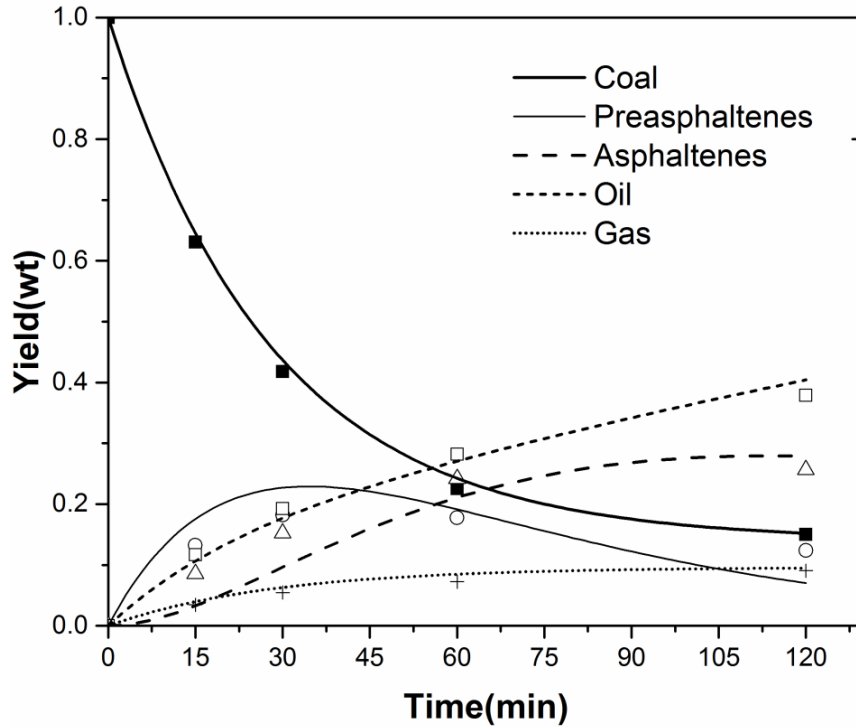
Figure 5–13: Comparison of experimental and predicted values of model 4 at 400°C
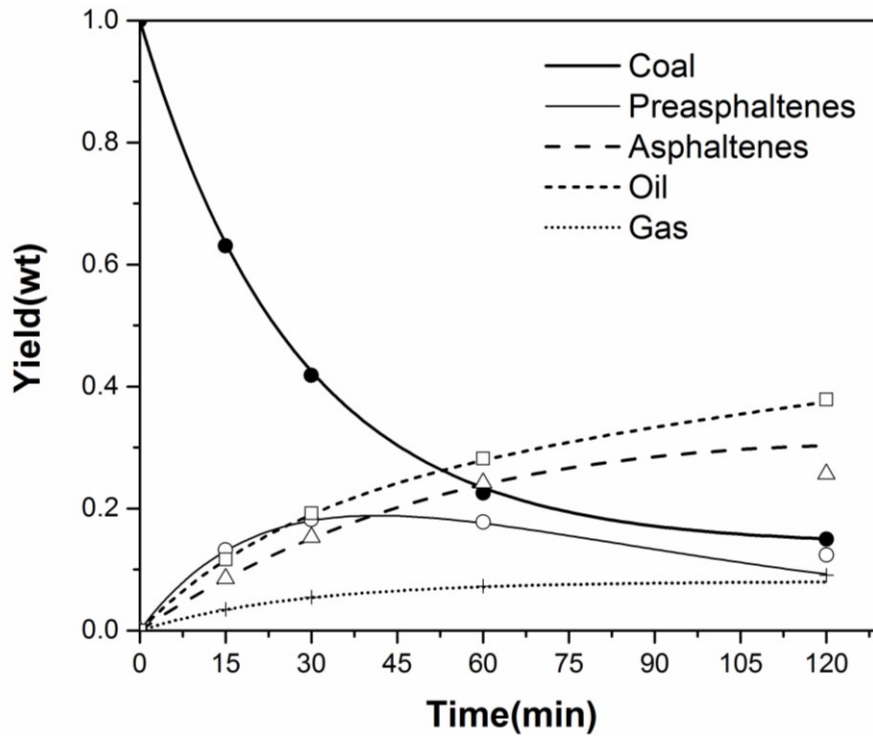
Figure 5–14: Comparison of experimental and predicted values of model 5 at 400°C

5.5.4 Scanning electron microscope (SEM)

In order to compare the variations in char morphology at different temperature-time, scanning electron microscopy was employed to follow the changes of coal physical structure using a JEOL 6301F device. Several images were taken and representative images were selected for further investigation. These pictures reveal the degree of decomposition as a function of temperature at relatively high magnification. The SEM images also exhibit porous structure of the liquefaction char. These results are shown in Figure 5-6 to 5-8. From these figures, it can be seen that temperature plays an important role in the decomposition process. In this study, four different time-temperature regimes were chosen and presented for visual observation and comparison. Figure 5-6 shows the SEM images of the raw coal (A) at two different magnifications and liquefaction residue obtained at 350(B),375(C), 400(D) and 450°C for 2 hours reaction time(E).
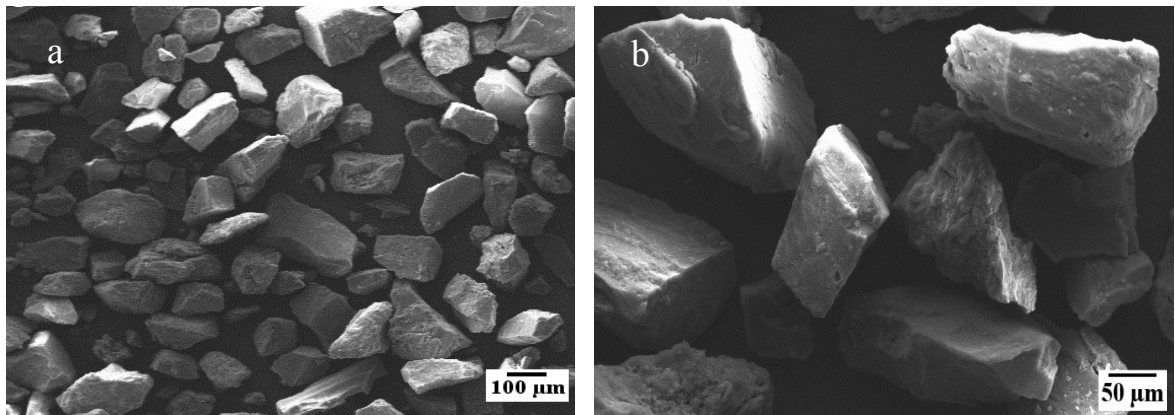
Figure 5-6: SEM images of raw coal at different magnifications; (a) 100X and (b)600X
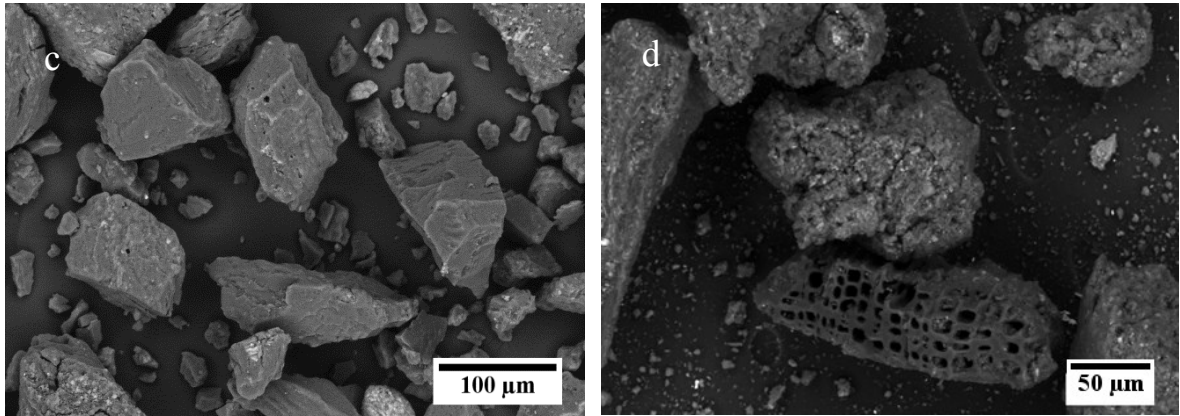
Figure 5-7: SEM images of residues; (c) 350°C and (d) 375°C
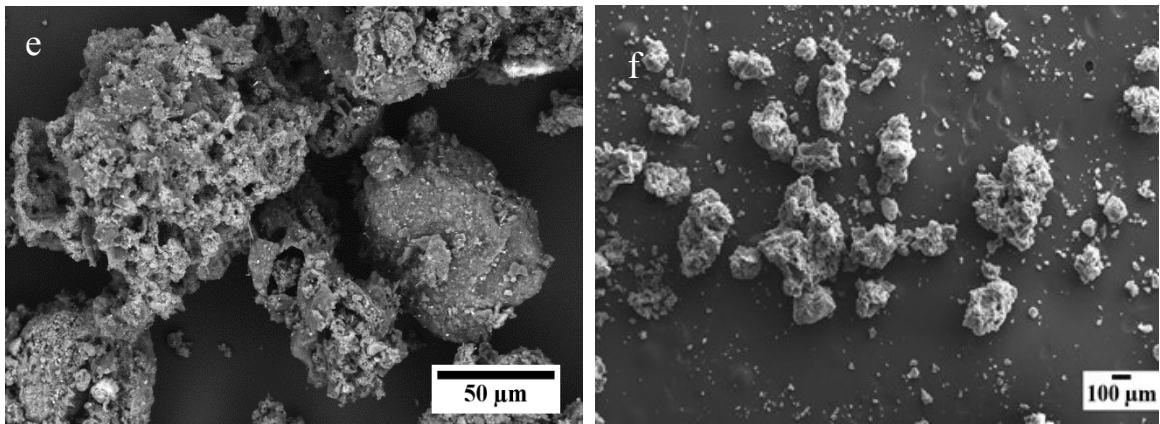
Figure 5-8: SEM images of residues; (e) 400°C and (f) 450°C

Figure 5-7 represents the liquefaction residue at lowest temperature regime. This residue was not expected to show major alteration as a result of swelling and thermal decomposition. Indeed, the temperature was not enough for complete thermal decomposition and disintegrates the coal particles. A closer look at Figure 5-7 (d) shows evidence of swelling and thermal decomposition of these particles and no evidence of agglomeration was observed

at this temperature-range. This initial decomposition stage is highly temperature sensitive, with the rate improving quickly as the temperature elevates from 375 to 400 "C.

The decomposition of the coal was drastic at this temperature and coal particles were disintegrated into shapeless structure which is in consistent with former works pointed on structural disintegration during devolatalization process [42,102,129,147-157]. At this stage porous structures were created and volatile matters were liberated from the coal network. At this temperature substantial disintegration has taken place and almost no original coal particles seem to remain intact. Therefore, the effect of initial coal particle size may not be important at elevated temperatures and longer reaction times implying that intraparticle diffusion is not a rate limiting parameter. At this stage size of cavities in particles developed. This morphological changing indicates that most acute reaction occurred over 400°C. These results indicate that the disintegration reaction takes place with rather high activation energy as indicated by the strong changes occurring with the relatively small changes in the temperatures. This high activation energy appears to imply that the coal liquefaction is more closely related to kinetically controlled, rather than a purely mass transfer controlled. Figure 5-8(f) presents SEM images of coal particles at highest temperature. This char photograph shows visual evidence of agglomeration at very high temperatures where rate of decomposition is higher than rate of hydrogenation, thus polymerization, i.e., retrograde reactions could take place. This is the basis for the formation of other large and insoluble molecular weight species. At very high temperatures about 450°C coal some particles were cleaved and dissolved during the liquefaction process and the others were agglomerated and generated larger size fraction than its original raw size during liquefaction. These effects are more pronounced at longer reaction times. Understanding onset temperature of retrograde

reactions is considerable for development of DCL process. One of the main improvements in this model was the inclusion of reversible reactions in the kinetic network as a result of retrograde reaction.

5.5.5 X-RAY diffraction analysis (XRD)

Powder XRD patterns were obtained using a Rigaku Powder X-Ray diffractometer which is equipped with a cobalt tube, graphite monochromator and scintillation detector. XRD analysis was performed on samples of the raw coal and coal liquefaction residues at different temperatures.

Figure 5-9 shows XRD spectra of raw coal and residues at four different temperatures. Quartz, calcium sulphate and pyrite were the main composition of the sample which are detected in the coal sample. Sodium, titanium and manganese were not found in the sample maybe because low concentrations of these elements exist in the coal. Generally most of the calcium in lignite coals is in the form of salts of humic acids. During the coal liquefaction the Ca humates in the coal decompose to form calcium carbonate solids as shown in XRD patterns and deposite on the reactor wall which can be a significant operational problem in a commercial plant [158, 159].

It has been reported that some inherent mineral matters such as pyrite can act beneficially as a catalyst for coal liquefaction [160, 161]. The major mineral transformations in the coal liquefaction seem to be reduction of pyrite to pyrrhotite and disappeared in the residue. The contribution of catalysis from mineral matters can be considered due to high ash content of the raw coal which can promote hydrocracking reactions of large fragments into smaller ones and hydrogenation of those molecules to stabilize them. The peaks intensity in residues are dramatically stronger than that of the raw coal which means that the residues

contain more mineral matters than raw coal. The residues obtained at higher temperatures have lower reactivity than those from less sever condition because most of volatile matters are evolved at higher temperatures and the organic structure of the coal which remains in the residue is more rigid and inflexible than those from less severe conditions.
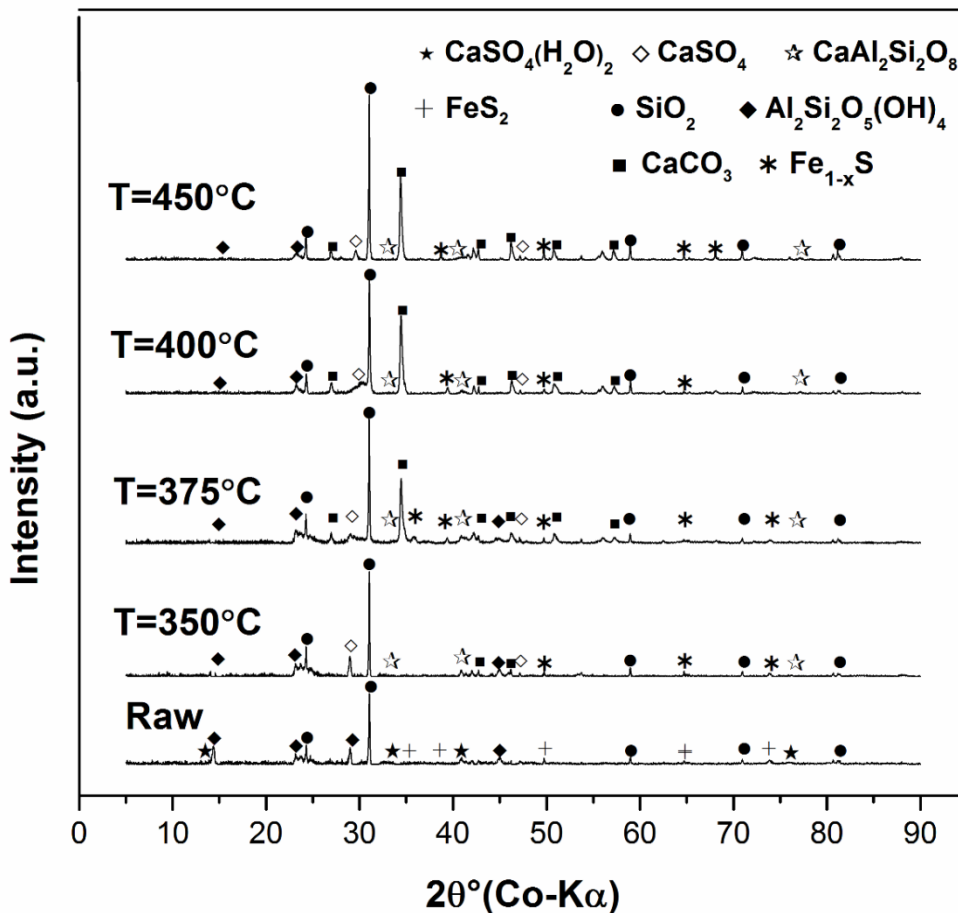
Figure 5-9: XRD spectra at different reaction temperatures

5.5.6 GC-MS analysis

A Varian CP3800 gas chromatograph with flame ionization detector (FID) and Saturn 2200 GC/MS ion trap spectrometer (Varian) were employed for analyzing the coal liquid. A

Helium carrier gas flow rate of 2 ml/min was used for GC column. A30m×0.25mm-id fused silica was used for the GC-MS work. The injector temperature was 300 °C .After removing THF from coal liquid, the extract was introduced to (GC-MS) for further analysis. The extract was obtained after reaction at four different temperatures and diluted in CS_2 to inject into gas (GC-MS).The results of gas chromatography of coal liquid at four temperatures are presented in Figure5-10 to 5-13.

Identification was based on the retention time and the mass spectral fragmentation pattern. It is believed that as a result of dehydrogenation of tetralin products naphthalene and dihydronaphthalene can be obtained [17,38,41,42,141,162,163,171]. The first peak of the GC spectra is decalin and the highest peak represents tetralin as hydrogen donor solvent. Main compounds of coal liquefaction are listed in Table 4.3. These results showed that even at low temperature and inert atmosphere hydrogen shuttling can takes place. At this region free radicals are formed due to thermal decomposition of bond linkages which can be capped by the abstraction of hydrogen atom from the donor molecule leading to formation of products with low molecular weight that can be dissolved in the solvent.
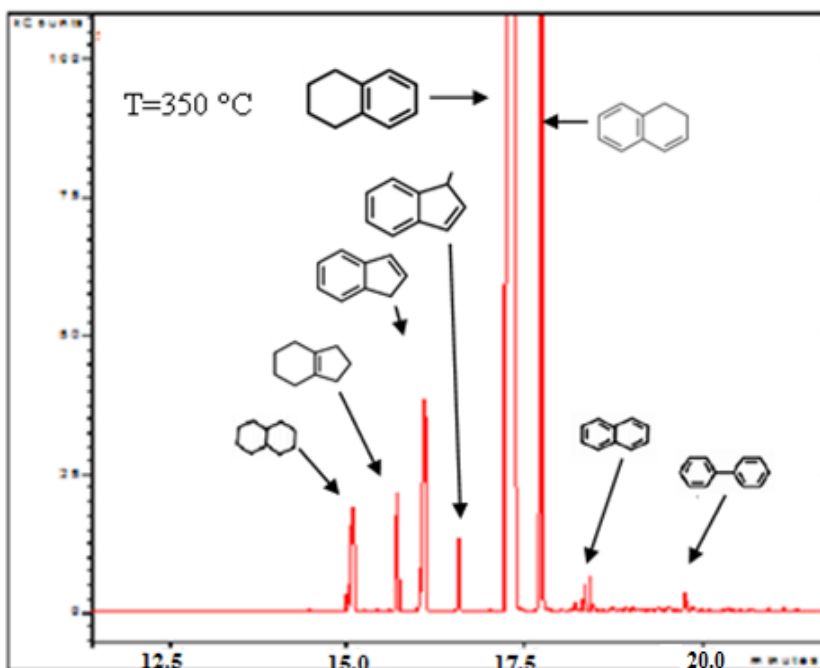
Figure 5-10: Gas chromatography of coal liquid at 350°C
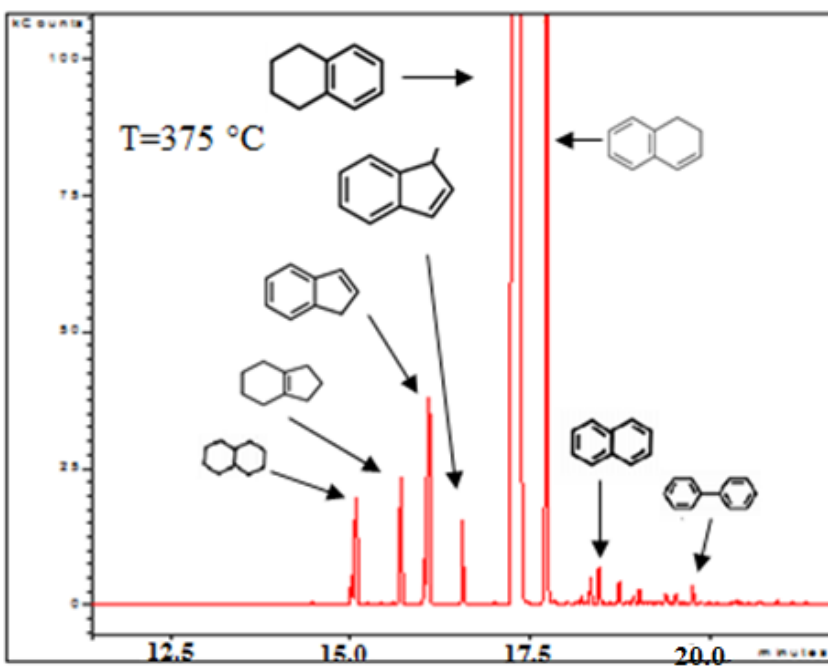
Figure 5-11: Gas chromatography of coal liquid at 375°C
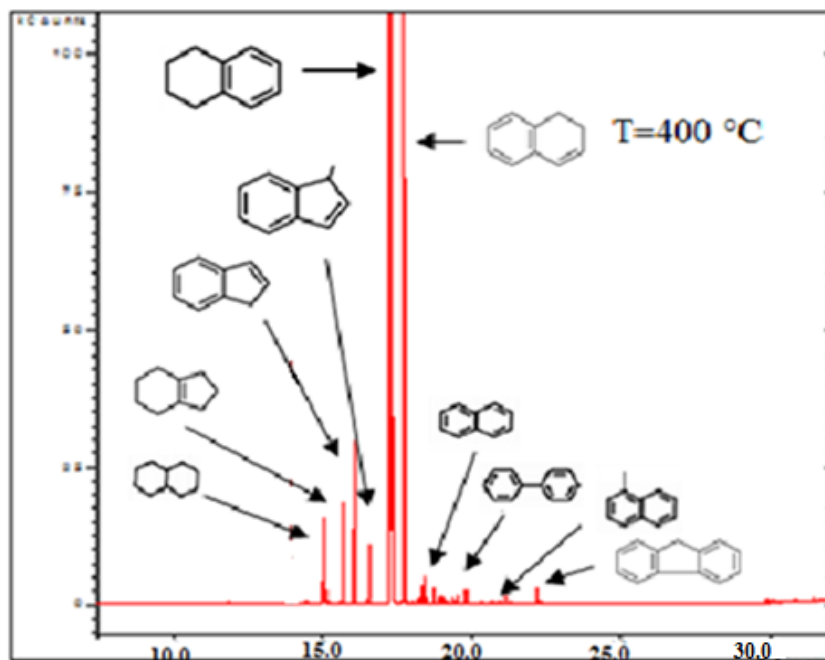
Figure 5–15: Gas chromatography of coal liquid at 400°C
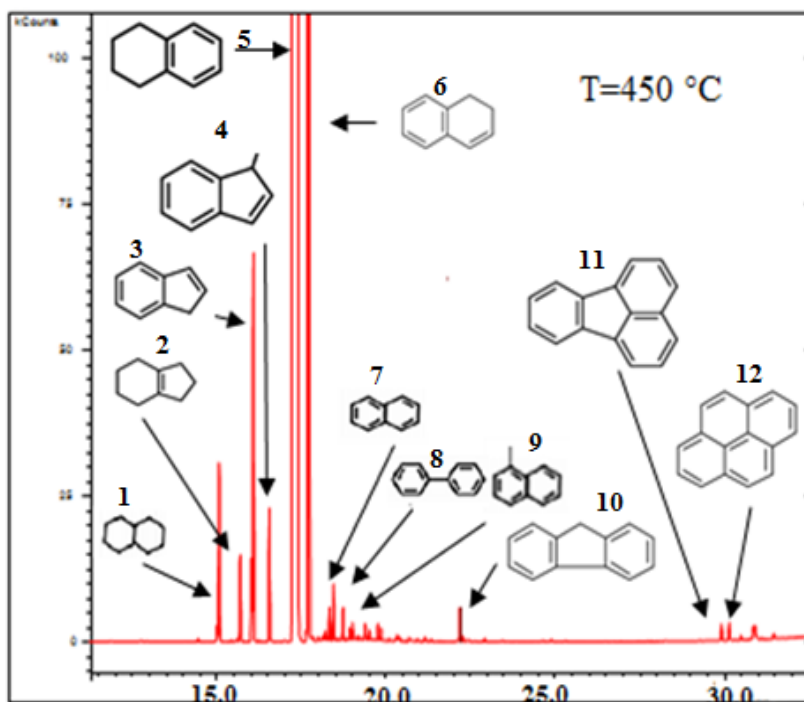
Figure 5-13 Gas chromatography of coal liquid at 450°C

It has been shown that the number of peaks as well as the intensity of peaks in the coal liquid obtained from different temperatures was changed and therefore the product distribution was formed in higher level at high temperatures compared to lower ones. It is shown at very high temperature (450°C) aromatic compounds are dominant at longer retention times. At this stage undesirable retrograde reactions with higher molecular weight can be produced which are discussed before. This result is in agreement with those previous results which discussed earlier. Therefore temperature is one of the most important factors that can alter quality of products.

CHAPTER 6

Optimization of kinetic parameters

6.1 Non-linear parameter estimation program

The aim of parameter estimation regression is to obtain the values of these parameters that cause the proposed equations to give the best possible fit to the data. The measure of fit depends on the residuals (differences between the observed values of certain variables and the values predicted by equations). A common measure of this difference is provided by sum of the squares of the residuals which is defined as Eq.6.64.

$$RSS = \sum_{i=1}^{n} (y_{i(exp)} - y_{i(cal)})^2 \qquad (6.1)$$

Where RSS is sum of the square of deviations, $y_{i(exp)}$ is the experimental concentration for component i, $y_{i(cal)}$ is the calculated value by the model.

6.2 Application of Genetic Algorithm (GA)

A genetic algorithm (GA) optimization method was applied to find the optimal set of parameters for the probability distribution functions. Genetic algorithm GA is an iterative numerical optimization method inspired by natural selection and evolution. Genetic Algorithms were developed by John Holland [164]. GA is generally exhibited as having higher flexibility and being more efficient with computation simulations than traditional optimization methods for nonlinear problems. The GA method succeeds in avoiding local extremum (minimum or maximum) that may result from using conventional optimization methods. GA is an efficient and powerful technique and has been broadly applied across a

number of research areas such as chemical engineering, medicine, economics, image processing that require optimization of complex nonlinear problems. GA generates improved solutions as succeeding populations evolve from former generations via operations of selection, crossover, and mutation. GA initiates with a population of primary solutions to a particular problem and evolves them towards the best solution. "Generation by generation this population is evolved in such a way that the best solutions win over the worst ones as in natural evolution" [165]. In this method, individuals (candidate solutions) which is a combination of a series of possible solution is randomly selected to generate an optimum solution, can be considered as an equivalent string. Each candidate solution has its own fitness that is applied to measure the quality of each candidate solution. The fitness is a representative of the survival potential and propagation capacity of an individual in the subsequent generations. Fitness is measured by the value of the objective function, i.e. least square calculated with each candidate solution. A candidate with a better value of fitness has this priority to be selected for reproduction. A population of randomly created candidates generates a discrete evolution which is known as a generation. The fitness of every candidate is calculated in each generation. Generally, a successive generation which contains individuals with an average fitness higher than the prior one due to the process of selection so each generation progressed itself through duplicate application of selection. The iterative nature of GA requests a terminate rule to end the algorithm. Normally it occurs when a fixed number of iterations is finished, maximum number of generations have been produced or the fitness level is reached a desired value. The individual with the best fitness in the final generation is occupied as the solution of the nonlinear optimization problem. The flow diagram of GA optimization is given here:
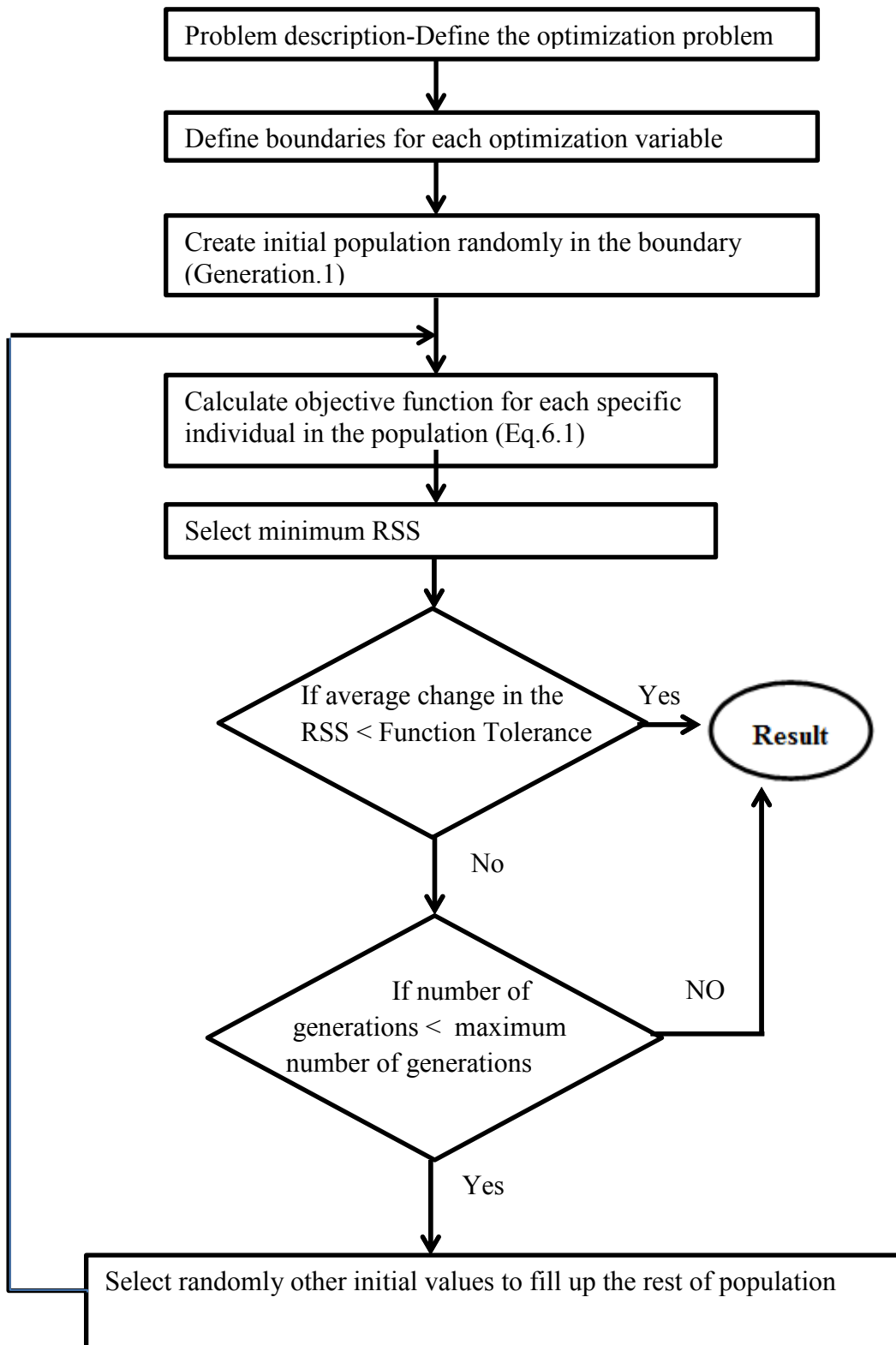
Figure 6–1: GA optimization flow diagram

The population size explains how many individuals are in a generation. A proper population size depends on the nature of the optimization problem. Too few individuals would leave GA with few possibilities to reach to the optimal point and may converge too quickly to a local optimal point that might not be the best answer. Too many individuals will make GA take longer time for any improvement. Therefore, the number of population size is important for each specific problem. The advantage of using GA over other conventional optimization methods is its global perspective to find optimal solutions. Moreover this method does not require an initial guess to be known for the problems being established to solve. Thus this method can provide a wide and pragmatic solution for many research areas.

6.3   Estimation of rate constants

The estimates of rate constants are shown in Table 6-1. These constants can be estimated by numerical solution of related differential equation and comparison of results with experimental data. Usually, conventional and sophisticated optimization methods have been used in the literature to estimate these constants as discussed above. To the best of our knowledge, there is no information regarding estimation of rate constants using genetic algorithm for modeling of direct coal liquefaction.

In this algorithm, rate constants defined as optimization variable and the boundaries for each rate constants are considered between (0-0.1). The iteration was terminated when our objective function became less than error criterion or maximum number of generation was reached. The kinetic constants obtained in this study were within the range of those predicted in the literature [106,110-112,116,120,166].

After calculating the rate constants by GA, they will be employed for solving differential equation by Runge-Kutta algorithm to find yield of liquid products. The activation energy

and frequency factor are calculated using Arrhenius equation. Model 6 which is considered the best model in this study was found to fit the experimental data properly for all temperatures. The magnitudes of the rate constants k_1, k_7, k_6, k_5 represent the significance of reactions leading directly from coal to pasphaltenes, asphaltenes, oils, and gases. Also the magnitudes of k_2, k_3, k_4 indicate the importance of the hydrocracking reactions preasphaltenes to asphaltenes, asphaltenes preasphaltenes to oils. Rate constant $k1$ was estimated highest among other constant which reveals the high amount of preasphaltenes at the beginning of the reaction. This model shows that the preliminary products of liquefaction are preasphaltenes and lesser amount asphaltenes. This is consistent with those previous researchers who believed that thermal cracking is the major contributor to coal liquefaction at the early stage of this process.

On the other hand, value of k_8 dictates the substance of retrograde reactions at high temperatures. Although rate constants of the reverse reactions are rather smaller than those of the corresponding forward reactions, they will not be negligible at high temperatures where these residual products become dominant. It was interesting that the magnitudes of kinetic constants k_1, k_7, k_6 were about the same order at high temperatures. The hydrocracking reaction of asphaltenes to oils proceeds favorably where as preasphaltenes to oils proceeds at lower rates. It can be assumed that the major oils compound in formed as a result of hydrogenation of asphaltenes rather than preasphaltenes. All kinetic constants extracted from this model followed Arrhenius equation. As could be seen in this table, with increasing the temperature, rate constants improve. The activation energies and frequency factors for this model are listed in Table 6-2. The activation energies changed from 48.3 KJmol^{-1} to 175.58 KJmol^{-1}.

These estimations are generally in good agreement with those given in the literature [50, 81,100,111,120,168,169]. The small discrepancy may be due to different reaction network and different feedstock used.

Table 6-1: Kinetic rate constants (min^{-1}) of model 6

T(°C)	k_1	k_2	k_3	k_4	k_5	k_6	k_7	k_8
350	0.00611	0.00198	0.00315	0.00049	0.00148	0.00292	0.00500	-
375	0.01707	0.00620	0.00492	0.00054	0.0042	0.00534	0.00933	-
400	0.02805	0.00802	0.00754	0.00196	0.00393	0.01372	0.01705	0.00112
450	0.03506	0.00914	0.01226	0.00211	0.00646	0.01415	0.01803	0.00876

Table 6-2: Kinetic parameters of direct liquefaction of lignite coal

	activation energy(KJmol^{-1})	frequency factor(min^{-1})
k_1	62.36	1.38×10^{03}
k_2	52.21	6.94×10^{01}
k_3	50.88	6.16×10^{01}
k_4	60.69	7.52×10^{01}
k_5	50.92	3.93×10^{01}
k_6	61.19	4.78×10^{02}
k_7	48.30	6.87×10^{01}
k_8	175.58	4.24×10^{10}

CHAPTER 7

CONCLUSION AND FUTURE WORK

7.1 Conclusion

The following main conclusions could be derived at:

- ## Drying methods

  1) Among three thermal drying methods as discussed in Chapter 3, Pretreatment by drying under vacuum condition represented highest conversion.

- ## Devolatilization

  1) Different devolatilization techniques such as the Kissinger method and the isoconversional methods of Ozawa, Kissinger-Akahira-Sunose and Friedman are employed and compared in order to analyze non-isothermal kinetic data and investigate thermal behavior of coals. The arithmetic means of the activation energy calculated by KAS, FWO and Friedman method are 282, 275, 283 kJ mol^{-1}, respectively, which are close to average activation energy obtained from the Kissinger method(281.03 kJ mol^{-1}). Experimental results showed that the activation energy values obtained by the isoconversional methods were in good agreement, but the Friedman method was considered to be the best among the model free methods to evaluate kinetic parameters for solid-state reactions. Among two samples of this work, sample No.1 exhibited lower activation energy as a result of pyrolysis. Moreover, the proximate and ultimate analysis of this

sample also was superior to the other one. It was thus chosen as the experimental sample in the present study.

➢ Particle size selection

1) Reactivity of lignite coals is high and contains fewer impurities such as Sulphur and heavy metal. It was thus chosen as the experimental sample in the present work.

2) The results presented and discussed in chapter 4 indicate that initial coal particle size can be considered an important factor for coal liquefaction. The results showed that liquefaction of coal in the presence of hydrogen-donor solvent affected total liquefaction conversion at short reaction time where most of the volatile matters evolved at this stage. In this study, particle size (150-212 µm) was detected for the subsequent kinetic modeling experiments. Image analysis of particles has been performed with Image J software to show the disintegration phenomena during coal liquefaction experiment. These results are presented in APPENDIX A.

➢ Kinetic modeling

1) The results show that lignite coal is readily liquefied, with its conversion exceeds 80% at 400 °C. Six different kinetic models have been proposed and examined to describe distributions of products such as preasphaltene, asphaltene, oil and gas. It can be concluded that simple models did not provide an adequate representation for coal liquefaction especially at high temperature.

2) The capability of the fit for all six models was tested by computing the sum of the square of deviations and BIC method at average temperature. Model 6 was considered to be the best among the six models studied and gave minimum deviation which indicates the superior fit to the data.

3) The results of this work showed that at high temperature and extended time undesirable retrograde reactions may take place. Thus incorporation of reversible reactions in needed to describe the residual concentration especially at high temperature. In this study the reaction network incorporated all series, parallel and reversible reaction steps to provide suitable expressions for direct liquefaction of coal and also to show the complexity of coal liquefaction.

4) This research also differs from previous studies in application of genetic algorithms (GA) for solving the nonlinear mathematical models. A genetic algorithm (GA) optimization method was applied to find the optimal set of kinetic parameters. The GA technique achieved in avoiding to be trapped in local extremum (minimum or maximum) that may result from using conventional optimization methods. Rate constants for each of the specified reaction network have been calculated by nonlinear regression analysis. The fourth order Runge-Kutta algorithm was applied to solve the set of differential equations for each model. The activation energies were obtained using Arrhenius equation. A good agreement has been found between experimental and predicted values by the model. These results are also useful to predict product distribution at different temperature and time under non-isothermal condition.

7.2 Recommendations for future work

1) Although lignite coals have similar composition, the kinetic parameters can be estimated for a few typical lignite coals with H/C and fuel ratio as input parameters for calculation of kinetic constants.

2) It is recommended to develop a comprehensive model which can treat a wide variety of coals and solvents under different conditions. Liquefaction runs with different coals and estimation of kinetic parameters using the same objective function or using design of experiment techniques would give the required background for such studies.

3) The mineral matters in coals are believed to have catalytic effects. Performing Experiments after coal deashing may give helpful information for these studies. Also it is useful to do petrographic analysis to measure the inert component of organic part of coal. This may give us the insight how to predict the maximum conversion that we can obtain at extended times.

4) Although tetralin is broadly used in the coal liquefaction studies as a good hydrogen donor solvent, the alternate solvent such as coal-drived liquid can be considered for liquefaction experiments.

5) Even though Canadian lignite coal is readily liquefied with high extraction yields even without catalyst, it is perhaps preferable to carry out liquefaction runs under catalytic condition to investigate the effect of catalyst on product distribution.

BIBLIOGRAPHY

[1] International energy Agency, "World Energy outlook" Available at: http:// www.iea.org.

[2] Vasireddy, S., Morreale, B., Cugini, A., Song, C., & Spivey, J. J. (2011). Clean liquid fuels from direct coal liquefaction: chemistry, catalysis, technological status and challenges. Energy & Environmental Science, 4(2), 311-345.

[3] Elliott, M. A. (1981).Chemistry of coal utilization. Second supplementary volume, John Wiley, New York, 1845-1910.

[4] Khan, M. R. (Ed.). (2011). Advances in clean hydrocarbon fuel processing: science and technology. Woodhead Pubishing Series in Energy,15-29.

[5] Spaite, P. W. (1986).Emerging clean coal technologies.3-51.

[6] Prasad, G. N., Wittmann, C. V., Agnew, J. B., & Sridhar, T. (1986). Modeling of coal liquefaction kinetics based on reactions in continuous mixtures. Part I: Theory. AIChE journal, 32(8), 1277-1287.

[7] Schobert, H.H.(1987).Coal, the energy source of past and future .ACS Publications, 614,41-53

[8] Lee, S., Speight, J. G., & Loyalka, S. K. (Eds.). (2007). Handbook of alternative fuel technologies. CRC, 17-123.

[9] B. G. Miller, Coal Energy Systems, Elsevier, Amsterdam, Boston, 2005.

[10] Li, X., Hu, S., Jin, L., & Hu, H. (2008). Role of iron-based catalyst and hydrogen transfer in direct coal liquefaction. Energy & Fuels, 22(2), 1126-1129.

[11] Brooks, D. G., Guin, J. A., Curtis, C. W., & Placek, T. D. (1983). Pyrite catalysis of coal liquefaction, hydrogenation, and intermolecular hydrogen transfer reactions. Industrial & Engineering Chemistry Process Design and Development, 22(3), 343-349.

[12] WILLSON, W. G., Walsh, D. A. N., & Irwinc, W. (1997). Overview of low-rank coal (LRC) drying. Coal Perparation, 18(1-2), 1-15.

[13] Couch, G. R. (1990). Lignite upgrading. UK: IEA Coal Research.

[14] Gronhovd, G. H., Sondreal, E. A., Kotowski, J., & Wiltsee, G. (1982). Low-rank coal technology: lignite and subbituminous.

[15] Asokan, P., Saxena, M., & Asolekar, S. R. (2005).Coal combustion residues—environmental implications and recycling potentials. Resources, conservation and recycling, 43(3), 239-262.

[16] Liu, Z., Shi, S., & Li, Y. (2010).Coal liquefaction technologies—Development in China and challenges in chemical reaction engineering. Chemical Engineering Science, 65(1), 12-17.

[17] Fentone, D.(2001). Direct Liquefaction of Coal with Coal-Derived Solvents to Produce Precursors for Carbon Products.MSc thesis, West Virginia University.

[18] Höök, M., & Aleklett, K. (2009).A review on coal-to-liquid fuels and its coal consumption. international journal of energy research, 34(10), 848-864.

[19] Berkowitz, N. (2012). An introduction to coal technology. Elsevier,257.

[20] Merrick, D. (1984). Coal combustion and conversion technology. Macmillan.

[21] Kabe, T., Ishihara, A., Qian, E. W., Sutrisna, I. P., & Kabe, Y. (2004). Coal and coal-related compounds: structures, reactivity and catalytic reactions (Vol. 150). Elsevier.

[22] Williams, R. H., & Larson, E. D. (2003).A comparison of direct and indirect liquefaction technologies for making fluid fuels from coal. Energy for Sustainable Development, 7(4), 103-129.

[23] Lobnitz, M. M. (1983). Direct and indirect coal conversion technology in Kentucky: an environmental perspective.

[24] Vallentin, D. (2008).Driving forces and barriers in the development and implementation of coal-to-liquids (CtL) technologies in Germany. Energy Policy, 36(6), 2030-2043.

[25] Taunton, J. W., Trachte, K. L., & Williams, R. D. (1981). Coal feed flexibility in the Exxon Donor Solvent coal liquefaction process. Fuel, 60(9), 788-794.

[26] Onozaki, M., Namiki, Y., Ishibashi, H., Kobayashi, M., Itoh, H., Hiraide, M., & Morooka, S. (2000). A process simulation of the NEDOL coal liquefaction process. Fuel processing technology, 64(1), 253-269.

[27] Song, C., Schobert, H. H., & Andresen, J. M. (2005). Premium carbon products and organic chemicals from coal. IEA Coal Research, Clean Coal Centre.

[28] Comolli, A. G., Lee, T. L., Popper, G. A., & Zhou, P. (1999). The Shenhua coal direct liquefaction plant. Fuel Processing Technology, 59(2), 207-215.

[29] Hirano, K. (2000). Outline of NEDOL coal liquefaction process development (pilot plant program). Fuel processing technology, 62(2), 109-118.

[30] Dadyburjor, D. B., Liu, Z., & Davis, B. H. (2004). Coal liquefaction. John Wiley & Sons, Inc.

[31] Song, C., Schobert, H. H., & Hatcher, P. G. (1992).Temperature-programmed liquefaction of a low-rank coal.Energy & fuels, 6(3), 326-328.

[32] Pullen, J. R. (1981).Solvent extraction of coal. IEA Coal Research, London, 9-110.

[33] Shaw, J. M. (1985).Novel design criteria for direct coal liquefaction reactors. PhD thesis, University of British Columbia.

[34] Ergun, S., Wen, C. Y., & Lee, E. S. (1979). Coal Conversion Technology. Chicago .

[35] Neavel, R. C., Knights, C. F., & Schulz, H. (1981).Exxon Donor Solvent Liquefaction Process [and Discussion].Philosophical Transactions of the Royal Society of London. Series A, Mathematical and Physical Sciences, 300(1453), 141-156.

[36] McMillen, D. F., & Malhotra, R. (2006).Hydrogen transfer in the formation and destruction of retrograde products in coal conversion. The Journal of Physical Chemistry A, 110(21), 6757-6770.

[37] Li, X., Hu, H., Jin, L., Hu, S., & Wu, B. (2008).Approach for promoting liquid yield in direct liquefaction of Shenhua coal.Fuel Processing Technology, 89(11), 1090-1095.

[38] Derbyshire, F. J., & Duayne, W. D. (1981). Study of coal conversion in polycondensed aromatic compounds. Fuel, 60(8), 655-662.

[39] Vernon, L. W. (1980). Free radical chemistry of coal liquefaction: role of molecular hydrogen. Fuel, 59(2), 102-106.

[40] Wiser, W. H., Hill, G. R., & Kertamus, N. J. (1967).Kinetic Study of Pyrolysis of High Volatile Bituminous Coal. Industrial & Engineering Chemistry Process Design and Development, 6(1), 133-138.

[41] Provine, W. D., Porro, N. D., LaMarca, C., Klein, M. T., Foley, H. C., Bischoff, K. B., ... & Tait, A. M. (1992). Development of a pulse-injection short contact time coal liquefaction flow reactor. Industrial & engineering chemistry research, 31(4), 1170-1176.

[42] Bhole, M. R. (2002).The effect of solvents and processing conditions on the solvent extraction of coal.PhD thesis, West Virginia University.

[43] Miknis, F. P., Netzel, D. A., Turner, T. F., Wallace, J. C., & Butcher, C. H. (1996). Effect of different drying methods on coal structure and reactivity toward liquefaction. Energy & fuels, 10(3), 631-640.

[44] Schobert, H. H. The geochemistry of coal. Part I. The classification and origin of coal. Journal of Chemical Education 66, 242.

[45] Skorupska, N. M. (1993). Coal specifications-impact on power station performance. London: IEA Coal Research.

[46] Karthikeyan M, Zhonghua W, Mujumdar AS .Low-rank coal drying technologies-Current status and new developments.Dry Technol. 2009;27:403-415.

[47] Channiwala SA, Parikh PP. A unified correlation for estimating HHV of solid, liquid and gaseous fuels. Fuel. 2002;81:1051-1063.

[48] Karaca, H., & Koyunoğlu, C. (2010). The co-liquefaction of Elbistan lignite and biomass. Part II: The characterization of liquefaction products. Energy Sources, Part A: Recovery, Utilization, and Environmental Effects, 32(13), 1167-1175.

[49] De Vlieger, J. J., Kieboom, A. P., & Van Bekkum, H. (1984). Behaviour of tetralin in coal liquefaction: examination in long-run batch-autoclave experiments. Fuel, 63(3), 334-340.

[50] Cronauer, D. C., Jewell, D. M., Shah, Y. T., & Kueser, K. A. (1978). Hydrogen transfer cracking of dibenzyl in tetralin and related solvents. Industrial & Engineering Chemistry Fundamentals, 17(4), 291-297.

[51] Brown M. Introduction to thermal analysis: techniques and applications Springer; 2001.

[52] Varol M, Atimtay AT, Bay B, Olgun H. Investigation of co- combustion characteristics of low quality lignite coals and biomass with thermogravimetric analysis. Thermochim Acta. 2010;510:195-201.

[53] Howard HC. Chemistry of coal utilization. Second supplementary volume, John Wiley, New York; 1963.pp.340-345.

[54] Lawson GJ. Differential Thermal Analysis, Fundamental Aspects, Academic Press, New York; 1970.pp.705.

[55] Anthony DB, Howard JR. Coal devolatilization and hydrogastification. AICHE J. 1976;22:625-656.

[56] Hathi VV. Thermal and kinetic analysis of the pyrolysis of coals. The university of Oklahoma. PhD Thesis. 1978.

[57] Scaccia, S.TG–FTIR and kinetics of devolatilization of Sulcis coal. J Anal Appl Pyrol. 2013;104:95-102.

[58] Idris, S. S., Rahman, N. A., Ismail, K., Alias, A. B., Rashid, Z. A., & Aris, M. J. (2010). Investigation on thermochemical behaviour of low rank Malaysian coal, oil palm biomass and their blends during pyrolysis via thermogravimetric analysis (TGA). Bioresource technology, 101(12), 4584-4592.

[59] Jiang, G., Nowakowski, D. J., & Bridgwater, A. V. (2010). A systematic study of the kinetics of lignin pyrolysis. Thermochimica Acta, 498(1), 61-66.

[60] Sbirrazzuoli N, Vincent L, Mija A, Guigo N. Integral, differential and advanced isoconversional methods: complex mechanisms and isothermal predicted conversion–time curves. Chemometr Intell Lab. 2009;96:219-226.

[61] Khawam A. Application of solid-state kinetics to desolvation reactions. Iowa University PhD Thesis. 2007.

[62] Zsako, J. (1968). Kinetic analysis of thermogravimetric data. The Journal of Physical Chemistry, 72(7), 2406-2411.

[63] Miura K. A new and simple method to estimate f (E) and k0 (E) in the distributed activation energy model from three sets of experimental data. Energ Fuel. 1995; 9: 302-307.

[64] Aboyade AO, Carrier M, Meyer EL, Knoetze JH, Görgens JF. Model fitting kinetic analysis and characterization of the devolatilization of coal blends with corn and sugarcane residues. Thermochim Acta. 2012;530:95-106.

[65] Niu, S. L., Han, K. H., & Lu, C. M. (2011). Characteristic of coal combustion in oxygen/carbon dioxide atmosphere and nitric oxide release during this process. Energy Conversion and Management, 52(1), 532-537.

[66] Vuthaluru HB. Investigations into the pyrolytic behaviour of coal/biomass blends using thermogravimetric analysis. Bioresource Technol. 2004;92:187-195.

[67] Ulloa CA, Gordon AL, García XA. Thermogravimetric study of interactions in the pyrolysis of blends of coal with radiate pine sawdust. Fuel Process Technol. 2009; 90:583-590.

[68] Haykiri-Acma S, Yaman. Synergy in devolatilization characteristics of lignite and hazelnut shell during co-pyrolysis. Fuel. 2007;86:373–380.

[69] KissingerHE. Reaction kinetics in differential thermal analysis.Anal Chem.1957;29:1702-1706.

[70] Aboyade, A. O., Görgens, J. F., Carrier, M., Meyer, E. L., & Knoetze, J. H. (2013). Thermogravimetric study of the pyrolysis characteristics and kinetics of coal blends with corn and sugarcane residues. Fuel Processing Technology, 106, 310-320.

[71] Güldoğan, Y., Durusoy, T., & Bozdemir, T. (2002). Effects of heating rate and particle size on pyrolysis kinetics of Gediz lignite. Energy sources, 24(8), 753-760.

[72] Sharma, S., & Ghoshal, A. K. (2010). Study of kinetics of co-pyrolysis of coal and waste LDPE blends under argon atmosphere. Fuel, 89(12), 3943-3951.

[73] Güneş, M., & Güneş, S. K. (2008). Distributed activation energy model parameters of some Turkish coals. Energy Sources, Part A, 30(16), 1460-1472.

[74] Ceylan, S., & Topçu, Y. (2014). Pyrolysis kinetics of hazelnut husk using thermogravimetric analysis. Bioresource technology, 156, 182-188.

[75] Gašparovič, L., Koreňová, Z., & Jelemenský, Ľ. (2010). Kinetic study of wood chips decomposition by TGA. Chemical Papers, 64(2), 174-181.

[76] Vyazovkin, S., & Sbirrazzuoli, N. Isoconversional kinetic analysis of thermally stimulated processes in polymers. Macromol Rapid Comm. 2006;27: 1515-1532.

[77] Wu, W., Cai, J., & Liu, R. Isoconversional Kinetic Analysis of Distributed Activation Energy Model Processes for Pyrolysis of Solid Fuels. Ind Eng Chem Res. 2013;52;14376-14383.

[78] Asbury, R. S. (1934).Action of Solvents on Coal Extraction of Edenborn Coal by Benzene at Elevated Temperatures. Industrial & Engineering Chemistry, 26(12), 1301-1306.

[79] Giri, C. C., & Sharma, D. K. (2000).Mass-transfer studies of solvent extraction of coals in N-methyl-2-pyrrolidone. Fuel, 79(5), 577-585.

[80] Curran, G. P., Struck, R. T., & Gorin, E. (1967).Mechanism of Hydrogen-Transfer Process to Coal and Coal Extract. Industrial & Engineering Chemistry Process Design and Development, 6(2), 166-173.

[81] Abichandani, J. S., Wieland, J. H., Shah, Y. T., & Cronauer, D. C. (1984).Kinetics of short contact time coal liquefaction. Part I: Effect of operating variables. AIChE journal, 30(2), 295-303.

[82] Pradhan, V. R., Tierney, J. W., Wender, I., & Huffman, G. P. (1991). Catalysis in direct coal liquefaction by sulfated metal oxides. Energy & fuels, 5(3), 497-507.

[83] Szladow, A. J., & Given, P. H. (1981).Models and activation energies for coal liquefaction reactions. Industrial & Engineering Chemistry Process Design and Development, 20(1), 27-33.

[84] Joseph, J. T. (1991). Liquefaction behaviour of solvent-swollen coals. Fuel,70(2), 139-144.

[85] Shui, H., Wang, Z., & Cao, M. (2008).Effect of pre-swelling of coal on its solvent extraction and liquefaction properties. Fuel, 87(13), 2908-2913.

[86] Hu, H., Sha, G., & Chen, G. (2000).Effect of solvent swelling on liquefaction of Xinglong coal at less severe conditions. Fuel processing technology, 68(1), 33-43.

[87] Whitehurst, D. D., Mitchell, T. O., & Farcasiu, M. (1980). Coal liquefaction: The chemistry and technology of thermal processes. New York, Academic Press, Inc., 280-355.

[88] Plett, E. G., Alkidas, A. C., Rogers, F. E., & Summerfield, M. (1977). Coal particle integrity in high-temperature solvents, with and without agitation. Fuel,56(3), 241-244.

[89] Akhtar, J., & Amin, N. A. S. (2011). A review on process conditions for optimum bio-oil yield in hydrothermal liquefaction of biomass. Renewable and Sustainable Energy Reviews, 15(3), 1615-1624.

[90] Schlosberg, R. H. (1985).Chemistry of coal conversion.Springer, New York. 3-91.

[91] Vasquez, E. and O. Trass. (1987) "Mechano-Chemical Liquefaction of Coal", Proc. Can. Chem. Eng. Grad. Student, Conf., Kingston, ON, pp.293–299.

[92] Karaca, H., & Koyunoğlu, C. (2010). Co-liquefaction of Elbistan lignite and biomass. Part I: The effect of the process parameters on the conversion of liquefaction products. Energy Sources, Part A: Recovery, Utilization, and Environmental Effects, 32(6), 495-511.

[93] Ma, B. W., Zhu, X. S., Li, W. B., Zhang, X. J., & Du, S. F. (2013). Study on reaction characteristics of phenolic hydroxyl in coal by using the model compound during direct coal liquefaction. Journal of Coal Science and Engineering (China), 19(4), 540-545.

[94] Ferrance, J. P., & Holder, G. D. (1996). Development of a general model for coal liquefaction. Preprints of papers-american chemical society division fuel chemistry, 41, 941-945.

[95] SZLADOW, A. J., & GIVEN, P. H. (1982). Analysis of Coal Dissolution Reaction Engineering. Chemical Engineering Communications, 19(1-3), 115-127.

[96] Akash, B. A., Muchmore, C. B., Koropchak, J. A., Kim, J. W., & Lalvani, S. B. (1992). Investigations of simultaneous coal and lignin liquefaction: kinetic studies. Energy & fuels, 6(5), 629-634.

[97] Shui, H., Chen, Z., Wang, Z., & Zhang, D. (2010). Kinetics of Shenhua coal liquefaction catalyzed by/ZrO 2 solid acid. Fuel, 89(1), 67-72.

[98] Martinez, M. T., Benito, A. M., & Callejas, M. A. (1997). Thermal cracking of coal residues: kinetics of asphaltene decomposition. Fuel, 76(9), 871-877.

[99] Weller, S., Pelipetz, M. G., & Friedman, S. (1951). Kinetics of coal hydrogenation conversion of asphalt. Industrial & Engineering Chemistry, 43(7), 1572-1575.

[100] Falkum, E., & Glenn, R. A. (1952). Coal hydrogenation process studies III—Effects of time on restricted hydrogenolysis of Spitsbergen coal with Adkins catalyst. Fuel, 31, 133.

[101] Pelipetz, M. G., Salmon, J. R., Bayer, J., & Clark, E. L. (1955). Uncatalyzed coal hydrogenolysis. Industrial & Engineering Chemistry, 47(10), 2101-2103.

[102] Hill, G. R., Hariri, H. A. S. S. A. N., Reed, R. I., & Anderson, L. L. (1966).Kinetics and Mechanism of Solution of High Volatile Coal. Coal Science, Advances in Chemistry Series, 55, 427-447.

[103] Brunson, R. J. (1979). Kinetics of donor-vehicle coal liquefaction in a flow reactor. Fuel, 58(3), 203-207.

[104] Struck, R. T., Clark, W. E., Dudt, P. J., Rosenhoover, W. A., Zielke, C. W., & Gorin, E. (1969). Kinetics of hydrocracking of coal extract with molten zinc chloride catalysts in batch and continuous systems. Industrial & Engineering Chemistry Process Design and Development, 8(4), 546-551.

[105] Liebenberg, B. J., & Potgieter, H. G. (1973). The uncatalysed hydrogenation of coal. Fuel, 52(2), 130-133.

[106] Yoshida, R., Maekawa, Y., Ishii, T., & Takeya, G. (1976). Mechanism of high-pressure hydrogenolysis of Hokkaido coals (Japan). 1. Simulation of product distributions. Fuel, 55(4), 337-340.

[107] Cronauer, D. C., Shah, Y. T., & Ruberto, R. G. (1978). Kinetics of thermal liquefaction of Belle Ayr subbituminous coal. Industrial & Engineering Chemistry Process Design and Development, 17(3), 281-288.

[108] Shah, Y. T., Cronauer, D. C., McIlvried, H. G., & Paraskos, J. A. (1978). Kinetics of catalytic liquefaction of Big Horn coal in a segmented bed reactor. Industrial & Engineering Chemistry Process Design and Development, 17(3), 288-301.

[109] Chiba, T., & Sanada, Y. (1978). On the kinetics of coal hydrogenation. J. Fuel Soc.(Japan), 57, 259.

[110] Shalabi, M. A., Baldwin, R. M., Bain, R. L., Gary, J. H., & Golden, J. O. (1979). noncatalytic Coal Liquefaction in a Donor Solvent. Rate of Formation of Oil,Asphaltenes, and Preasphaltenes. Industrial & Engineering Chemistry Process Design and Development, 18(3), 474-479.

[111] Mohan, G., & Silla, H. (1981). Kinetics of donor-solvent liquefaction of bituminous coals in nonisothermal experiments. Industrial & Engineering Chemistry Process Design and Development, 20(2), 349-358.

[112] Gertenbach, D. D., Baldwin, R. M., & Bain, R. L. (1982). Modeling of bench-scale coal liquefaction systems. Industrial & Engineering Chemistry Process Design and Development, 21(3), 490-500.

[113] Abichandani, J. S., Shah, Y. T., Cronauer, D. C., & Ruberto, R. G. (1982). Kinetics of thermal liquefaction of coal. Fuel, 61(3), 276-282.

[114] Brandes, S. D. (1995). A characterization and evaluation of coal liquefaction process streams. Status assessment (No. DOE/PC/93054--14). CONSOL, Inc., Library, PA (United States).

[115] Radomyski, B., & Szczygiel, J. (1984). Mathematical analysis of the kinetics of hydrogenating depolymerization of benzene-insoluble coal extract fraction in the absence of catalyst. Fuel, 63(6), 744-746.

[116] Ozawa, S., Matsuura, M., Matsunaga, S. I., & Ogino, Y. (1984). Kinetics and reaction scheme of coal liquefaction over molten tin catalyst. Fuel, 63(5), 719-721.

[117] Gollakota, S. V., Guin, J. A., & Curtis, C. W. (1985). Parallel thermal and catalytic kinetics in direct coal liquefaction. Industrial & Engineering Chemistry Process Design and Development, 24(4), 1148-1154.

[118] Nagaishi, H., Moritomi, H., Sanada, Y., & Chiba, T. (1988). Evaluation of coal reactivity for liquefaction based on kinetic characteristics. Energy & fuels, 2(4), 522-528.

[119] Giralt, J., Fabregat, A., & Giralt, F. (1988). Kinetics of the solvolysis of a catalan lignite with tetralin and anthracene oil. Industrial & engineering chemistry research, 27(7), 1110-1114.

[120] Angelova, G., Kamenski, D., & Dimova, N. (1989). Kinetics of donor-solvent liquefaction of Bulgarian brown coal. Fuel, 68(11), 1434-1438.

[121] Salvadó, J., Giralt, J., Fabregat, A., & Giralt, F. (1990). Catalytic hydroliquefaction of Bergueda lignite with fuel oil and anthracene oil under various reactive atmospheres. Fuel, 69(6), 743-746.

[122] Pradhan, V. R., Holder, G. D., Wender, I., & Tierney, J. W. (1992). Kinetic modeling of direct liquefaction of Wyodak coal catalyzed by sulfated iron oxides. Industrial & engineering chemistry research, 31(8), 2051-2056.

[123] Ferrance, J., & Warzinski, R. P. (1996). A liquefaction kinetic research needs assessment. preprints of papers-american chemical society division fuel chemistry, 41, 928-934.

[124] Ikeda, K., Sakawaki, K., Nogami, Y., Inokuchi, K., & Imada, K. (2000). Kinetic evaluation of progress in coal liquefaction in the 1t/d PSU for the NEDOL process. Fuel, 79(3), 373-378.

[125] Kidoguchi, A., Itoh, H., Hiraide, M., Kaneda, E., Ishibashi, H., Kobayashi, M., ... & Inokuchi, K. (2001). Simulation of initial stage reactions in the direct coal liquefaction of sub-bituminous coals. Fuel, 80(9), 1325-1331.

[126] Song, C., Saini, A. K., & Schobert, H. H. (1994). Effects of drying and oxidation of Wyodak subbituminous coal on its thermal and catalytic liquefaction. Spectroscopic characterization and products distribution.Energy & fuels, 8(2), 301-312.

[127] Yu, J., Tahmasebi, A., Han, Y., Yin, F., & Li, X. (2013). A review on water in low rank coals: the existence, interaction with coal structure and effects on coal utilization. Fuel Processing Technology, 106, 9-20.

[128] Itay, M., Hill, C. R., & Glasser, D. (1989). A study of the low temperature oxidation of coal. Fuel Processing Technology, 21(2), 81-97.

[129] Guin, J., Tarrer, A., Taylor Jr, L., Prather, J., & Green Jr, S. (1976). Mechanisms of coal particle dissolution. Industrial & Engineering Chemistry Process Design and Development, 15(4), 490-494.

[130] Joseph, J. T., Cronauer, D. C., Rosenbaum, N. H., & Davis, A. (1994). Effect of Temperature on the Functionality Changes During Coal Liquefaction. preprints of papers-american chemical society division fuel chemistry, 39, 103-103.

[131] Flatman-Fairs, D. P., & Harrison, G. (1999).Suitability of UK bituminous and Spanish lignitous coals, and their blends for two stage liquefaction. Fuel, 78(14), 1711-1717.

[132] Huang, H., Wang, K., Wang, S., Klein, M. T., & Calkins, W. H. (1998).Studies of coal liquefaction at very short reaction times. 2. Energy & fuels, 12(1), 95-101.

[133] Rodriguez, I.,Chomón, M. J., Caballero, B., Arias, P. L., & Legarreta, J. A. (1998). Liquefaction behaviour of a Spanish subbituminous A coal under different conditions of hydrogen availability.Fuel processing technology, 58(1), 17-24.

[134] Storch, H. H., Fisher, C. H., Eisner, A., & Clarke, L. (1940). Hydrogenation of a Pittsburgh Seam Coal. Industrial & Engineering Chemistry, 32(3), 346-353.

[135] Rudnick, L. R., & Whitehurst, D. D. (1980, May).The Effect of Solvent Composition of the Liquefaction Behavior of Western Sub-Bituminous Coal.In EPRI Contractor's Meeting, Palo Alto, CA, 154-170.

[136] Loganbach, J. R., Droege, J. R., & Chauhan, S. P. (1978).Short Residence Time Coal Liquefaction.Electric Power Research Institute.166-177.

[137] Chandaliya, V. K., Banerjee, P. K., & Biswas, P. (2012).Optimization of Solvent Extraction Process Parameters of Indian Coal. Mineral Processing and Extractive Metallurgy Review, 33(4), 246-259.

[138] Wang, Z., Li, L., Shui, H., Wang, Z., Cui, X., Ren, S., ... & Kang, S. (2011). Study on the aggregation of coal liquefied preasphaltene in organic solvents by UV–vis and fluorescence spectrophotometry. Fuel, 90(1), 305-311.

[139] Steedman, W. (1985). Coal asphaltenes: a review. Fuel processing technology, 10(3), 209-238.

[140] Hortal, A. R., Hurtado, P., Martínez-Haya, B., & Mullins, O. C. (2007). Molecular-weight distributions of coal and petroleum asphaltenes from laser desorption/ionization experiments. Energy & Fuels, 21(5), 2863-2868.

[141] Cugini, A. V., Rothenberger, K. S., Ciocco, M. V., & Veloski, G. A. (1994).The Effect of Pressure and Solvent Quality on First Stage Coal Liquefaction with Dispersed Catalysts. ACS, 39, 695-695.

[142] Tang, Q. J., & Wang, Z. H. (2012).The Effect of Technological Parameter on the Co-liquefaction of Coal with Lignin.Advanced Materials Research, 577, 167-170.

[143] Okuma, O. (2000). Liquefaction process with bottom recycling for complete conversion of brown coal. Fuel, 79(3), 355-364.

[144] Cai, J., Wang, Y., & Huang, Q. (2008). Rapid liquefaction of Longkou lignite coal by using a tubular reactor under methane atmosphere. Fuel, 87(15), 3388-3392.

[145] Miura, K., Shimada, M., Mae, K., & Sock, H. Y. (2001).Extraction of coal below 350° C in flowing non-polar solvent. Fuel, 80(11), 1573-1582.

[146] Mochida, I., Takayama, A., Sakata, R., & Sakanishi, K. (1990). Hydrogen-transferring liquefaction of an Australian brown coal with polyhydrogenated condensed aromatics: roles of donor in the liquefaction. Energy & Fuels, 4(1), 81-84.

[147] Okutani, T., Yokoyama, S., & Maekawa, Y. (1984). Viscosity changes in coal paste during hydrogenation. Fuel, 63(2), 164-168.

[148] Traeger, R. K. (1980). Engineering kinetics of short residence time coal liquefaction processes. Industrial & Engineering Chemistry Product Research and Development, 19(2), 143-147.

[149] Krichko, A. A., & Gagarin, S. G. (1990). New ideas of coal organic matter chemical structure and mechanism of hydrogenation processes. Fuel, 69(7), 885-891.

[150] Sakaki, T., Shibata, M., & Hirosue, H. (1995). Effect of coal rank on rheological behavior of coal-solvent slurries during heating. Energy & fuels, 9(2), 314-318.

[151] Gabzdyl, W.,n & Varma, A. (1993). Thermogravimetric studies in prediction of coal behaviour during coal liquefaction. Journal of Thermal Analysis and Calorimetry, 39(1), 31-40.

[152] Sakaki, T., Shibata, M., & Hirosue, H. (1995). Effect of coal rank on rheological behavior of coal-solvent slurries during heating. Energy & fuels, 9(2), 314-318.

[153] Sakaki, T., Yasuda, S., Arita, S., Hirosue, H., & Honda, H. (1991). Reduction in size of coal particles by heating with petroleum asphalt. Fuel Processing Technology, 28(3), 275-285.

[154] Syamlal, M., & Wittmann, C. V. (1985). Continuous reaction mixture model for coal liquefaction kinetics. Industrial & engineering chemistry fundamentals, 24(1), 82-90.

[155] Wen, C. Y., & Han, K. W. (1975). Kinetics of coal liquefaction. Am. Chem. Soc., Div. Fuel Chem, 20(1), 216-233.

[156] White, C. M., Douglas, L. J., Perry, M. B., & Schmidt, C. E. (1987). Characterization of extractable organosulfur constituents from Bevier seam coal. Energy & fuels, 1(2), 222-226.

[157] Bendale, P. G., Zeli, R. A., & Nishioka, M. (1994). Mechanism of coal solubilization by high temperature soaking: Investigation by extractability after soaking under various conditions. Fuel, 73(2), 251-255.

[158] Cloke, M., Hamilton, S., & Wright, J. P. (1987). Evidence for mineral matter forms in coal liquefaction extracts. Fuel, 66(12), 1685-1690.

[159] Stone, J. B., Trachte, K. L., & Poddar, S. K. (1978). Calcium carbonate deposit formation during the liquefaction of low rank coals. In Proceedings EPRI Contractor's Conference on Coal Liquefaction (pp. 1-10).

[160] Li, X., Hu, S., Jin, L., & Hu, H. (2008). Role of iron-based catalyst and hydrogen transfer in direct coal liquefaction. Energy & Fuels, 22(2), 1126-1129.

[161] Ikenaga, N. O., Taniguchi, H., Watanabe, A., & Suzuki, T. (2000). Sulfiding behavior of iron based coal liquefaction catalyst. Fuel, 79(3), 273-283.

[162] Miller, R. E., & Stein, S. E. (1981, February). A fundamental chemical kinetics approach to coal conversion. In Chemistry and Physics of Coal Utilization-1980 (Vol. 70, No. 1, pp. 466-467). AIP Publishing.

[163] Cronauer, D. C., Jewell, D. M., Shah, Y. T., & Modi, R. J. (1979). Mechanism and kinetics of selected hydrogen transfer reactions typical of coal liquefaction. Industrial & Engineering Chemistry Fundamentals, 18(2), 153-162.

[164] Holland, J. H. (1975). Adaptation in natural and artificial systems: an introductory analysis with applications to biology, control, and artificial intelligence. U Michigan Press.

[165] Castillo, L., & González, A. (1998). Distribution network optimization: finding the most economic solution by using genetic algorithms. European Journal of Operational Research, 108(3), 527-537.

[166] Ramdoss, P. K., & Tarrer, A. R. (1997). Kinetic model development for single-stage coal coprocessing with petroleum waste. Fuel processing technology, 51(1), 83-100.

[167] Schwarz, G. (1978). Estimating the dimension of a model. The annals of statistics, 6(2), 461-464.

[168] Ding, W., Liang, J., & Anderson, L. L. (1997). Kinetics of thermal and catalytic coal liquefaction with plastic-derived liquids as solvent. Industrial & engineering chemistry research, 36(5), 1444-1452.

[169] Xu, B., & Kandiyoti, R. (1996). Two-stage kinetic model of primary coal liquefaction. Energy & fuels, 10(5), 1115-1127.

[170] Tissot, B. P., & Welte, D. H. (1984). Coal and its Relation to Oil and Gas. In Petroleum Formation and Occurrence (pp. 229-253). Springer Berlin Heidelberg.

[171] Panvelker, S. V. (1982). Hydrogen transfer reactions in coal liquefaction. PhD thesis, University of Pittsburgh.

[173] Rahman, M., Samanta, A., & Gupta, R. (2013). Production and characterization of ash-free coal from low-rank Canadian coal by solvent extraction. Fuel Processing Technology, 115, 88-98.

[174] Murasawa, N., Koseki, H., Li, X. R., Iwata, Y., & Sakamoto, T. (2012). Study on thermal behaviour and risk assessment of biomass fuels. International Journal of Energy Engineering, 2(5), 242-252.

[175] Mark Niemczyk, available at http://mirandamusic.com/mpnorganic/rotovap.html

[176] Parees, D. M., & Kamzelski, A. Z. (1982). Characterization of coal-derived liquids using fused silica capillary column GC-MS. Journal of Chromatographic Science, 20(10), 441-448.

[177] Mochida, I., Okuma, O., & Yoon, S. H. (2013). Chemicals from direct coal liquefaction. Chemical reviews, 114(3), 1637-1672.

[178] Karaca, H. (2006). Effect of coal liquefaction conditions on the composition of the product oil. Energy Sources, Part A, 28(16), 1483-1492

APPENDIX A

Image analysis of coal particles

The thermal decomposition of the coal occurs during liquefaction and particles were disintegrated into shapeless structure which is in consistent with former works pointed on structural disintegration during devolatalization process [42,102,129,147-157]. Image analysis of particles has been performed with Image J software to show the disintegration phenomena during coal liquefaction experiment. Particles of 150-212 μm size fractions were selected for particle size distribution. The raw image and residues were compared to exhibit the area differences as a result of reaction time.
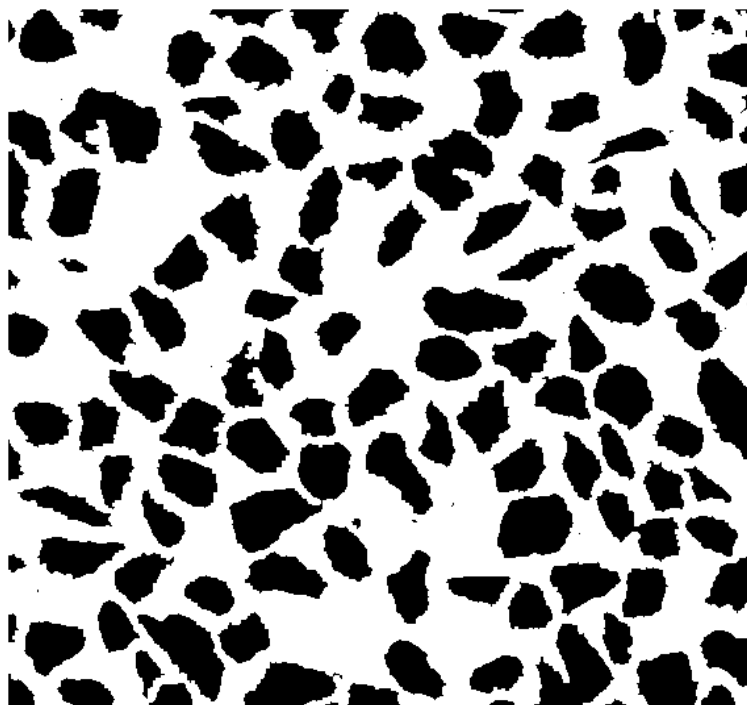
Figure   A -1: Image analysis of 150-212 μm size fractions (Raw coal)
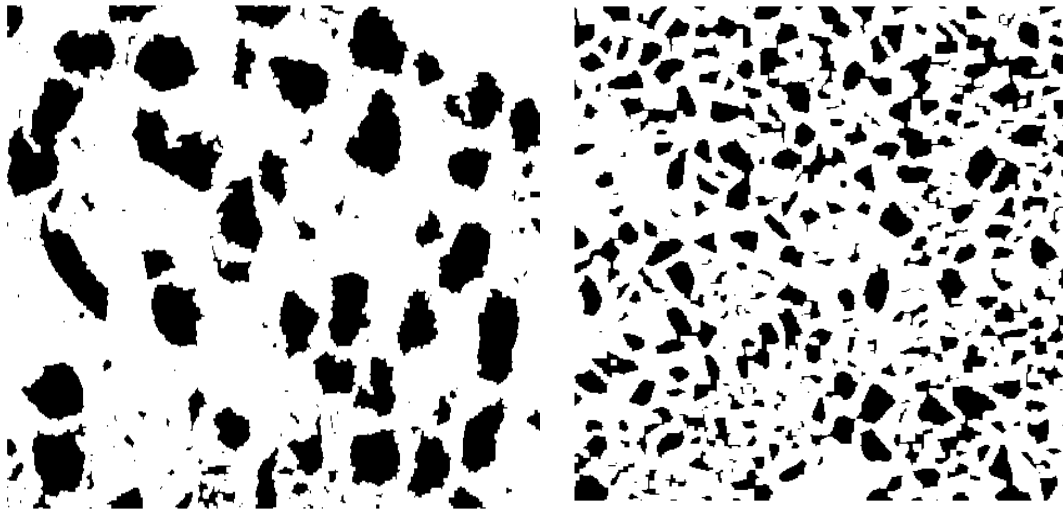
Figure   A -2: Image analysis of residues after 15 min and 30 min reaction times and 400°C
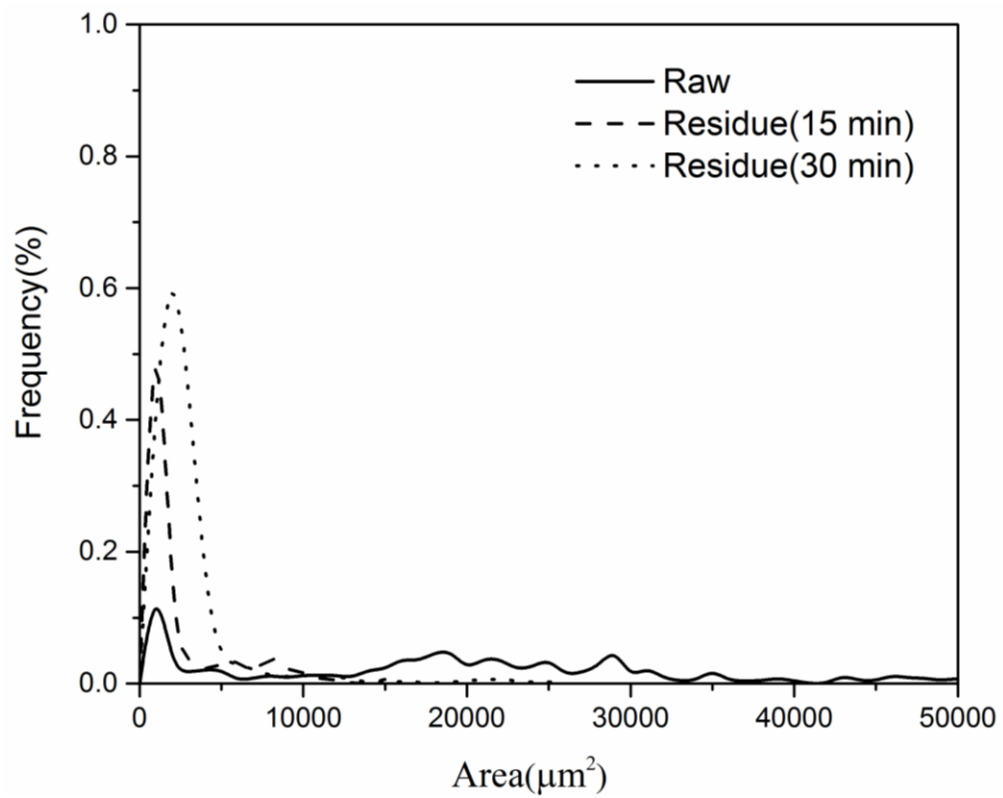
Figure   A- 3: Particle size distribution of coal and its residue

APPENDIX B

Mass Balance

Following expression was considered for calculating coal liquefaction conversion based on the dry and ash-free basis,

$$X\left(daf\ wt\%\right) = \frac{M_c - M_R}{M_c} \tag{B.1}$$

Where, M_c and M_R are the weight fractions of the raw coal and residue respectively.

The experiments were repeated under identical conditions to check the reproducibility of the results. The general mass balance for this experiment can be explained as follows:

$$M_C + M_S = M_P \tag{B.2}$$

$$M_P = M_{PA} + M_A + M_O + M_G \tag{B.3}$$

Where, M_C, M_S, M_P are the mass of the coal sample, solvent and M_{PA}, M_A, M_O and M_G represent mass of Preasphaltene, Asphaltene, Oil and Gas respectively.

Sample calculation for Run NO.1

Reaction condition

Mass of empty reactor=227.9 g

Weight of filter: 0.9604 g

Weight of residue with filter: 1.3825 g

T=350°C, t=120 min, P=60 (bar), M_C=1.2564 g, S/C=7:1, M_S=8.78 g

M_R (THF Ins)= 0.4221g

Coal ash= 21.5%, Weight of ash in residue: 0.1388 g, Residue ash (wt %) =32.9,

$X(daf\ wt\%)=0.67$

Initial reactor weight (before reaction) =238.95 g

Final reactor weight (after reaction) =237.87 g

Weight of gas produced by reaction: 0.06282 g

M_{PA} (Toluene Insoluble) =0.38 (wt %), M_A (Heptane Insoluble) = 0.24 (wt %),

M_O (Heptane soluble)=0.23 (wt %)

Run NO.1: M_{PA} (wt %) =0.30, M_A (wt %) =0.19, M_O (wt %) =0.18, M_G (wt %) =0.052
Same calculation has been performed for other runs at this reaction condition as follows:

Run NO.2: M_{PA} (wt %) =0.30, M_A (wt %) =0.20, M_O (wt %) =0.12, M_G (wt %) =0.073
Run NO.3: M_{PA} (wt %) =0.31, M_A (wt %) =0.17, M_O (wt %) =0.19, M_G (wt %) =0.031

Standard deviation of products:

STD (PA) =0.0058, STD (A) =0.0153, STD (O) =0.038, STD (G) =0.021

As can be observed from the standard deviation data, the highest deviation is related to Oil measurement and the lowest is related to Preasphaltene. The reason somewhat arises from the fact that during the experiment some of this deviation could belong to the sequence of experiment because the weight fraction of first component (Preasphaltene) has been measured first and with progress of time the deviation may increase as previous error may affect to the next error. It also arises because direct determination of oil measurement in the liquid product is very sophisticated since both THF and oil are not distinguishable by solvent

extraction methods as both components are heptane soluble. Moreover, it was very difficult to isolate THF from extract by rotary evaporator equipment because of high interaction between THF and coal liquid. Therefore, the yield of oil will be slightly overestimated if THF remains in the extract. So the yield of oil can be was determined by the difference of sum of the other components and 100. This technique allowed us to reduce the experimental error which may occur by the operator. The results of other runs are given here:

Run NO.1	Run NO.2	Run NO.3
Temperature:350°C	**Temperature=350°C**	**Temperature=350°C**
Reaction time=15 min	**Reaction time=15 min**	**Reaction time=15 min**
Mass of empty reactor=227.8 g	Mass of empty reactor=227.2 g	Mass of empty reactor=227.6 g
Mc=1.0523 g	Mc=1.0251 g	Mc=1.0344 g
Ms=7.36 g	Ms=7.18 g	Ms=7.24 g
M_R= 0.8176 g	M_R= 0.8325 g	M_R= 0.8384 g
Residue ash= 27.25%	Residue ash= 26.2%	Residue ash= 26.8 %
Conversion=0.1849	Conversion=0.1357	Conversion=0.1445

Run NO.1	Run NO.2	Run NO.3
Temperature=350°C	**Temperature=350°C**	**Temperature=350°C**
Reaction time=30 min	**Reaction time=30 min**	**Reaction time=30 min**
Mass of empty reactor=227.4 g	Mass of empty reactor=227.1 g	Mass of empty reactor=228.2 g
Mc=1.1236 g	Mc=1.1145 g	Mc=1.0894 g
Ms=7.85 g	Ms=7.80 g	Ms=7.60 g
M_R= 0.7703 g	M_R= 0.7511 g	M_R= 0.7228 g
Residue ash= 29.8 %	Residue ash= 31.7 %	Residue ash= 32.9 %
Conversion=0.306 %	Conversion=0.3362 %	Conversion=0.3580 %

Run NO.1	Run NO.2	Run NO.3
Temperature=350°C	**Temperature=350°C**	**Temperature=350°C**
Reaction time=60 min	**Reaction time=60 min**	**Reaction time=60 min**
Mass of empty reactor=227.9	Mass of empty reactor=227.5	Mass of empty reactor=227.9
Mc=1.0885 g	Mc=1.1125 g	Mc=1.042 g
Ms=7.61 g	Ms=7.78 g	Ms=7.294 g
M_R= 0.5391 g	M_R= 0.5058 g	M_R= 0.5228 g
Residue ash= 32.1 %	Residue ash= 32.7 %	Residue ash= 34.6 %
Conversion=0.5150 %	Conversion=0.5587 %	Conversion=0.5268 %

Run NO.1	Run NO.2	Run NO.3
Temperature=350°C	**Temperature=350°C**	**Temperature=350°C**
Reaction time=120 min	**Reaction time=120 min**	**Reaction time=120 min**
Mass of empty reactor=227.9 g	Mass of empty reactor=226.4 g	Mass of empty reactor=225.4 g
Mc=1.2564 g	Mc=1.3126 g	Mc=1.1294 g
Ms=8.78 g	Ms=9.17 g	Ms=7.9 g
M_R= 0.4221 g	M_R= 0.4733 g	M_R= 0.3781 g
Residue ash= 32.9%	Residue ash= 32.6%	Residue ash= 33.8%
Conversion=0.6749	Conversion=0.6495	Conversion=0.6804

Run NO.1	Run NO.2	Run NO.3
Temperature=375°C	**Temperature= 375°C**	**Temperature= 375°C**
Reaction time=15 min	**Reaction time=15 min**	**Reaction time=15 min**
Mass of empty reactor=226.8 g	Mass of empty reactor=227.8 g	Mass of empty reactor=227.2 g
Mc=1.2621 g	Mc=1.2452 g	Mc=1.2132 g
Ms=8.83 g	Ms=8.71 g	Ms=8.49 g
M_R= 0.8693 g	M_R= 0.8982 g	M_R= 0.8719 g
Residue ash= 27.9 g	Residue ash= 27.4 g	Residue ash= 26.3 g
Conversion=0.2839%	Conversion=0.2448%	Conversion=0.2362%

Run NO.1	Run NO.2	Run NO.3
Temperature=375°C	Temperature= 375°C	Temperature= 375°C
Reaction time=30 min	Reaction time=30 min	Reaction time=30 min
Mass of empty reactor=226.8 g	Mass of empty reactor=227.8 g	Mass of empty reactor=227.4 g
Mc=1.2234 g	Mc=1.0561 g	Mc=1.2024 g
Ms=8.55 g	Ms=7.39 g	Ms=8.41 g
MR= 0.7435 g	MR= 0.6064 g	MR= 0.6992 g
Residue ash= 27.4 %	Residue ash= 28.9 %	Residue ash= 29.6 %
Conversion=0.3638%	Conversion=0.4109%	Conversion=0.4096%

Run NO.1	Run NO.2	Run NO.3
Temperature=375°C	**Temperature= 375°C**	**Temperature= 375°C**
Reaction time=60 min	**Reaction time=60 min**	**Reaction time=60 min**
Mass of empty reactor=226.4 g	Mass of empty reactor=227.2 g	Mass of empty reactor=225.5 g
Mc=1.0151 g	Mc=1.0395 g	Mc=1.1274 g
Ms=7.1 g	Ms=7.26 g	Ms=7.9 g
M_R= 0.4352 g	M_R= 0.4184 g	M_R= 0.4108 g
Residue ash= 28.4%	Residue ash= 29.9%	Residue ash= 30.4%
Conversion=0.5573	Conversion=0.5931	Conversion=0.6343

Run NO.1	Run NO.2	Run NO.3
Temperature=375°C	**Temperature= 375°C**	**Temperature= 375°C**
Reaction time=120min	**Reaction time=120 min**	**Reaction time=120min**
Mass of empty reactor=225.9 g	Mass of empty reactor=224.2 g	Mass of empty reactor=228.6 g
Mc=1.0127g	Mc=1.0579g	Mc=1.0927g
Ms=7.1g	Ms=7.4g	Ms=7.64g
M_R= 0.2652g	M_R= 0.2434g	$M_{R=}$0.2736g
Residue ash= 29.8%	Residue ash= 31.4%	Residue ash= 32.8%
Conversion=0.7349	Conversion=0.7724	Conversion=0.7573

Run NO.1	Run NO.2	Run NO.3
Temperature=400°C	**Temperature=400°C**	**Temperature=400°C**
Reaction time=15 min	**Reaction time=15 min**	**Reaction time=15 min**
Mass of empty reactor=224.3 g	Mass of empty reactor=226.2 g	Mass of empty reactor=227.9 g
Mc=1.026 g	Mc=1.068	Mc=1.029 g
Ms=7.18 g	Ms=7.48 g	Ms=7.2 g
M_R= 0.6504 g	M_R= 0.7006 g	M_R= 0.7201 g
Residue ash= 34.8%	Residue ash= 33.5%	Residue ash= 34.1%
Conversion=0.404	Conversion=0.3709	Conversion=0.335

Run NO.1	Run NO.2	Run NO.3
Temperature=400°C	**Temperature=400°C**	**Temperature=400°C**
Reaction time=30 min	**Reaction time=30 min**	**Reaction time=30 min**
Mass of empty reactor=224.3g	Mass of empty reactor=228.2g	Mass of empty reactor=227.1g
Mc=1.0284g	Mc=1.2113g	Mc=1.1237g
Ms=7.2g	Ms=8.48g	Ms=7.86g
M_R= 0.4824g	M_R= 0.4689g	M_R= 0.5201g
Residue ash= 33.9%	Residue ash= 34.4%	Residue ash= 35%
Conversion=0.5529	Conversion=0.6338	Conversion=0.5708

Run NO.1	Run NO.2	Run NO.3
Temperature=400°C	**Temperature=400°C**	**Temperature=400°C**
Reaction time=60 min	**Reaction time=60 min**	**Reaction time=60 min**
Mass of empty reactor=225.4g	Mass of empty reactor=225.8g	Mass of empty reactor=227.7g
Mc=1.0435g	Mc=1.2416g	Mc=1.0238g
Ms=7.3g	Ms=8.69g	Ms=7.16g
M_R= 0.2851g	M_R= 0.2864g	M_R= 0.2573g
Residue ash= 34.6%	Residue ash= 36.8%	Residue ash= 36.1%
Conversion=0.7423	Conversion=0.7897	Conversion=0.7684

Run NO.1	Run NO.2	Run NO.3
Temperature=400°C	**Temperature=400°C**	**Temperature=400°C**
Reaction time=120min	**Reaction time=120 min**	**Reaction time=120min**
Mass of empty reactor=228.9g	Mass of empty reactor=226.2g	Mass of empty reactor=227.4g
Mc=1.0332g	Mc=1.047g	Mc=1.1283g
Ms=7.23g	Ms=7.33g	Ms=7.89g
M_R= 0.1598g	M_R= 0.2434g	M_R=0.2736g
Residue ash= 37.4%	Residue ash= 38.7%	Residue ash= 38.3%
Conversion=0.8604	Conversion=0.8485	Conversion=0.8416

Run NO.1	Run NO.2	Run NO.3
Temperature=450°C	**Temperature=450°C**	**Temperature=450°C**
Reaction time=15 min	**Reaction time=15 min**	**Reaction time=15 min**
Mass of empty reactor=227.3 g	Mass of empty reactor=226.5 g	Mass of empty reactor=228.3 g
Mc=1.0124 g	Mc=1.0362 g	Mc=1.0325 g
Ms=7.08 g	Ms=7.25 g	Ms=7.22 g
M_R= 0.4764 g	M_R= 0.5584 g	M_R= 0.5842 g
Residue ash= 39.2%	Residue ash= 39.7%	Residue ash= 40.3%
Conversion=0.5874	Conversion=0.5314	Conversion=0.5129

Run NO.1	Run NO.2	Run NO.3
Temperature=450°C	**Temperature=450°C**	**Temperature=450°C**
Reaction time=30 min	**Reaction time=30 min**	**Reaction time=30 min**
Mass of empty reactor=227.3 g	Mass of empty reactor=227.9 g	Mass of empty reactor=225.8 g
Mc=1.013g	Mc=1.0317 g	Mc=1.0158 g
Ms=7.09g	Ms=7.22 g	Ms=7.11 g
M_R= 0.2801g	M_R= 0.2593 g	M_R= 0.2273 g
Residue ash= 41.2%	Residue ash= 40.9%	Residue ash= 41.5%
Conversion=0.7655	Conversion=0.7858	Conversion=0.8112

Run NO.1	Run NO.2	Run NO.3
Temperature=450°C	**Temperature=450°C**	**Temperature=450°C**
Reaction time=60 min	**Reaction time=60 min**	**Reaction time=60 min**
Mass of empty reactor=229.4 g	Mass of empty reactor=227.8 g	Mass of empty reactor=228.7 g
Mc=1.0159 g	Mc=1.0295 g	Mc=1.0133 g
Ms=7.11 g	Ms=7.2 g	Ms=7.09 g
M_R= 0.1535 g	M_R= 0.1505 g	M_R= 0.2116 g
Residue ash= 41.6%	Residue ash= 42.5%	Residue ash= 41.8%
Conversion=0.8724	Conversion=0.8788	Conversion=0.8245

Run NO.1	Run NO.2	Run NO.3
Temperature=450°C	Temperature=450°C	Temperature=450°C
Reaction time=120min	Reaction time=120 min	Reaction time=120min
Mass of empty reactor=227.9 g	Mass of empty reactor=228.6 g	Mass of empty reactor=227.3 g
Mc=1.0147 g	Mc=1.0223 g	Mc=1.0272 g
Ms=7.1 g	Ms=7.15 g	Ms=7.19 g
MR= 0.1598 g	MR= 0.1441 g	MR=0.1901 g
Residue ash= 42.9 %	Residue ash= 43.7 %	Residue ash= 43.5 %
Conversion=0.8703	Conversion=0.8855	Conversion=0.8492